SYNTHETIC FUELS FROM CRACKING OF POLYETHYLENE USING ZEOLITE CATALYSTS IN BATCH AND CONTINUOUS PROCESSES

CHAIWAT TACHAKRITIKUL

A THESIS SUBMITTED IN PARTIAL FULFILLMENT

OF THE REQUIREMENT FOR THE DEGREE OF

MASTER OF SCIENCE IN PETROCHEMICALS AND HYDROCARBON CHEMISTRY

SCHOOL OF GRADUATE STUDIES

KING MONGKUT'S INSTITUTE OF TECHNOLOGY LADKRABANG

2001

ISBN 974-648-478-8

หัวข้อวิทยานิพนธ์	เชื้อเพลิงสังเคราะห์จากการแตกตัวของพอลิเอทิลีนด้วยตัวเร่งปฏิกิริยาซีโอไลต์ในกระบวนการแบบกะและแบบต่อเนื่อง
นักศึกษา	นายชัยวัฒน์ เตชะเกียรติกูร
รหัสประจำตัว	41065112
ปริญญา	วิทยาศาสตรมหาบัณฑิต
สาขาวิชา	ปิโตรเคมีและเคมีไฮโดรคาร์บอน
พ.ศ.	2544
อาจารย์ผู้ควบคุมวิทยานิพนธ์	ผศ. ดร.ตะวัน สุขน้อย

บทคัดย่อ

งานวิจัยนี้เป็นการออกแบบและจัดสร้างชุดปฏิกรณ์ (Reactor) เพื่อใช้ศึกษาการแตกตัวของพอลิเอทิลีนในกระบวนการแบบต่อเนื่อง (Continuous process) เปรียบเทียบกับกระบวนการแบบกะ (Batch process) โดยใช้ซีโอไลต์ชนิด H-ZSM-5 และ H-Beta เป็นตัวเร่งปฏิกิริยา จากการศึกษาด้วยเทคนิคเทอร์โมกราวิเมทรี (TGA) พบว่าอัตราส่วนตัวเร่งปฏิกิริยาทั้ง 2 ชนิดต่อพอลิเอทิลีนที่ 20 เปอร์เซ็นต์โดยน้ำหนักมีค่าเหมาะสมที่สุด ซึ่งในกระบวนการแบบกะได้ทำการทดลองที่อุณหภูมิ 430 องศาเซลเซียส เป็นเวลา 15 และ 30 นาที ภายใต้บรรยากาศก๊าซไฮโดรเจนและฮีเลียมที่มีอัตราการไหลของก๊าซตัวพา (Carrier gas) 100 มิลลิลิตรต่อนาที โดยทำการศึกษาถึงผลของขนาดรูพรุนจุลภาคของซีโอไลต์ ผลการเสื่อมสภาพของตัวเร่งปฏิกิริยา เวลาในการทำปฏิกิริยา และผลของก๊าซตัวพา จากการศึกษาพบว่าเมื่อใช้ซีโอไลต์ชนิด H-ZSM-5 ที่มีรูพรุนขนาดกลางเป็นตัวเร่งปฏิกิริยาจะได้ผลิตภัณฑ์ที่เป็นก๊าซมาก ในขณะที่ใช้ซีโอไลต์ชนิด H-Beta ซึ่งมีรูพรุนขนาดใหญ่จะได้ผลิตภัณฑ์ที่เป็นของเหลวมากกว่า ดังนี้ขนาดรูพรุนจุลภาคของซีโอไลต์สามารถควบคุมชนิดของผลิตภัณฑ์ได้ เมื่อใช้ซีโอไลต์ที่ใช้แล้วกลับมาใช้ใหม่โดยไม่ได้ทำการปรับสภาพ พบว่าอัตราการเสื่อมสภาพของซีโอไลต์ชนิดเดียวกันที่มีผลึกขนาดเล็กกว่าจะต่ำกว่า และเมื่อเปรียบเทียบระหว่างชนิดของซีโอไลต์พบว่าซีโอไลต์ H-ZSM-5 มีอัตราการเสื่อมสภาพต่ำกว่า H-Beta นอกจากนั้นพบว่าอัตราการแตกตัวของพอลิเอทิลีนเกิดขึ้นเร็วภายในระยะเวลา 15 นาที และเมื่อใช้ก๊าซตัวพาเป็นไฮโดรเจนจะเกิดกากคาร์บอน (Coke formation) บนตัวเร่งปฏิกิริยาซีโอไลต์น้อยกว่าเมื่อใช้ก๊าซตัวพาเป็นฮีเลียม

สำหรับกระบวนการแบบต่อเนื่องปฏิกิริยาการแตกตัวถูกทดสอบในชุดปฏิกรณ์ที่ออกแบบและจัดสร้างขึ้นเพื่อใช้สำหรับป้อนสารและแยกตัวเร่งปฏิกิริยาที่ใช้แล้วกับสารประกอบแว็กซ์ออก ชุดปฏิกรณ์ประกอบด้วย 3 ส่วนคือ ส่วนป้อนสาร ถังปฏิกรณ์ และส่วนเก็บผลิตภัณฑ์ โดยตัวเร่งปฏิกิริยาที่ใช้แล้วสามารถแยกออกจากส่วนล่างของถังปฏิกรณ์ ซึ่งจะช่วยลดปริมาณตัวเร่งปฏิกิริยาที่สะสมในถังปฏิกรณ์ทำให้สามารถนำมาปรับสภาพและหมุนเวียนตัวเร่งปฏิกิริยากลับมาใช้ใหม่ได้

การแตกตัวในกระบวนการแบบต่อเนื่องได้ทำการศึกษาที่อุณหภูมิ 350-430 องศาเซลเซียส ภายใต้บรรยากาศก๊าซฮีเลียม อัตราการป้อนพอลิเอทิลีน 90 กรัมต่อชั่วโมง จากการทดลองโดยป้อนสารที่มีอัตราส่วนของซีโอไลต์ชนิด H-Beta ต่อพอลิเอทิลีน 5 เปอร์เซ็นต์โดยน้ำหนักที่อุณหภูมิ 375 ถึง 430 องศาเซลเซียส พบว่าจะได้ผลิตภัณฑ์ที่เป็นของเหลว 45-65 เปอร์เซ็นต์ และผลิตภัณฑ์ที่เป็นก๊าซ 30-40 เปอร์เซ็นต์ ส่วนที่อุณหภูมิ 350 องศาเซลเซียสไม่เกิดปฏิกิริยาการแตกตัวขึ้น เมื่อใช้อัตราส่วนของ H-Beta 2 เปอร์เซ็นต์โดยน้ำหนัก จะเกิดผลิตภัณฑ์ที่เป็นของเหลวลดลง จากการวิเคราะห์ผลิตภัณฑ์ด้วยเทคนิคนิวเคลียร์แมกเนติกเรโซแนนซ์ (NMR) พบว่าผลิตภัณฑ์ของเหลวที่มีน้ำหนักโมเลกุลต่ำ (LCL) มีค่าออกเทนประมาณ 110-140 และมีองค์ประกอบของไอโซพาราฟินและโอเลฟินมาก ส่วนอะโรเมติกน้อย ผลิตภัณฑ์ของเหลวที่มีน้ำหนักโมเลกุลสูง (HCL) มีปริมาณอะโรเมติกสูงกว่า LCL ในขณะที่ปริมาณของโอเลฟินและไอโซพาราฟินต่ำกว่า เมื่อเพิ่มอุณหภูมิและอัตราส่วนของซีโอไลต์ในการทำปฏิกิริยาจะได้อะโรเมติกมากขึ้นและโอเลฟินลดลง

Thesis Title	Synthetic Fuels from Cracking of Polyethylene using Zeolite Catalysts in Batch and Continuous Processes
Student	Mr. Chaiwat Tachakritikul
Student ID.	41065112
Degree	Master of Science
Programme	Petrochemicals and Hydrocarbon Chemistry
Year	2001
Thesis Advisor	Assist. Prof. Dr. Tawan Sooknoi

ABSTRACT

In this thesis, design and construction of a catalytic reactor for continuous cracking of polyethylene were studied and compared with a batch process using zeolite H-ZSM-5 and H-Beta as catalysts. The effect of catalyst/polymer ratio was primarily investigated using TGA. It was found that suitable ratio was 20 % (w/w). The effect of pore size of zeolites, catalyst deactivation, residence time and carrier gas were investigated in the batch process. The experiments were carried out at 430°C for 15 and 30 minutes residence time, using hydrogen and helium as a carrier gas at flow rate of 100 ml/min. Cracking reaction catalyzed by the medium pore zeolite H-ZSM-5 produced higher yield of gas. In contrast, the large pore zeolite H-Beta produced higher yield of liquid. It was suggested that product distribution can be controlled by pore size of the catalyst. When the catalysts were reused without regeneration, the extent of the decline in the degradation rate was found to be lower for zeolite H-ZSM-5 as compared to zeolite H-Beta and for small crystal as compared in the same zeolites. In addition, catalysis using hydrogen as carrier gas showed a possibility to reduce coke formation, when compared with that of helium. The rate of cracking was so fast within 15 minutes residence time.

For continuous process, the cracking reaction was tested in the reactor that was particularly designed and constructed for continuous feeding and for removal of the used catalysts and heavy residues. The reactor consists of 3 parts; the feeder, the reactor chamber and the product collector. Used catalysts can be separated from the bottom of the reactor chamber. This would reduce catalyst accumulation in the reactor and facilitates recycle and regeneration of the used catalysts. In the continuous process, the effect of temperature and the catalyst/polymer ratio were also investigated. The experiment was carried out at 350-430°C using helium as a carrier

gas. Polyethylene was fed by the extruder at a rate of 90 g/hr. Compared with thermal degradation, the 5% H-Beta/polyethylene (w/w) feed was cracked at temperature range of 375-430^{o}C, successively producing 45-65% liquid product and 30-35% gas product. However, no catalytic activity was significantly observed from the reaction at 350^{o}C. The reaction using 5% catalyst produced higher amounts of liquid products than that using 2% catalyst. From NMR results, the light cracked liquid products (LCL) possessed an estimate octane number about 110-140 and contained a large amount of isoparaffins and olefins, with a small amount of aromatics. For the heavy cracked liquid products (HCL), the amount of aromatics was higher than LCL, while the amount of olefins and isoparaffins were lower. When the reaction temperature was increased, more aromatics were produced, whereas the yields of the olefins decreased.

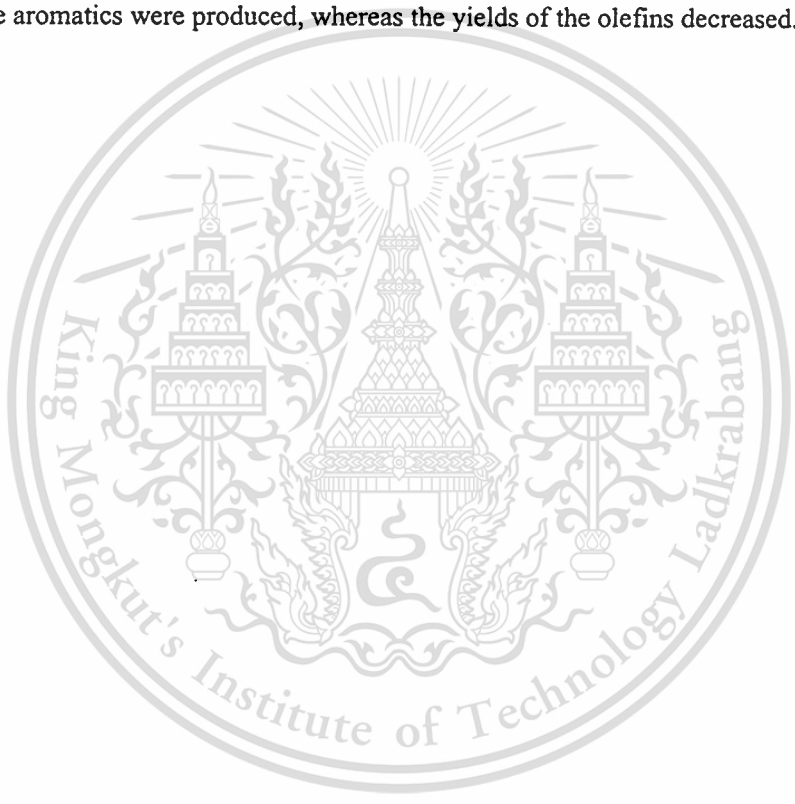

ACKNOWLEDGEMENTS

The author would like to thank and express his profound gratitude to his advisor, Assist. Prof. Dr. Tawan Sooknoi for encouraging guidance, advice, discussion and helpful suggestions throughout this thesis. He is also grateful to Assist. Prof. Dr. Metta Chareonpanich, Assist. Prof. Dr. Ittipol Jangchud and Dr. Chonlada Ritvirulh for serving as the chairperson and the committees, and their valuable comments.

Special thanks are also due to National Energy Policy Office of Thailand for financial support. He also appreciates the supports from the Department of Chemistry, Faculty of Science, King Mongkut's Institute of Technology Ladkrabang for the equipment, chemicals and facilities.

The author would like to extend his sincere appreciation to all of his teachers, and his friends for their support and encouragement.

Finally, the author dedicates his work to his above parents, brothers and sister for their moral support.

Chaiwat Tachakritikul

CONTENTS

CONTENTS (CONTINUED)

CONTENTS (CONTINUED)

CONTENTS (CONTINUED)

LIST OF TABLES

LIST OF TABLES (CONTINUED)

LIST OF TABLES (CONTINUED)

LIST OF FIGURES

LIST OF FIGURES (CONTINUED)

Figure **Page**

LIST OF FIGURES (CONTINUED)

LIST OF FIGURES (CONTINUED)

LIST OF ABBREVIATIONS

FID	Flame Ionization Detector
GC	Gas Chromatograph
HCL	Heavy Cracked Liquid Products
H-Beta (S)	Zeolite H-Beta (synthesis)
H-Beta (C)	Zeolite H-Beta (commercial)
H-ZSM-5 (S)	Zeolite H-ZSM-5 (synthesis)
H-ZSM-5 (C)	Zeolite H-ZSM-5 (commercial)
LCL	Light Cracked Liquid Products
MFI	Melt Flow Index
NMR	Nuclear Magnetic Resonance
PE	Polyethylene
SEM	Scanning Electron Microscope
TEAOH	Tetraethylammonium hydroxide
TGA	Thermogravimetric Analyzer
TPABr	Tetrapropylammonium bromide
UV	UV-Vis Spectrophotometer
XRD	X-ray Powder Diffractometer

CHAPTER 1

INTRODUCTION

1.1 Statement and significance of the problems

At present, plastics have been used worldwide due to their numerous advantages such as high strength, low weight, etc. However, used plastics are difficult to degrade biologically which causes environmental problems regarding to waste treatment. The disposal of waste polymers becomes a difficult social problem due to the above reason. Most waste polymers are disposed of by landfilling or incineration but soil contamination and air pollution make it necessary to find more effective disposal methods. Furthermore, landfilling and incineration are inefficient uses of resources since there is no attempt to recover any of the residual value of used products. Therefore, several alternatives have been considered. In particular, recycling of plastic wastes is one of the alternative ways which is currently an environmental requirement. Since waste polymers can be converted to a mixture of lower hydrocarbons which can be effectively used as fuels, the degradation of waste polymers is a promising method of tertiary recycling. However, based on the current price of fuels, the costs of tertiary plastic waste recycling methods cannot presently be recovered. Nevertheless, future increases in landfilling costs coupled with lower collecting and sorting costs may make tertiary plastic waste recycling economically viable in the future.

There are numerous papers reporting the effect of the operating conditions on catalytic processes using adiabatic batch and fixed-bed reactors. However, the literature available involving the catalytic cracking of polyethylene in a continuous process is rather scarce. Therefore, new development of waste polymer cracking processes will require models of reactor system which can be used for solving environmental problem and further development in industrial level. In addition, this would help reduce plastic waste and recycle them for energy compensation.

1.2 Goal and objectives

The ultimate objective of this thesis is to study the cracking of polyethylene in a continuous process, particularly on development and design of a reactor. The specific objectives are as follows:

1. To obtain a designed reactor which can produce fuels from polyethylene
2. To obtain suitable conditions for fuel production from polyethylene cracking in continuous process
3. To reduce the environmental problem occurred from plastic waste by efficient utilization
4. To obtain an alternative approach for energy compensation

1.3 Scopes of the study

The scopes of the study on catalytic cracking of polyethylene in batch and continuous processes are as follows:

1. Synthesis of zeolite ZSM-5 and Beta (for batch process)
2. Characterization of zeolites
3. Study of the appropriate catalyst/polymer ratio for cracking of polyethylene in batch process
4. Study on cracking of polyethylene in batch process
5. Design and construct reactor for cracking of polyethylene in continuous process
6. Study on catalytic cracking of polyethylene by continuous process using designed reactor
7. Analyse products from the reaction

1.4 Expected results

1. This research would produce fuels from degradation of polyethylene.
2. This research would reduce the problem according to conventional process.
3. The reactor can be used as a model for further development for large scale cracking systems.
4. This process can be applied for energy conservation.

CHAPTER 2

LITERATURE REVIEWS AND THEORY

2.1 Zeolites

Zeolites are natural or synthetic microporous, crystalline aluminosilicates. They have been widely used as ion exchangers, sorbents, molecular sieve, and catalysts in industrial processes. Most zeolites are synthesized from a slurry containing a silica source (e.g. sodium silicate), an alumina source (e.g. sodium aluminate), and caustic [1]. Other compounds, such as organic templates, may also be present during synthesis. The synthesized zeolite is modified by ionic exchange and thermal or chemical treatment in order to obtain an active catalyst.

The word 'Zeolite' has Greek roots and means 'boiling stones', an allusion to the visible loss of water noted when the natural zeolites are heated. This property, of course, illustrates their easy water loss and is described as 'intumescence' [2].

2.1.1 Zeolite ZSM-5 [1, 3-7]

Zeolite ZSM-5 is medium-pore zeolite used in some dewaxing catalysts. This zeolite is a member of the "pentasil" family of high-silica zeolite whose structure is characterized by two types of intersecting channels with 10-membered ring openings (Figure 2.1). One channel system is sinusoidal and has near-circular (0.54×0.56 nm) openings. The other channel is straight and has elliptical (0.51×0.57 nm) openings. The channel intersections have a diameter of about 0.9 nm and are probably the locus of strong acid sites and of catalytic activity. This zeolite has been synthesized with silica-to-alumina ratios varying from about 20 to 8000.

The ZSM-5 has a low aluminium content and consequently few cations are present in crystallographic sites. Similarly their water contents are low. Their frameworks have hydrophobic tendencies, in sharp contrast to the normally highly hydrophilic character of most other known zeolites. In the hydrogen form, zeolite ZSM-5 has Brønsted and Lewis acidity, with acidic OH groups located at the channel intersections. The presence of acidic sites explains the cracking activity of the zeolite. The concentration of strong acid sites is proportional to the concentration of framework aluminum. Steaming results in framework dealumination and a decrease in Brønsted acidity.

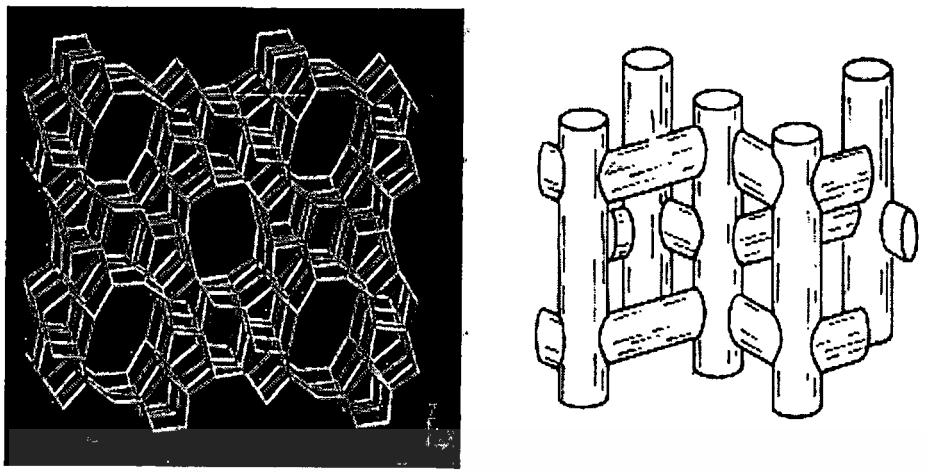

(a) (b)

Figure 2.1 Representation of three-dimensional structure of ZSM-5 [7]

(a) Structure formed by stacking of sequences of layers (010)

(b) Schematic representation of the intracrystalline pore structure

Zeolite ZSM-5 shows unique shape-selective properties due to the presence of medium-size pores. These properties play a key role in their uses as dewaxing catalysts. Zeolite pore geometry and diffusion limitations are often the controlling factors that determine the catalytic activity and selectivity. Shape selectivity controls the size and shape of molecules diffusing into and out of the zeolite pore network. In catalytic dewaxing with ZSM-5-based catalysts, only normal and lightly branched paraffins (e.g. with one CH_3 branch) diffuse into the zeolite pores, where they are cracked. Isoparaffins with longer or multiple branches remain practically unaffected. Such selective cracking results in a product with improved properties. Shape-selective hydrocracking of n-paraffins takes place also over catalysts containing other medium-pore size zeolites, such as offretite or erionite.

2.1.2 Zeolite Beta [8-10]

The zeolite Beta has three-dimensional interconnecting channel system with 12-membered ring pore opening (Figure 2.2). It can be crystallized in wide range of silica to alumina ratio, $10 < SiO_2/Al_2O_3 < 200$, but the efficiency of crystallization is lower when it crystallizes at silica to alumina ratio lower than 19 (6 aluminium atoms per 1 unitcell). Zeolite Beta, like many other molecular sieve zeolites, is synthesized by the hydrothermal digestion of a reaction mixture comprising silica, alumina, an alkaline earth metal and an organic templating agent. The organic

agent acts as a template in the nucleating and growth of the zeolite Beta crystal. Once the crystals are formed, it is conventional practice to carry out a calcination treatment in order to remove the organic material from the interstitial channels of the molecular sieve network.

Zeolite Beta is a crystalline aluminosilicate molecular sieve zeolite which finds applications in a number of industrial processes including as a catalyst in various hydrocarbon conversion reactions such as hydrocracking, hydroisomerization and dewaxing. In addition, it can be used in alkylation process. Alkylation process employing zeolite Beta which is said to be especially useful in the production of ethylbenzene from benzene and ethylene and production of cumene from benzene and propylene. Moreover, it may often be desirable to incorporate a metal component into the zeolite Beta. Suitable metal components include those found in groups VIB and VIII of the periodic table. Specific metals include chromium, molybdenum, tungsten, vanadium, iron, cobalt, nickel, copper, platinum and palladium.

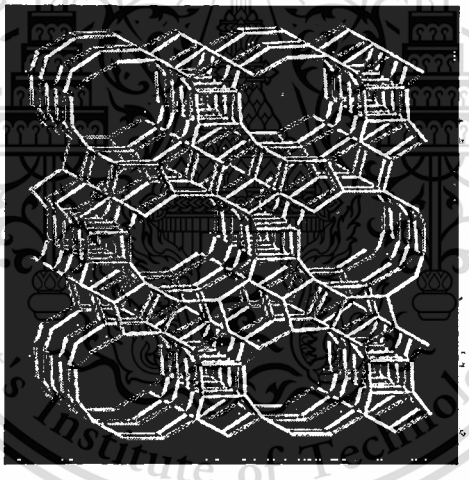

Figure 2.2 Structure formed by stacking of sequences of layers (100)

2.2 Catalysis by zeolites

Zeolites are catalysts which offer advantages of high densities of catalytic active sites combined with stability at high temperatures. The latter is an advantage characterizing many inorganic solids and accounts for their wide applications as industrial catalysts. The industrial applications of zeolites involve acid-catalyzed reactions. Almost the reactions catalyzed by acids in solutions and in polymer matrices can be catalyzed by zeolites incorporating acidic groups. This generalization is based on experimental evidence for hundreds of catalytic reactions. The

exceptions involve the fact that reactants are too large to enter the zeolite pores and products are too large to form in, or leave, the pores.

The major commercial processes using zeolite catalysts are listed in Table 2.1. Reviewing zeolite catalyst literature and patents suggest that other areas of the globe may make use of natural clinoptilolites and mordenites in their oil and chemical industries.

Table 2.1 Commercial processes using zeolite catalysts [2]

Process	**Catalysts**	**Advantage in using zeolite-based catalysts**
Catalytic cracking	REY (REX, REHY, REMgY, HY)	Selectivity and high conversion rates
Hydrocracking	X, Y, mordenite, erionite loaded with Co, Mo, W, Ni, also HY, US-Y, Ca MgY and H-ZSM-5	High conversion rates
Selectoforming	Ni erionite, clinoptilolite	Increase in octane number via LPG production
Hydroisomerization	Pt mordenite	Converts low octane, pentane and hexane feeds to higher octane yields
Dewaxing	Pt mordenite, ZSM-5	Improved pour points
Benzene Alkylation	ZSM-5	Ethylbenzene and styrene production with low by-product yield
Xylene isomerization	ZSM-5	Increase in p-xylene yield with low by-product yield
Methanol to gasoline conversion	ZSM-5	High gasoline yield with high octane rating
No_x reduction	H-mordenite	Effluent clean-up in nitric acid and nuclear reprocessing plants

2.3 Cracking reaction

Cracking is the process for decomposition of high molecular weight materials which are converted to lower molecular weight products at elevated temperatures. Cracking reactions

involve carbon-carbon bond cleavage and are thermodynamically favored at high temperatures [11]. Cracking is affected by one of three general methods, i.e., thermal cracking, catalytic cracking, or hydrocracking.

2.3.1 Thermal cracking

One of the earliest processes used in petroleum, after distillation, is the noncatalytic conversion of higher boiling point petroleum stocks into lower boiling point products, known as thermal cracking. Thermal cracking is a free radical chain reaction and does not produce any degree of branching in the products other than that already present in the feedstock [12]. However, certain products may interact with one another to produce higher molecular weight products than that in the original feedstock.

Two general types of reactions occur during cracking are:

1. The decomposition of large molecules into small molecules (primary reactions):

2. Reactions by which some of the primary products interact to form higher molecular weight materials (secondary reactions):

Free radicals are very reactive. A free radical reacts with a hydrocarbon by abstracting a hydrogen atom to produce a stable end product and a new free radical:

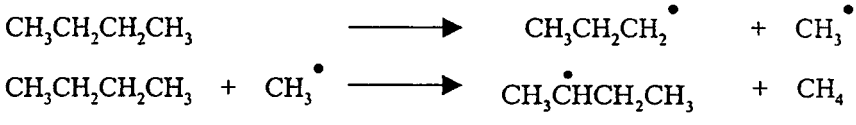

Other reactions, such as

One of the significant features of hydrocarbon free radicals is their resistance to isomerization, for example, migration of an alkyl group:

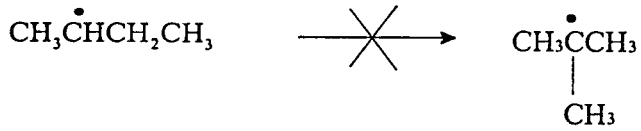

An increase in pressure inhibits the formation of low molecular weight gaseous products and therefore promotes the formation of higher molecular weight materials [13].

2.3.2 Catalytic cracking

Catalytic cracking is simply the thermal decomposition of hydrocarbons in the presence of a catalyst. Thermal cracking has essentially been replaced by catalytic cracking as the process for gasoline manufacture. Catalytic cracking produces more gasoline of higher octane than thermal cracking because gasoline produced by catalytic cracking is richer in branched paraffins, cycloparaffins, and aromatics [14]. This is due to the effect of the catalyst, which promotes isomerization and dehydrocyclization reactions. Catalytic cracking also results in the production of the maximum amount of C_4 hydrocarbons (butanes and butenes) rather than C_2 hydrocarbons (ethane and ethylene).

In general, catalytic cracking may be regarded as the modern method for converting high boiling point petroleum fractions, such as gas oil, into high quality gasoline and other low boiling point fractions. Thus, catalytic cracking in the usual commercial process involves contacting a gas oil fraction with an active catalyst under suitable conditions of temperature, pressure, and residence time, so that a substantial part (>50%) of the gas oil is converted into gasoline and lower boiling products, usually in a single-pass operation.

However, during the cracking reaction, carbonaceous material is deposited on the catalyst, which markedly reduces its activity, and removal of the deposit is extremely necessary. This is usually accomplished by burning the deactivated catalyst in the presence of air until the catalyst activity is reestablished [1].

A major difference between thermal and catalytic cracking is that reactions through catalytic cracking occur via carbonium ion intermediate, compared to the free radical intermediate in thermal cracking. Carbonium ions are longer lived and accordingly more selective than free radicals [15-16]. Moreover, the degradation products are distributed in a narrow range of carbon

number compared with those obtained by thermal degradation. The acid catalysts first used in catalytic cracking were amorphous solids composed of approximately 87% silica (SiO_2) and 13% alumina (Al_2O_3) and were designated to low-alumina catalysts. On the other hand, high-alumina catalysts contain 25% alumina and 75% silica [11]. However, this type of catalyst is now being replaced by crystalline aluminosilicates (zeolites) or molecular sieves. The following illustrates the different ways by which carbonium ions may be generated by:

1. Abstraction of a hydride ion (H^-) by a Lewis acid site from a hydrocarbon:

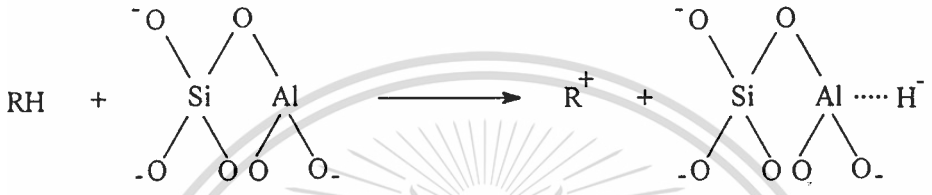

2. Reaction between a Brønsted acid site (H^+) and an olefin:

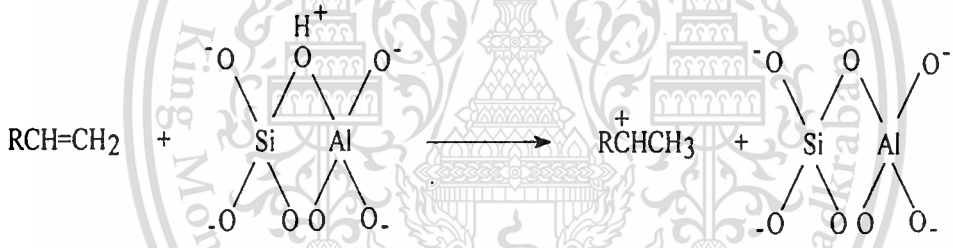

3. Reaction of the carbonium ion formed, from step 1 or 2, with another hydrocarbon by abstraction of a hydride ion:

Abstraction of a hydride ion from a tertiary carbon is easier than from a secondary, which is easier than from a primary position. The formed carbonium ion can rearrange through a methide-hydride shift similar to catalytic reforming. This isomerization reaction is responsible for a high ratio of branched isomers in the products.

The most important cracking reaction, however, is the carbon-carbon beta bond scission. A bond at a position beta to the positively-charged carbon breaks heterolytically, yielding an olefin and another carbonium ion. This can be represented by the following example:

The new carbonium ion may experience another beta scission, rearrange to a more stable carbonium ion, or react with a hydrocarbon molecule in the mixture and produce a paraffin. However, carbonium ions are not formed by cleavage of a carbon-carbon bond:

$$RCH_2CH_2R \longrightarrow RCH_2^+ + RCH_2^- \qquad 260 \text{ kcal/mol}$$

but

$$RCH_2CH_2R \longrightarrow 2RCH_2^{\bullet} \qquad 76 \text{ kcal/mol}$$

In essence, the use of a catalyst permits alternate routes for cracking reactions, usually by lowering the free energy of activation for the reaction [14].

2.3.3 Hydrocracking

Hydrocracking is essentially catalytic cracking in the presence of hydrogen. Relatively high pressures of hydrogen (100-2000 psi) are employed [2], and the overall result is usually a change in the character or quality of the products. It produces less olefinic hydrocarbons whatsoever as the added hydrogen traps the intermediate species to yield saturated products. Such processes are generally expensive because of the considerable amount of hydrogen used and the high operating pressure. The bifunctional catalysts used in hydrocracking provide high surface area cracking sites and hydrogenation-dehydrogenation sites. The cracking function is provided by an acidic support, whereas the hydrogenation-dehydrogenation function is provided by metals. The acidic support consists of (a) amorphous oxides (e.g. silica-alumina), (b) crystalline zeolite (mostly modified zeolite Y) plus a binder (e.g. alumina), or (c) a mixture of crystalline zeolite and amorphous oxides. Cracking and isomerization reactions take place on the acidic support [17]. Catalysts with strong acidic activity promote isomerization, leading to a high iso/normal ratios. The metals providing the hydrogenation-dehydrogenation function can be noble metals (palladium and platinum), or nonnoble metal sulfides from group VIA (molybdenum and tungsten) and group VIIIA (cobalt and nickel) [1]. These metals catalyze the hydrogenation of the feedstock, making it more reactive for cracking and heteroatom removal, as well as reducing the coking rate. The metals also initiate the cracking by forming a reactive olefin intermediate via dehydrogenation.

The main hydrocracking reaction could be illustrated by the first step formation of a carbonium ion over the catalyst surface:

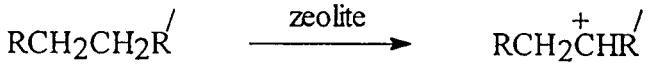

The carbonium ion may rearrange, eliminate a proton to produce an olefin, or crack at a beta (β) position to yield an olefin and new carbonium ion. Under the atmosphere of hydrogen and in the presence of a catalyst with hydrogenation-dehydrogenation activity, the olefins are hydrogenated to paraffinic compounds. This reaction sequence could be represented as follows:

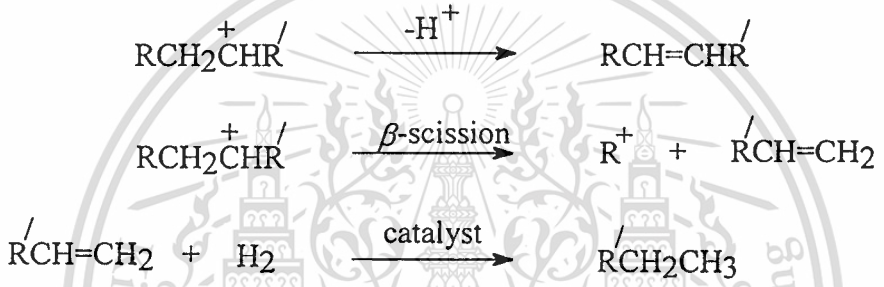

As anticipated, most products from hydrocracking are saturated. For this reason, gasolines from hydrocracking units have lower octane ratings than those produced by catalytic cracking units since they have a lower aromatic content due to the high hydrogenation activity. Products from hydrocracking units are suitable for jet fuel use. Hydrocracking also produces light hydrocarbon gases (LPG) suitable as petrochemical feedstocks.

Other reactions which take place during hydrocracking are the fragmentation followed by hydrogenation (hydrogenolysis) of the complex asphaltenes and heterocyclic compounds normally present in the feeds [14]. The following is a representative example of hydrocracking of a substituted anthracene.

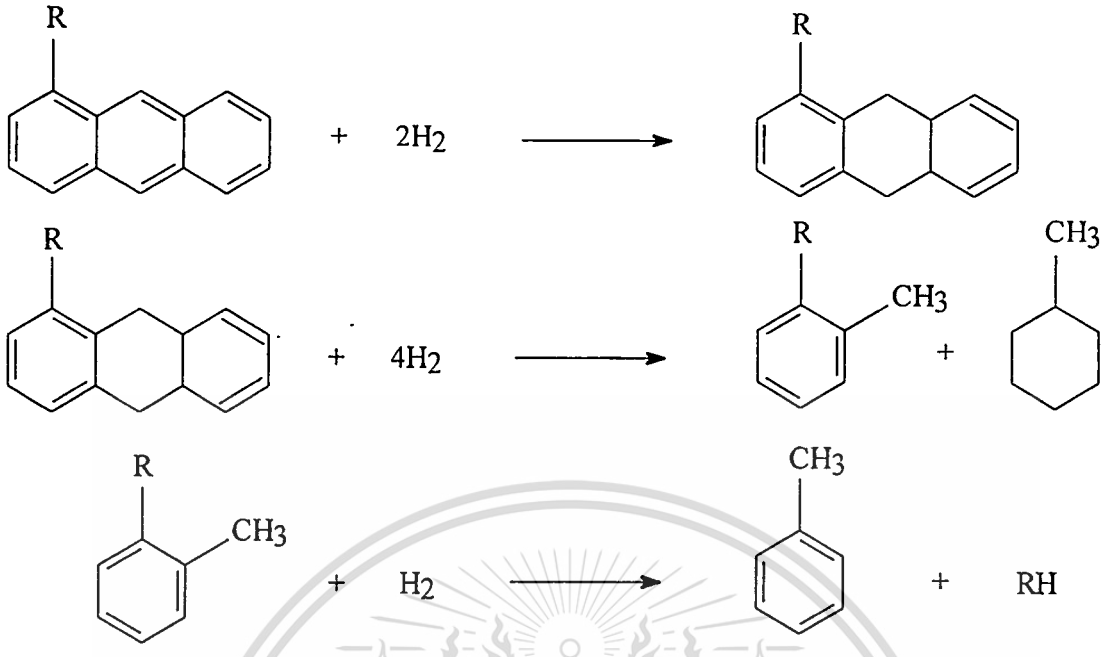

It should be noted, however, that this reaction sequence may be different from what may actually be occurred in the reactor. The reactions proceed at different rates depending on the process variables. Hydrodesulfurization of complex sulfur compounds such as dibenzothiophene also occurs under these conditions. The desulfurized product may crack to give two benzene molecules:

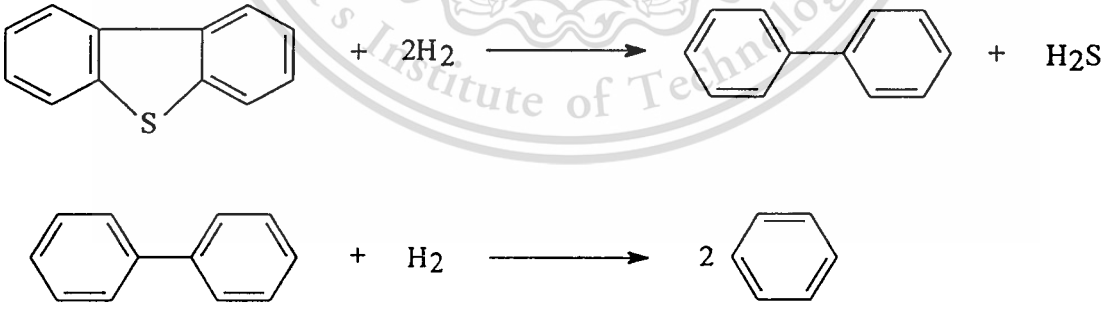

2.4 Polyethylene (PE)

2.4.1 History of polyethylene

The study of polyethylene begins most conveniently with low density polyethylene (LDPE), the most general and fundamental model for organic polymer structures. The simple chemical composition, derived directly from very low-cost petrochemical sources, provides a

polymer whose low price may be its most important property in the tremendous markets where other properties are relatively unimportant.

The original ICI process for polymerizing ethylene was developed in the 1940s and produces low density polyethylene (LDPE) with a density in the range of 910 to 935 kgm^{-3}. It involves compressing ethylene to very high pressures (1400 to 2400 bar) and polymerizing it at a high temperature (200 to 250°C) using free radical catalysts [18]. There are both short and long chain branches on the molecules because of side reactions in the process. If the polymerization pressure is increased, the molecular mass increases and the number of branches decreases.

From 1955 onwards a number of processes for producing high density polyethylene (HDPE), with densities in the range of 955-970 kgm^{-3}, were introduced. These used organometallic catalysts which allowed polymerization at low to medium pressures of 1 to 200 bar. There are less side reactions and hence fewer short chain branching (0.5 to 1% of the C atoms) and no long chain branching. Catalysts used for HDPE production are either of the Zieglar-type (a complex of $Al(C_2H_5)_3$ and α-$TiCl_4$) or silica-alumina impregnated with a metal oxide such as chromium oxide or molybdenum oxide.

Reaction conditions are generally mild, but they differ from one process to another. In a newer Unipol process used to produce both HDPE and LLDPE, the reaction occurs in the gas phase. Ethylene and the comononers (propene, 1-butene, etc.) are fed to the reactor containing a fluidized bed of growing polymer particles. Operation temperature and pressure are approximately 100°C and 20 atmospheres. A single-stage centrifugal compressor circulates unreacted ethylene. The circulated gas fluidizes the bed and removes some of the exothermic reaction heat. The product from the reactor is mixed with additives and then pelletized. New modifications for gas-phase processes have been reviewed by Sinclair [19].

The polymerization of ethylene can also occur in a liquid-phase system where a hydrocarbon diluent is added. This requires a hydrocarbon recovery system.

2.4.2 Properties and uses of polyethylene

The most important structural feature of HDPE is the balance between (a) its high crystallinity and (b) its lack of polarity or any other type of intermolecular bonding [20]. Thus, the polymer can be melted sharply at a moderate temperature, providing easy processing by many techniques. Crystallinity gives the solid polymer reasonably good rigidity and strength, while

weakness of any other intermolecular bonds still makes it somewhat softer and weaker than more polar or sterically hindered structures. The heat deflection temperature is reasonable but not high. Crystalline growth into spherulites can produce translucency and opacity, unless they are kept small by quenching or stretching during processing. Crystallinity produces high solvent resistance; but rigidity accentuates the danger of stress-cracking, unless a little comonomer is used to soften and flexibilize the structure somewhat.

The flexibility of the polyethylene molecule is potentially an important feature of polymer structure, but its effect on solid properties is masked into insignificance by packing it into the highly-ordered crystalline lattice. In the molten state during processing, on the other hand, molecular flexibility plays an important role in providing the easy processing which, along with low price, makes polyethylene the optimum material for many major applications.

HDPE is characterized by a higher crystallinity and higher melting temperature than LDPE due to the absence of branching. Some branching could be incorporated in the backbone of the polymer by adding variable amounts of comononers such as hexene. These comononers modify the properties of HDPE for specific applications.

Polyethylene is an inexpensive thermoplastic which can be molded into almost any shape, extruded into fiber or filament, and blown or precipitated into film or foil. The production of bottles and other containers by blow molding accounts for about 40% of the HDPE made [21]. The adjustment of structure variables to obtain high resistance to environmental stress cracking, allowing the material to be used in detergent bottles, produced a large expansion in this field. About 25% of the HDPE produced is used in the injection molding of crates, pails, tubs, caps and closures, and housewares. The higher stiffness and heat resistance of the HDPE have led to its replacement of LDPE in applications where these properties are important.

2.5 Literature reviews

In recent years, the production and consumption of plastics have increased drastically. As a consequence, the responsible disposal of plastic wastes has created serious social and environmental arguments. Consecutively, there has been a growing interest in plastics recycling as well as their potential for using as resources. The simplest option, incinerating plastics for energy recovery, is viewed adversely by the public and is an unattractive approach. A secondary recycling, mechanical recycling, in which mixed plastics are ground, remelted, and then shaped

into new products, results in a loss of material strength from degradation during heating. The next method is feedstock production or tertiary recycling. The polymers can be broken down into their corresponding monomers or into petrochemicals and fuels. In contrast to the materials produced by mechanical recycling, products made from these low molecular weight chemicals are not limited in their applicability.

Therefore, the thermal and catalytic cracking of polymers have become an increasingly important method for the conversion of waste plastics into valuable chemicals and fuel oil. Numerous papers have reported about thermal cracking but these processes required high temperatures, typically higher than 500°C [22-29]. In addition, the thermal cracking of polyolefins produces many kinds of components with broadly comparable yields [23, 26-29]. Consequently, many workers effort to reduce the reaction temperature using catalysts. Catalysts have been chosen such as silica-alumina, Fe_2O_3/SO_4^{2-}, ZrO_2/SO_4^{2-}, Al_2O_3/SO_4^{2-}, and $TiCl_3$ [28-33]. In contrast, these catalysts give broad product distribution. A suitable catalyst, zeolite, has the ability to control both the product yield and product distribution from polymer cracking as well as to significantly reduce the reaction temperature, potentially leading to a cheaper process with more valuable products. Most zeolites are used as cracking catalysts such as Y, EMT, Mordenite and ZSM-5 [29-30, 32-40]. Zeolites have both channel and cage structures. Zeolites with channel structures which allow low deactivation rate are preferable [38, 41-42].

However, most of the previous reports on the thermal and catalytic cracking of plastics have focused on the effect of the operating conditions, particularly in the batch process. This causes the problem of catalyst deactivation due to the fact that the used catalysts are unable to be separated and regenerated consecutively. In addition, numerous paper studying the catalytic process using fixed-bed and fluidized-bed reactors are dealing with experimental parameters including temperature, contact time, conversion and product distribution [35, 38-39, 43-45]. Meanwhile, the continuous process where catalysts can be separated and regenerated are rather scarce.

2.6 Overview of this thesis

This thesis was focused on the investigation of the cracking of polyethylene using continuous process, compared with batch process. Zeolite Beta and ZSM-5 which possess channel structure are chosen in this thesis due to their low deactivation rates. Consequently, this

would reduce the amount of catalyst employed. The synthesized zeolites and commercial zeolites were characterized using conventional techniques which were shown in section 4.1. Thermogravimetric analysis (TGA) was used to investigate the effect of catalyst/polymer ratio and time-dependent activity of the catalyst as discussed in section 4.2. For batch process, the effects of zeolite pore sizes, catalyst deactivation, residence time, and carrier gas were discussed on the product yield and product distribution (section 4.3). For continuous process, the cracking reaction was tested in a reactor which was particularly designed and constructed for continuous feed and for removal of the used catalysts and heavy residues. The reactor system consists of 3 parts; the extruder (feeder), the reactor chamber, and the product collector. Details of each part used in the cracking study, were mentioned in section 4.4.1. The effects of reaction temperature and catalyst/polymer ratio were investigated on the product yield and product distribution (section 4.4.2.2-4.4.2.3). Time on stream was also focused on product yield as a function of temperature, catalyst/polymer ratio (section 4.4.2.1-4.4.2.3). In addition, the product types and octane number were also mentioned to determine the product quality (section 4.4.3).

CHAPTER 3

EXPERIMENTAL DETAILS

3.1 Reagents

1. Acetic acid (Mallinckrodt)
2. Air zero (TIG)
3. Aluminium nitrate (Fluka Chemika)
4. 1-Amino-2naphthol-4-sulphonic acid (Carlo Erba Reagenti)
5. Ammonium acetate (Merck)
6. Ammonium chloride (Merck)
7. Ammonium hydroxide solution (Baker Analyzed)
8. Ammonium molybdate (Fluka Chemika)
9. Ammonium nitrate (Fluka Chemika)
10. Chloroform (Carlo Erba Reagenti)
11. Distilled water
12. Gasoline fuel, octane 91 and 95 (PTT)
13. Helium gas (TIG)
14. Hydrochloric acid (Merck)
15. Hydrogen gas (TIG)
16. 8-Hydroxyquinoline (Merck)
17. Isooctane (Carlo Erba Reagenti)
18. Liquid nitrogen (TIG)
19. Liquefied petroleum gas (Siam Gas)
20. Ludox (suspension silica, 40% SiO_2 by weight) (Aldrich)
21. Nitrogen gas (TIG)
22. *n*-Heptane (Carlo Erba Reagenti)
23. *n*-Hexane (Mallinckrodt)
24. *n*-Nonane (Merck)
25. *n*-Pentane (Carlo Erba Reagenti)
26. Polyethylene (Melt flow index, MFI = 15 g/10min, pellet form, TPI)

27. Polyethylene (Melt flow index, MFI = 45 g/10min, powder form, TPI)
28. Silicic acid (Fluka Chemika)
29. Sodium aluminate (Rideal-de Haen)
30. Sodium hydrogen sulphite (Merck)
31. Sodium hydroxide (Carlo Erba Reagenti)
32. Sodium tetraborate (Merck)
33. Sulfuric acid (Mallinckrodt)
34. Tartaric acid (Merck)
35. Tetraethylammonium hydroxide (Fluka Chemika)
36. Tetrapropylammonium bromide (Fluka Chemika)
37. Zeolite ZSM-5 (Star Petroleum Refining Company)
38. Zeolite Beta (Tosoh Corporation)

3.2 Apparatus

1. Autoclave
2. Beaker
3. Buchner flask
4. Buchner funnel
5. Bunsen burner
6. Burett
7. Condenser
8. Furnace
9. Gas Adsorption Analyzer (Autosorb-1, Quantachrome)
10. Gas Chromatograph (3800 Gas Chromatograph, Varian)
11. Gas Chromatograph (910 Gas Chromatograph, Buck Scientific)
12. Heating mantle
13. Heating tape
14. Hotplate
15. Magnetic stirrer
16. Mechanical motor
17. Nickel crucible

18. Nuclear Magnetic Resonance Spectrometer (AVANCE DPX300, Bruker)
19. Oven
20. pH meter
21. Pipette
22. Scanning Electron Microscope (Scanning Microscope 6400, Joel)
23. Separatory funnel
24. Thermogravimetric Analyzer (TGA51, Dupont 9000)
25. UV-Vis Spectrophotometer (UV)
26. Vial
27. Volumetric flask
28. Water circulator
29. X-ray Powder Diffractometer (D8 Advance, Bruker)

3.3 Experimental procedure

3.3.1 Synthesis and modification of catalysts

1. Synthesis of zeolite ZSM-5 (Si/Al ≈ 20)
2. Synthesis of zeolite Beta (Si/Al ≈ 15)
3. Modification of zeolites to acidic catalysts

3.3.2 Characterization of zeolites

1. Determination of crystal morphology using Scanning Electron Microscope (SEM)
2. Determination of zeolite structure using X-ray Powder Diffractometer (XRD)
3. Determination of surface area using Gas Adsorption Analyzer (Autosorb)
4. Determination of acidity by petentiometric titration
5. Determination of silicon/aluminium ratio using UV-Vis Spectrophotometer (UV)

3.3.3 Catalytic testing

1. Study on cracking of polyethylene using thermogravimetric Analyzer (TGA)
    1) Effect of catalyst/polymer ratio
    2) Time-dependent activity of the catalyst

2. Study on cracking of polyethylene in batch process
    1) Effect of pore size of zeolites
    2) Effect of catalyst deactivation
    3) Effect of residence time
    4) Effect of carrier gas
3. Study on cracking of polyethylene in continuous process
    1) Time on stream
    2) Effect of reaction temperature
    3) Effect of catalyst/polymer ratio

3.3.4 Analysis of products

1. Determination of product composition using Gas Chromatograph (GC)
2. Determination of composition and octane number of gasoline using Nuclear Magnetic Resonance (NMR)

3.4 Experimental details

3.4.1 Synthesis and preparation of catalysts

3.4.1.1 Zeolite ZSM-5 [46]

Zeolite ZSM-5 (S) was synthesized hydrothermally from an aluminosilicate gel with a nominal composition of $40SiO_2 : Al_2O_3 : 4Na_2O : 2TPABr : 1200H_2O$, where TPABr stands for tetrapropylammonium bromide. Firstly, 1.10 grams of sodium hydroxide anhydrous was mixed with 41.54 grams of distilled water, followed by adding 2.46 grams of tetrapropylammonium bromide under stirring for 5 minutes. After that, 0.79 grams of sodium aluminate was added and stirred. Finally, 27.79 grams of colloidal silica (Ludox®AS-40), 40% SiO_2 mixed with 41.54 grams of distilled water, were added to the mixture. This mixture was then loaded to a teflon-lined stainless-steel autoclave and crystallized at 175°C for 72 hours. The crystalline product obtained was separated, washed with distilled water, dried at 110°C overnight and activated by calcination in air at 550°C (heating rate at 2°C/min) for 3 hours. Whereas, ZSM-5 (C) was supplied by Star Petroleum Refining Company (SPRC). ZSM-5 (C) was used in the batch process and compared with ZSM-5 (S).

3.4.1.2 Zeolite Beta [47]

The zeolite Beta (S) employed in the present study were synthesized hydrothermally from an aluminosilicate gel with a nominal composition of $30SiO_2 : Al_2O_3 : 0.9Na_2O : 6TEAOH : 290H_2O$, where TEAOH stands for tetraethylammonium hydroxide. In the first step, 0.99 grams of sodium aluminate was mixed with 8.05 grams of distilled water. 14.80 grams of tetraethylammonium hydroxide was added and stirred. After that, 30.19 grams of colloidal silica (Ludox®AS-40), 40% SiO_2, was added to the gel mixture. The gel prepared by mixing individual solutions was stirred vigorously at room temperature for 45 minutes and then loaded to a teflon-lined stainless-steel autoclave. The gel was kept at 160°C under autogenous pressure without stirring for 240 hours. At the end of the crystallization period, the autoclave was quenched in water and the zeolite was filtered and dried overnight at 110°C. The sample was then calcined in air at 550°C (heating rate at 2°C/min) for 5 hours. In addition, Beta (C) (Si/Al molar ratio of 13.5) was purchased from Tosoh Corporation of Japan. This zeolite Beta (C) was used in batch process and continuous process.

3.4.1.3 Modification of zeolites to acidic catalysts

Na-zeolite was ion-exchanged three consecutive times with 1 M ammonium nitrate solution at 80°C for 3 hours. The NH_4^+- zeolite was then dried at 110°C overnight. Finally, H-form zeolite was obtained by calcination in high-purity oxygen at 450°C (heating rate at 10° C/min) for 1 hour.

3.4.2 Characterization of zeolites

3.4.2.1 Determination of crystal morphology of zeolite using Scanning Electron Microscope (SEM)

The crystal morphology and crystal size were determined by scanning electron microscope (Jeol 6400 Scanning Microscope, Chulalongkorn University Instruments Service Center). The sample was prepared by thoroughly placing zeolite onto the sample holder. It was then coated with gold thin film by ion sputtering. The sample was placed in the sample chamber of scanning electron microscope and evacuated from ambient pressure to 10^{-4} torr. The scanning electron micrographs were taken at the magnification of 5500, 8,500, 10,000 and 30,000 times.

3.4.2.2 Determination of zeolite structure using X-ray Powder Diffractometer (XRD)

The zeolite structure was determined by X-ray diffractometer (D8 Advance, Bruker, Scientific Instruments Service Center; SISC). The sample was prepared by packing the zeolite in the sample holder. CuKα X-ray beam was used for analysis at 40 kV, 40 mA. The sample were scanned from 2θ angle 5° to 60° with 1 second/step time and 0.04 2θ/step increment. X-ray diffraction pattern of sample was compared with X-ray diffraction pattern of standard zeolite for determining the structure.

3.4.2.3 Determination of surface area of zeolites using Gas Adsorption Analyzer (Autosorb)

Surface area of zeolite was determined by Gas Adsorption Analyzer (Autosorb-1, Quantachrome). The sample was prepared by weighing 1 mg of zeolite sample into the cleaned and dried sample cell. The sample cell was attached to the out gassing station. Heating mantle was installed and the temperature was raised to 350 $^{\circ}$C. The sample was out-gassed for 24 hours. The sample cell was then removed from the out gassing station after the nitrogen was filled and was attached to the analysis station. The equilibration time is set to 3 minutes and the adsorption was tested at the partial pressure (P/P_0) ranged from 10^{-6} to 1.0.

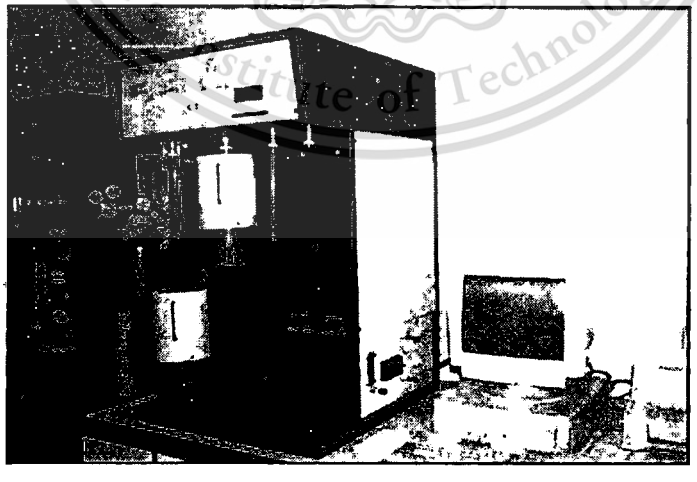

Figure 3.1 Gas Adsorption Analyzer (Autosorb-1, Quantachrome)

3.4.2.4 Determination of acidity of zeolite by potentiometric titration

1) Preparation of reagents

- **Preparation of 0.05 M sodium tetraborate solution**

Accurately weighed 1.9 grams of sodium tetraborate was dissolved with distilled water in a beaker. Then, the solution was diluted with distilled water by using 100 mL volumetric flask.

- **Preparation of 0.1 M hydrochloric acid solution**

Approximately 100 mL of distilled water was added into 250 volumetric flask. Then, 2.20 mL of concentrated hydrochloric acid was pipetted and transferred to the flask and the solution was diluted to 250 mL with distilled water.

- **Preparation of 0.05 M ammonium hydroxide solution**

Approximately 0.8 mL of 28% ammonium hydroxide solution was pipetted into 250 mL volumetric flask and this solution was diluted to 250 mL with distilled water.

2) Determination of certain HCl concentration

25 mL of 0.1 M hydrochloric acid was charged to 50 mL beaker. The solution was stirred and the pH was measured by dipping the glass electrode of a pH meter into the solution. After that, hydrochloric acid was titrated with 0.05 M sodium tetraborate solution by adding the titrant in 0.5 mL portions after each addition until pH value was constant. Titration was repeated again but volume of sodium tetraborate solution was changed from 0.5 mL to 0.2 mL toward the end point of titration. The difference in pH value, ΔpH, and the change in volume, ΔV, were calculated and plotted the ΔpH/ΔV versus the volume of added solution. Finally, the volume belonging to the equivalent point, Ve, was obtained from the volume which markedly change the pH value.

3) Determination of certain NH_4OH concentration

25 mL of 0.05 M ammonium hydroxide was charged to 50 mL beaker. The solution was stirred and the pH was measured by dipping the glass electrode of a pH meter into the solution. After that, ammonium hydroxide was titrated with hydrochloric acid by adding the titrant in 0.5 mL portions after each addition until pH value was constant. Titration was repeated again but volume of hydrochloric solution was changed from 0.5 mL to 0.2 mL toward the end point of titration. The equivalent point volume, Ve, was determined similarly to the case of hydrochloric acid.

4) Determination of acidity of zeolites by back titration technique

0.075 grams of H-zeolite was weighed into 50 mL beaker. After that, 25 mL of 0.05 M ammonium hydroxide solution and 0.1 grams of ammonium chloride were then added to the beaker. Temperature was kept at 70°C for 5 minutes. Then, the beaker was cooled to room temperature before the residual ammonium hydroxide was determined by back titration using hydrochloric acid as a titrant. The acidity of zeolite was calculated by this technique.

3.4.2.5 Determination of silicon/aluminium ratio of zeolites using UV-Vis Spectrophotometer (UV)

1) Determination of silicon [48]

- **Preparation of reagents**

  - Ammonium molybdate solution

Approximately 8.0 grams of ammonium molybdate crystals was dissolved in water. The solution was added by 9 mL of concentrated sulfuric acid, and then diluted to 100 mL with distilled water.

  - Reducing agent

Solution A was prepared by dissolving 10 grams of sodium hydrogen-sulphite in 70 mL of distilled water. Solution B was prepared by dissolving 0.8 grams of anhydrous sodium hydrogensulphite in 20 mL of distilled water, followed by adding 0.16 grams of 1-amino-2-naphthol-4-sulphonic acid. Then, the solution A and B were mixed together, and diluted to 100 mL. This solution must be prepared freshly in use.

- **Preparation of standard solution of silicon and sample solution**

The method for standard preparation was similar to that for the sample. Accurate 50 mg of each zeolite powder and 50 mg of standard silica (100 % SiO_2) were weighed in nickel crucibles. The zeolite sample was primarily prepared by heating the zeolite at 700 °C for 5 hours. One crucible was needed for the sample, and the other was needed for the standard. 5 mL of 30 percent weight sodium hydroxide solution (30% NaOH) was transferred to the crucible. After that, the crucible was heated to dry over gas burner for approximately 15 minutes. Each crucible was removed from the heater and swirled the melt around the sides. When the melt mass was just solidified, the crucible was washed by boiling water. This solution was then transferred to a 1 L beaker and 150 mL of distilled water was added. Then, 5 mL of 1+1 hydrochloric acid was added

to each beaker. Stirring was applied at each time of addition. The solution was then diluted with distilled water to a total volume of 250 mL in a plastic volumetric flask. Afterwards, 10 mL of solution from 250 mL volumetric flask was diluted into 100 mL volumetric flask.

At this step, the concentration of the standard solution was approximately 10 ppm and used as stock for further dilution. A calibration curve was constructed by using 2.5, 5.0, 7.5, and 10.0 mL of this standard silica solution. For the zeolite sample, 10 mL of the sample solution from 100 mL volumetric flask was added to a 100 mL beaker. The pH of the mixture was measured by a pH meter and adjusted to 4.5-5.0. 1 mL of ammonium molybdate solution was added, after 5 minutes, 5 mL of 10% tartaric acid solution was mixed to the solution. Then, 1.0 mL of the reducing agent was added and diluted to 100 mL in a graduated flask by distilled water. After 20 minutes, the sample and standard solution were scanned over 900-500 nm, against the blank, and the wavelength at maximum absorbance was measured (ca. 815 nm). The maximum wavelength was used to measure the absorbance of sample and standard solutions against the blank. The calibration curve was plotted and the concentration of sample can be calculated by comparing with the standard calibration curve.

2) **Determination of aluminium [49]**

- **Preparation of reagents**

- Acetate buffer solution

Acetate buffer solution was prepared by dissolving 25 grams of ammonium acetate in 70 mL of distilled water, followed by adding 5 mL of acetic acid (100%). This solution was then diluted to 100 mL by distilled water.

- Reagent solution

The reagent solution was prepared by dissolving 2 grams of 8-hydroxyquinoline in sufficient chloroform to make a 100 mL solution.

- **Preparation of standard solution of aluminium and sample solution**

25 mL of stock sample solution was transferred to 100 mL beaker, followed by adding 3 mL of acetate buffer solution. The pH value was measured by pH meter and adjusted to 6.0. The mixture was then transferred to a separatory funnel. After that, 20 mL of reagent solution was filled and shaked vigorously for 3 minutes. The organic phase was separated and measured in quartz cell at 410 nm against the blank.

The standard of the aluminium solution was diluted to 50 ppm and a calibration

curve was constructed by using 1, 2, 3, and 4 mL of this standard solution. The calibration curve was plotted and the concentration of sample can be calculated by comparing with the standard calibration curve.

3.4.3 Catalytic testing

3.4.3.1 Study on cracking of polyethylene using Thermogravimetric Analyzer (TGA)

1) Effect of catalyst/polymer ratio

Thermogravimetric behavior of polyethylene was investigated using TGA Dupont 9000. Approximately 30 mg of polyethylene or polyethylene mixed with catalyst (catalyst/polymer ratio ranging from 10 to 30%) was placed in a platinum pan and the sample was heated under a nitrogen flow (50 mL/min) from 40°C to 700°C at a heating rate of 10°C/min. The %weight loss due to the degradation was measured with the sample temperature.

2) Time-dependent activity of the catalyst

30 mg of polyethylene or polyethylene mixed with catalyst (catalyst/polymer ratio of 20%) was placed in the platinum pan. The sample was heated from 40°C to 330°C at a heating rate of 100°C/min. The temperature was then held for 20 minutes under nitrogen at a flow rate of 50 mL/min. The %weight loss due to degradation was measured with time.

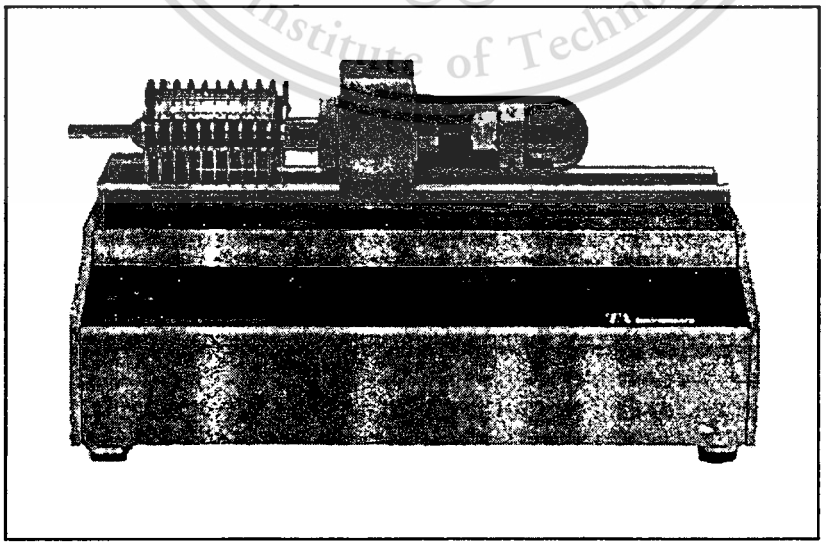

Figure 3.2 Thermogravimetric Analyzer (TGA51, Dupont 9000)

3.4.3.2 Study on cracking of polyethylene in batch process

Thermal and catalytic cracking of polyethylene, in pellet form (MFI = 15 g/10min), were carried out in a glass reactor under atmospheric pressure by batch operation. Figure 3.3 shows a schematic diagram of the apparatus used in the experiment. For the reaction, 2 grams of polyethylene for thermal cracking or 1.6 grams of polyethylene mixed with 0.4 grams of the catalyst for catalytic cracking were loaded into the reactor. In a typical run, after the reactor was set, air remaining in the reactor was removed by purging with a nitrogen stream at a flow rate of 100 mL/min. The reactor was then heated to 120°C at the rate of 2°C/min and held at 120°C for 30 minutes in order to drive off the absorbed water from the plastic sample. Carrier gas was changed from nitrogen to helium or hydrogen and the temperature was increased from 120°C to 430°C at a maximum rate of heating. The reaction time was usually carried out over a period of 15-30 minutes residence time. Gaseous and liquid products leaving the reactor were first collected by a liquid nitrogen trap cooled at -196°C. After the reaction, the gaseous fraction was separated from the liquid at room temperature and collected in a volumetric flask by replacing saturated NaCl solution. The reaction conditions for the study on cracking of polyethylene in batch process were summarized in Table 3.1.

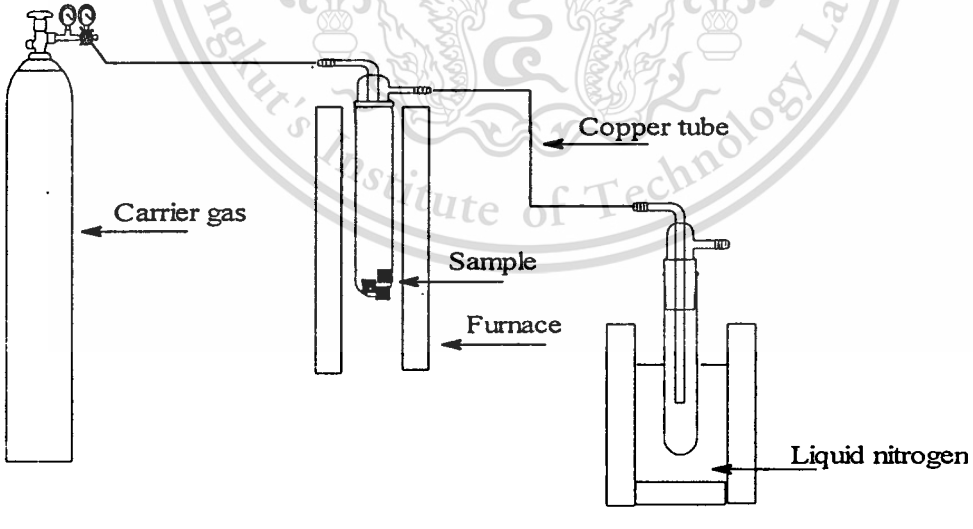

Figure 3.3 Schematic representation of batch process

Table 3.1 The reaction conditions for study on cracking of polyethylene in batch process

Reaction number	Catalyst	%Catalyst (w/w)	Repeated sample	Carrier gas	Residence time (minutes)
1	PE	-	-	He	30
2	PE + H-Beta (S)	20	fresh	He	30
3	PE + H-Beta (S)	20	1 st	He	30
4	PE + H-Beta (C)	20	Fresh	He	30
5	PE + H-Beta (C)	20	1 st	He	30
6	PE + H-Beta (C)	20	2 nd	He	30
7	PE + H-Beta (C)	20	3 rd	He	30
8	PE + H-ZSM-5 (S)	20	Fresh	He	30
9	PE + H-ZSM-5 (S)	20	1 st	He	30
10	PE + H-ZSM-5 (S)	20	2 nd	He	30
11	PE + H-ZSM-5 (S)	20	3 rd	He	30
12	PE + H-ZSM-5 (C)	20	Fresh	He	30
13	PE + H-ZSM-5 (C)	20	1 st	He	30
14	PE + H-ZSM-5 (C)	20	2 nd	He	30
15	PE + H-ZSM-5 (C)	20	3 rd	He	30
16	PE	-	-	H_2	30
17	PE + H-Beta (C)	20	Fresh	H_2	30
18	PE + H-Beta (C)	20	1 st	H_2	30
19	PE + H-Beta (C)	20	2 nd	H_2	30
20	PE + H-Beta (C)	20	3 rd	H_2	30

Table 3.1 (continued)

Reaction number	Catalyst	%Catalyst (w/w)	Repeated sample	Carrier gas	Residence time (minutes)
21	PE + H-ZSM-5 (C)	20	Fresh	H_2	30
22	PE + H-ZSM-5 (C)	20	1 st	H_2	30
23	PE + H-ZSM-5 (C)	20	2 nd	H_2	30
24	PE + H-ZSM-5 (C)	20	3 rd	H_2	30
25	PE + H-Beta (C)	20	Fresh	He	15
26	PE + H-Beta (C)	20	1 st	He	15
27	PE + H-Beta (C)	20	2 nd	He	15
28	PE + H-Beta (C)	20	3 rd	He	15
29	PE + H-ZSM-5 (C)	20	Fresh	He	15
30	PE + H-ZSM-5 (C)	20	1 st	He	15
31	PE + H-ZSM-5 (C)	20	2 nd	He	15
32	PE + H-ZSM-5 (C)	20	3 rd	He	15
33	PE + H-Beta (C)	20	Fresh	H_2	15
34	PE + H-Beta (C)	20	1 st	H_2	15
35	PE + H-Beta (C)	20	2 nd	H_2	15
36	PE + H-Beta (C)	20	3 rd	H_2	15
37	PE + H-ZSM-5 (C)	20	Fresh	H_2	15
38	PE + H-ZSM-5 (C)	20	1 st	H_2	15
39	PE + H-ZSM-5 (C)	20	2 nd	H_2	15
40	PE + H-ZSM-5 (C)	20	3 rd	H_2	15

1) Effect of pore size of zeolites

The effect of pore size of zeolites was determined by the reaction using medium pore H-ZSM-5 compared with large pore H-Beta as the catalyst.

2) Effect of catalyst deactivation

The effect of catalyst deactivation can be tested by repeating the catalyst three times without regeneration.

3) Effect of residence time

The effect of residence time was studied by comparing between 15 and 30 minutes residence time.

4) Effect of carrier gas

The effect of carrier gas was determined by the reaction using helium as a carrier gas compared with hydrogen at a flow rate of 100 mL/min.

3.4.3.3 Study on cracking of polyethylene in continuous process

The continuous flow reactor system comprises a feeder, the reactor chamber and the product collector. The schematic diagram and reactor used for continuous process were shown in Figures 3.4 and 3.5, respectively.

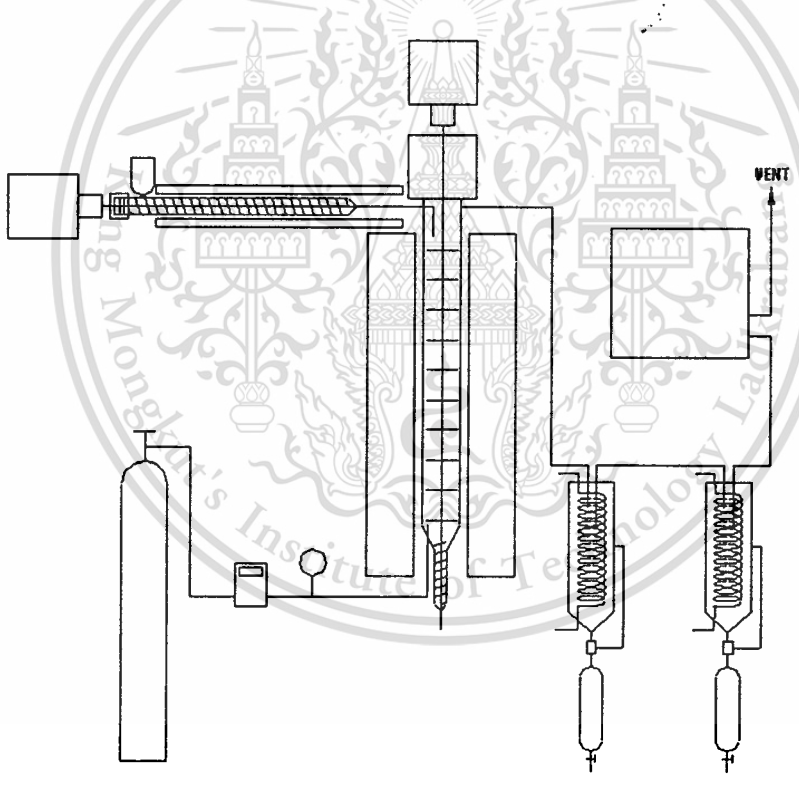

Figure 3.4 Schematic representation of continuous process

Polyethylene, in powder form (MFI = 45 g/10min), with or without catalyst was loaded into the extruder which was controlled at about 200°C. This material was molten and fed using the designed screw into the top of the reactor chamber at an average rate of 90 g/h using helium

as a carrier gas with a flow rate of 30 mL/min. Prior to start of the run, the screw extruder was heated by heating mantle and the reactor was purged with nitrogen for at least 20 minutes to remove oxygen in this reactor chamber. The temperature of the reactor chamber fitted in a three-zone vertical tube furnace was controlled in the range of 350-430°C. The waxy materials mixed with coking catalysts were separated by a screw at the bottom of reactor chamber. The output for volatile products was connected to the series of two cooling condensers. The liquid products were trapped at 20°C and -5°C, respectively. The gaseous products were analyzed by on-line gas chromatograph (GC).

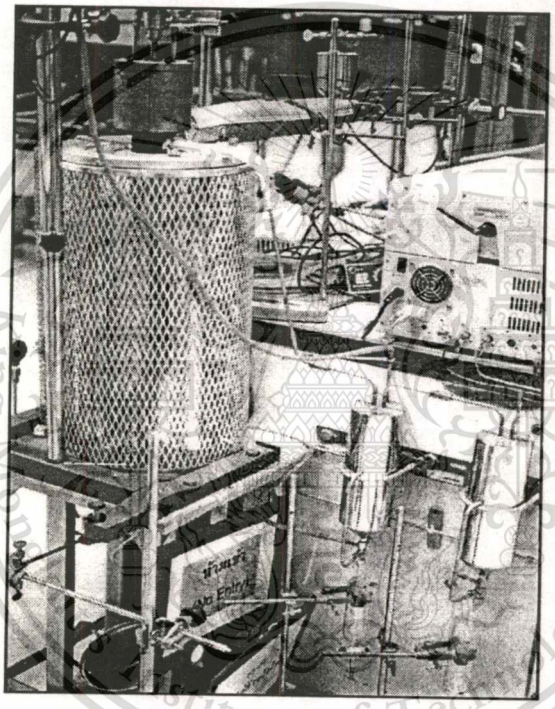

Figure 3.5 The reactor used for continuous process

1) Effect of reaction temperature

The effect of temperature was studied at reaction temperatures in the range of 350, 375, 400 and 430°C. Thermal reaction was compared with catalytic cracking under the same conditions.

2) Effect of catalyst/polymer ratio

The effect of catalyst/polymer ratio was determined by the reaction using catalyst ratio of 2% compared with 5% at 400°C.

3) Time on stream

The cracking activity was studied at a constant temperature as a function of time on stream (8 hours). Thermal reaction was compared with catalytic cracking under the same conditions.

3.4.4 Analysis of products

3.4.4.1 Determination of product composition using Gas Chromatograph (GC)

The gaseous and liquid products from the batch operation and liquid products trapped at 20°C from the continuous process were analyzed by gas chromatograph using 3800 Gas Chromatograph, Varian, with a capillary VA-1 column (15 m, 0.53 mm I.D.) and a flame ionization detector (FID). Helium was used as a carrier gas with a linear velocity of 12.3 cm/sec. Approximately 100 μL of gaseous products were injected to the injection port (220°C) of gas chromatograph using split ratio of 100. The programmed temperature was started at 30 °C and held for 5 minutes. Then, the temperature was raised to 200 °C with a rate of 5 °C/min and held at that temperature for 26 minutes. While, 0.1 μL of liquid products were injected to the injection port (220 °C) of gas chromatograph using split ratio of 100. The programmed temperature was started at 30 °C and held for 5 minutes. Then, the temperature was raised to 220 °C with a rate of 5 °C/min and held at that temperature for 22 minutes.

The gaseous products from continuous process flowed through a sample loop (100 μL) and were analyzed with an on-line 910 Gas Chromatograph, Buck Scientific, with a capillary HP-Plot column (30 m, 0.53 mm I.D.) and a flame ionization detector (FID). While, 0.01μL of liquid products trapped at -5°C were injected to the injection port. Helium was used as a carrier gas with a linear velocity of 53.6 cm/sec. The programmed temperature for gaseous and liquid products was started at 100°C and held for 10 minutes. Then, the temperature was raised to 190°C with a rate of 1°C/min and held at that temperature for 10 minutes.

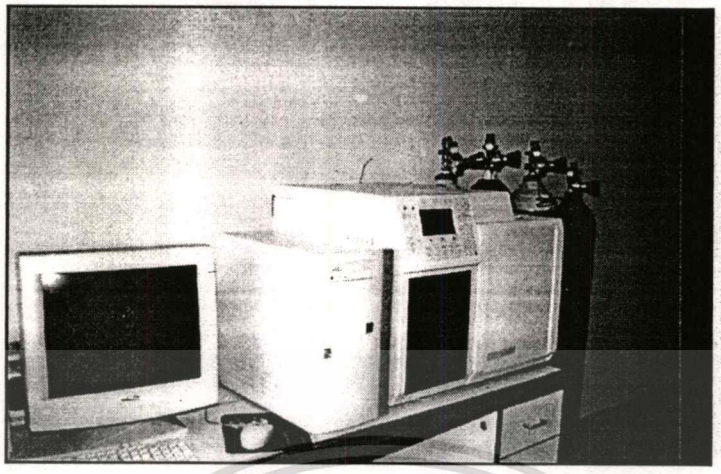

Figure 3.6 Gas Chromatograph (3800 Gas Chromatograph, Varian)

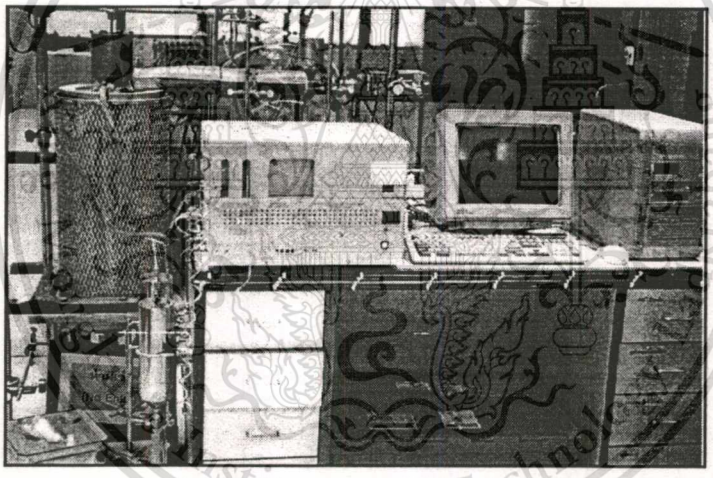

Figure 3.7 Gas Chromatograph (910 Gas Chromatograph, Buck Scientific)

3.4.4.2 Determination of composition and octane number of gasoline using Nuclear Magnetic Resonance (NMR)

The contents of paraffins, olefins and aromatics were estimated using the NMR method developed by Myers *et al.* [50-51]. The liquid products from the continuous process were diluted in TMS-containing deuterated chloroform. The determination was performed on a Bruker AVANCE DPX300 NMR spectrometer with 300-MHz proton resonance frequency. The integral spectra was obtained in separate scans from 0 to 10 parts per million (ppm). The RON and MON were also determined using the equation as shown in section 4.4.3.

CHAPTER 4

RESULTS AND DISCUSSION

4.1 Characterization of zeolites

4.1.1 Determination of the zeolite structure using X-ray Powder Diffractometer (XRD)

Zeolites used in this work were classified into 4 groups: Beta (S), Beta (C), ZSM-5 (S), and ZSM-5 (C). Zeolite (S) refers to the zeolite which was synthesized in the laboratory, while zeolite (C) refers to the zeolite which was commercially used in industry. X-ray diffraction pattern of the zeolites was obtained from D8 Advance Bruker X-ray Powder Diffractometer using Cu-Kα-radiation as shown in Figures 4.1-4.6.

4.1.1.1 Zeolite Beta

For non-calcined Na-Beta (S) (Figure 4.1), the X-ray diffraction pattern showed characteristic peaks at 2θ 7.68, 21.48, 22.48, 25.36, 26.48, and 29.56. Compared to X-ray diffraction pattern of standard Beta (Figure B.1), there was no difference in all peaks corresponding to the crystalline phases. These results confirmed that the obtained zeolite was Na-Beta.

After calcination of Na-Beta (S) (Figure 4.2), the relative intensity of the peak at 2θ 7.68 and 22.48 was altered, as compared with the non-calcined Na-Beta. This indicated that before calcination part of zeolite structure was still incomplete due to the presence of silanol groups. After calcination, the dehydration of silanol took place, and a 3-dimensional framework could be obtained. However, the crystallinity of the calcined sample was reduced due to the heat treatment as shown by a decrease in total intensity.

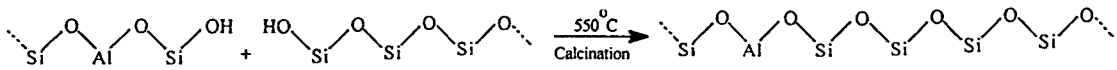

The X-ray diffraction pattern of NH_4-Beta (C) (Figure 4.3) was compared to X-ray diffraction pattern of the standard Beta. It revealed characteristic peaks at 2θ 7.68, 21.42, 22.50, 25.27, 26.93, and 29.51. The X-ray diffraction pattern was similar to the X-ray diffraction pattern

of the standard Beta. These results showed that the framework topology of zeolite Beta is retained.

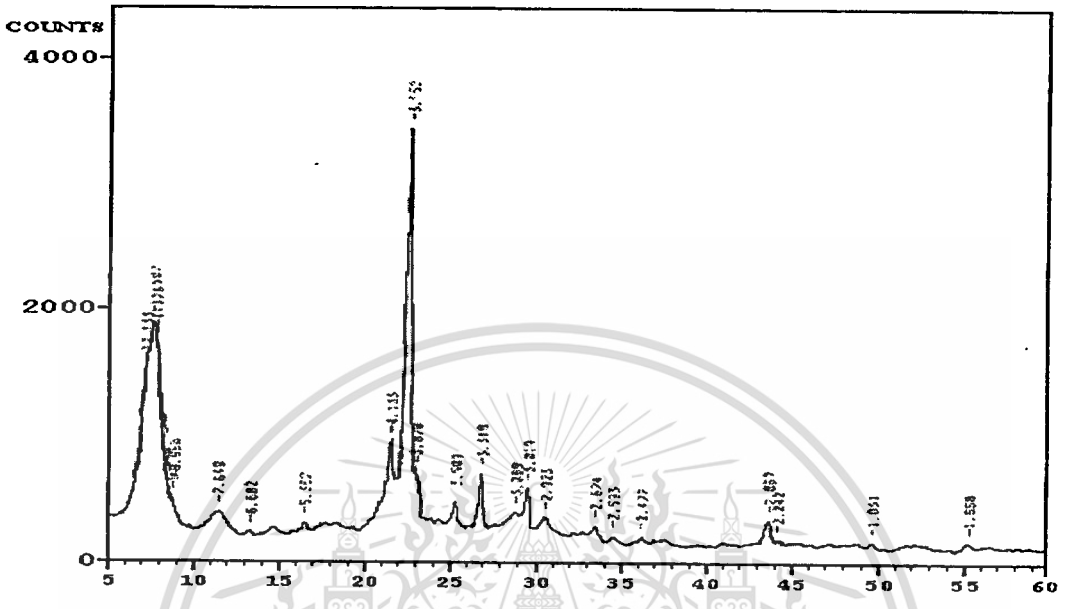

Figure 4.1 X-ray diffraction pattern of non-calcined Na-Beta (S)

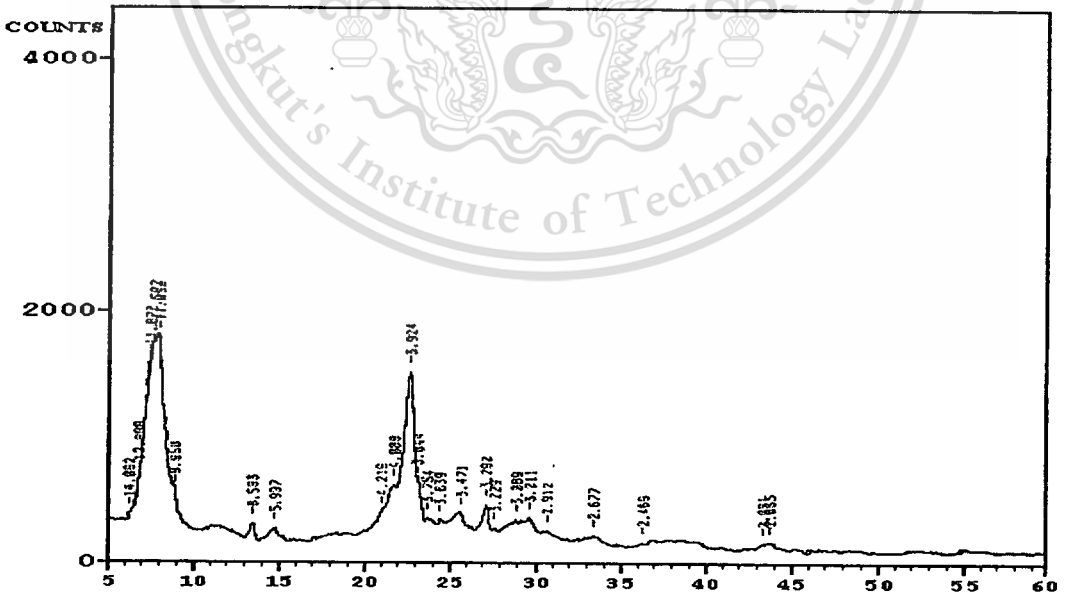

Figure 4.2 X-ray diffraction pattern of calcined Na-Beta (S)

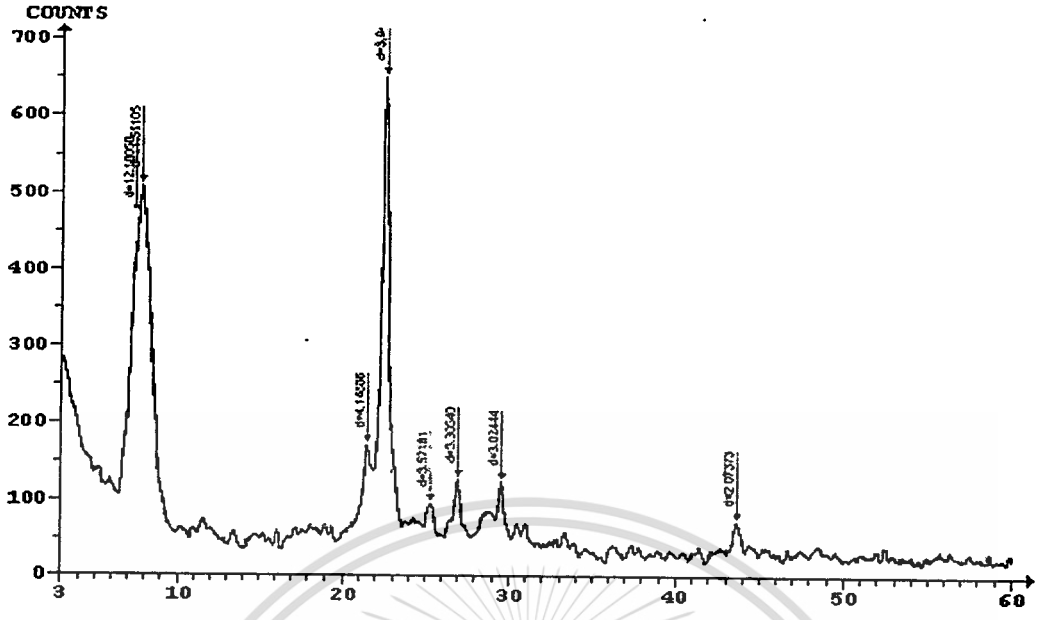

Figure 4.3 X-ray diffraction pattern of NH_4-Beta (C)

4.1.1.2 Zeolite ZSM-5

For non-calcined Na-ZSM-5 (S) (Figure 4.4), the characteristic peaks were shown at 2θ 7.92, 8.84, 23.12, 23.92, and 24.36. When compared to X-ray diffraction pattern of standard ZSM-5 (Figure B.2), it showed that Na-ZSM-5 retained ZSM-5 type structure.

For calcined Na-ZSM-5 (S) (Figure 4.5), the X-ray diffraction pattern was similar to that of the non-calcined Na-ZSM-5. Nevertheless, compared with non-calcined Na-ZSM-5, the calcined Na-ZSM-5 showed higher intensity at 2θ 7.92 and 8.84 due to the decomposition of organic template in the pore of Na-ZSM-5.

The X-ray diffraction pattern of H-ZSM-5 (C) (Figure 4.6) showed characteristic peak at 2θ 7.98, 8.94, 23.30, 23.94, and 24.38. Compared to X-ray diffraction pattern of standard ZSM-5, the X-ray diffraction pattern of H-ZSM-5 (C) appeared to be the same. These results confirmed that this catalyst contains H-ZSM-5. However, the baseline revealed part of amorphous material. This result is explained by the considerable amount of silica/alumina present in the sample. Silica/alumina is the amorphous material which is used for catalytic proposes.

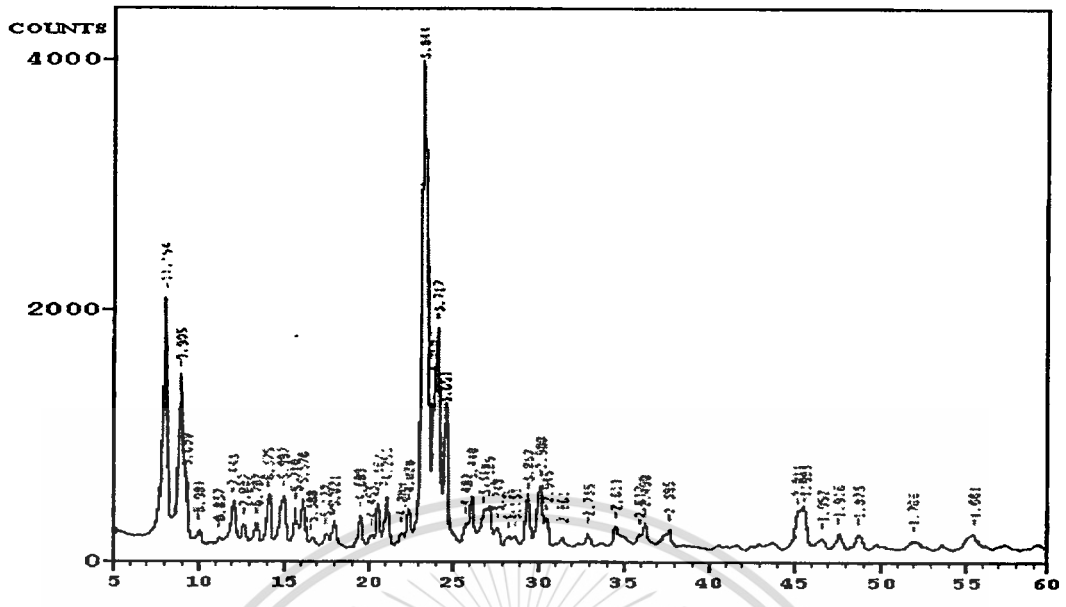

Figure 4.4 X-ray diffraction pattern of non-calcined Na-ZSM-5 (S)

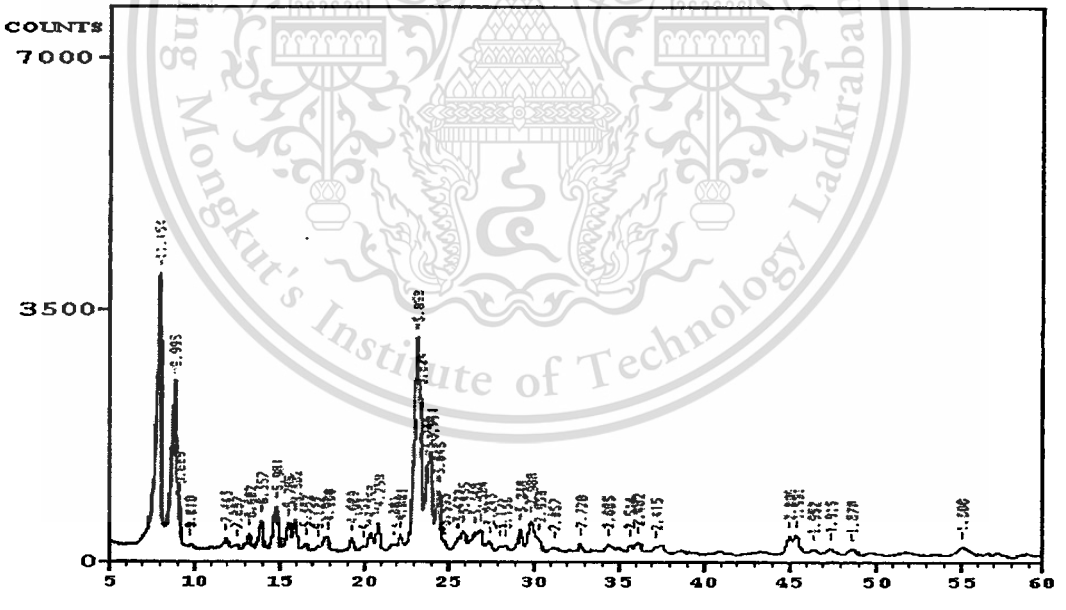

Figure 4.5 X-ray diffraction pattern of calcined Na-ZSM-5 (S)

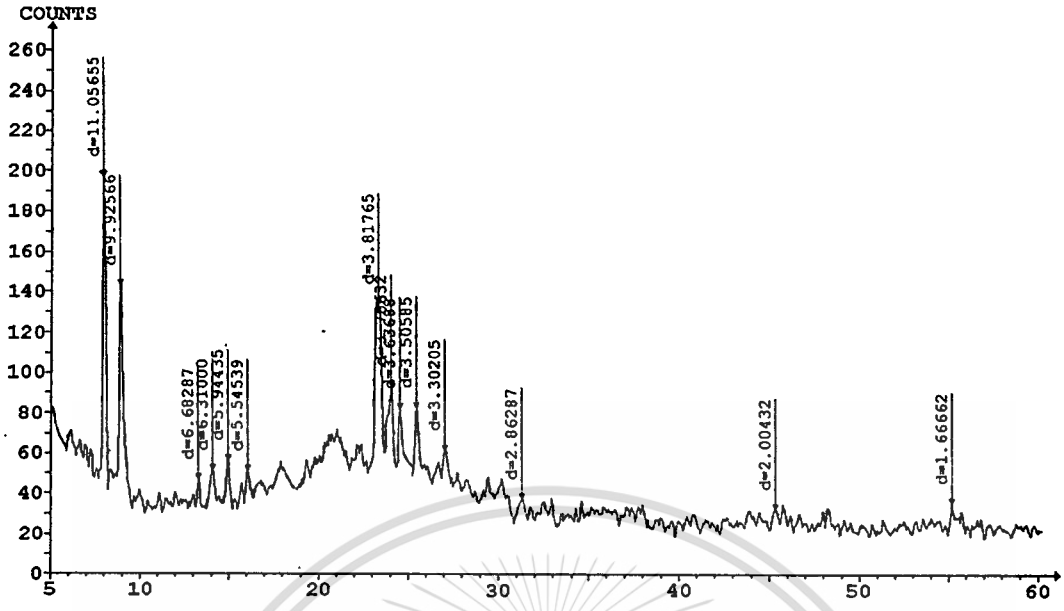

Figure 4.6 X-ray diffraction pattern of H-ZSM-5 (C)

4.1.2 Determination of the crystal morphology of zeolites using Scanning Electron Microscope (SEM)

The crystal morphology of the zeolites was obtained from Jeol 6400 Scanning Electron Microscope. The crystals of the two samples of zeolite Beta and the two samples of zeolite ZSM-5 used in this work were shown in Figures 4.7-4.10.

Non-calcined Na-Beta (S) (Figure 4.7) was made up of spherical particles with 1 μm in diameter. The NH_4-Beta (C) (Figure 4.8), however, showed smaller crystals (Approximately 0.2 μm in diameter) with spherical shape.

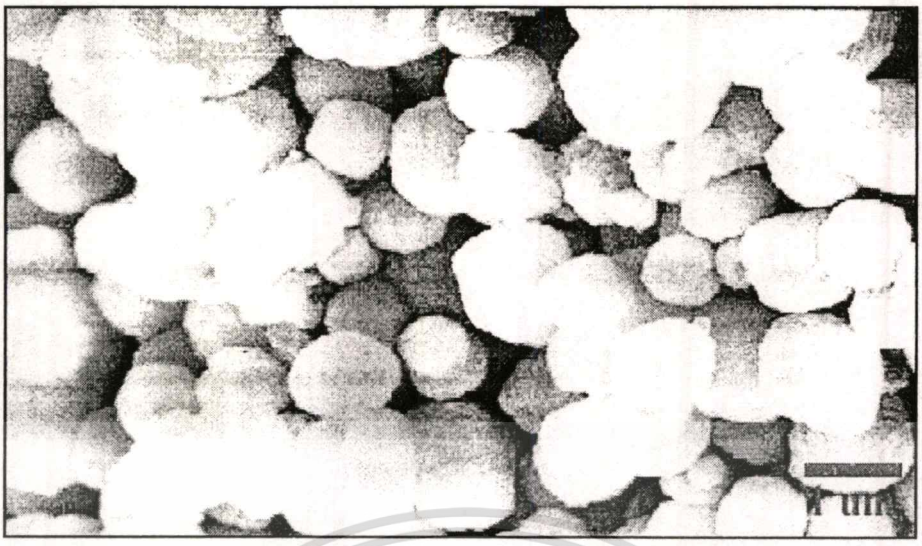

Figure 4.7 Scanning electron micrograph of the Na-Beta (S)

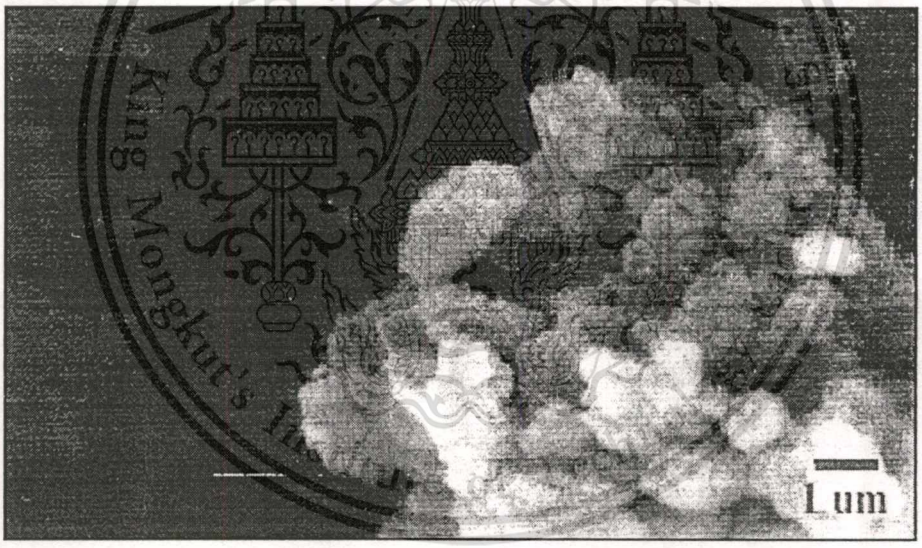

Figure 4.8 Scanning electron micrograph of the NH_4-Beta (C)

The morphology of Na-ZSM-5 (S) (Figure 4.9) showed orthorhombic shape with crystallite size approximately of 3×1 μm. In contrast, a non-uniformed particles was observed from H-ZSM-5 (C) (Figure 4.10).

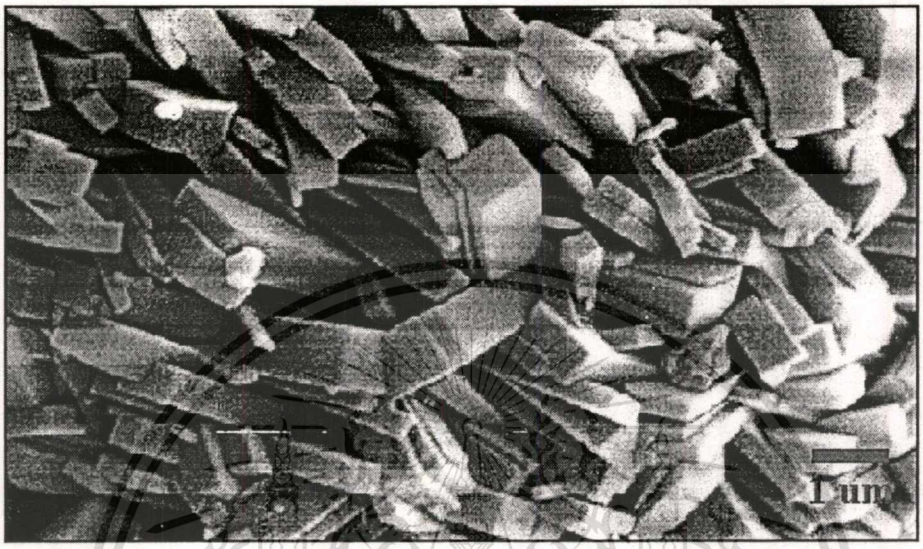

Figure 4.9 Scanning electron micrograph of the Na-ZSM-5 (S)

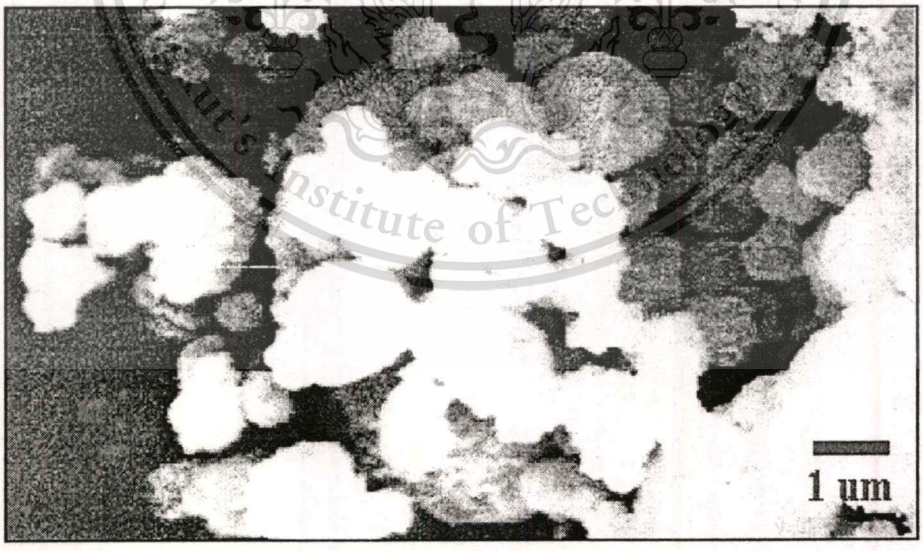

Figure 4.10 Scanning electron micrograph of the H-ZSM-5 (C)

Table 4.1 Crystal size, surface area, Si/Al ratio and acidity of the zeolites

Catalyst	Crystal size (μm)	BET area (m^2/g)	Si/Al ratio	Acidity (mmol /g of zeolite)
H-Beta (S)	1	632	18.1	0.68
H-Beta (C)	0.2	650	13.5	0.78
H-ZSM-5 (S)	3	413	18.6	0.54
H-ZSM-5 (C)	-	407	-	0.40

4.1.3 Determination of the surface area of zeolites using Gas Adsorption Analysis (Autosorb)

The surface areas of zeolites were determined using the BET equation and summarized in Table 4.1. Zeolite H-Beta (C) had a higher surface area (650 m^2/g), as compared to H-Beta (S) (632 m^2/g). It was noted that the smaller the crystal size, the higher the surface area. Whereas, the surface area of H-ZSM-5 (S) and H-ZSM-5 (C) was approximately 400 m^2/g.

4.1.4 Determination of the silicon/aluminium (Si/Al) ratio of zeolites using UV-Vis Spectrophotometer (UV)

The silicon/aluminium (Si/Al) ratios of zeolites were summarized in Table 4.1. H-Beta (S), H-Beta (C) and H-ZSM-5 (S) were classified as high silica samples. It was expected that these zeolites would possess high thermal stability and acid strength. Due to the presence of silica/alumina in H-ZSM-5 (C), the result of Si/Al ratio of zeolite in this sample cannot be certainly calculated.

4.1.5 Determination of the acidity of zeolites by potentiometric titration

The acidity of these zeolites was investigated by potentiometric titration with NH_4OH. The acidity of zeolites was summarized in Table 4.1. It was found that H-Beta (C) exhibited higher acidity than H-Beta (S) due to the higher aluminium content which implied a higher concentration of acid sites. The acidity of H-ZSM-5 (C) was lower than H-ZSM-5 (S). This was due to the fact that, in commercial, there is a considerable amount of silica/alumina in the sample. Therefore, the acidity determined as mole of H^+ per gram of catalyst, was relatively low.

4.2 Study on cracking of polyethylene using Thermogravimetric Analysis (TGA)

4.2.1 Effect of catalyst/polymer ratio

Polyethylene was decomposed over zeolite catalyst with different catalyst/polymer ratio ranging from 0 to 30%. Thermograms of decomposition of polyethylene were shown in Figures 4.11-4.12. The initial degradation temperature of polyethylene was summarized in Table 4.2.

Table 4.2 Initial degradation temperature of polyethylene with different catalyst/polymer ratio

Sample	% Catalyst/polymer ratio	Initial degradation temperature (^{o}C)
PE	-	445
PE + H-Beta (S)	10 %	350
PE + H-Beta (S)	20 %	305
PE + H-Beta (S)	30 %	300
PE + H-Beta (C)	10 %	315
PE + H-Beta (C)	20 %	295
PE + H-Beta (C)	30 %	283
PE + H-ZSM-5 (S)	10 %	392
PE + H-ZSM-5 (S)	20 %	358
PE + H-ZSM-5 (S)	30 %	346
PE + H-ZSM-5 (C)	10 %	420
PE + H-ZSM-5 (C)	20 %	415
PE + H-ZSM-5 (C)	30 %	410

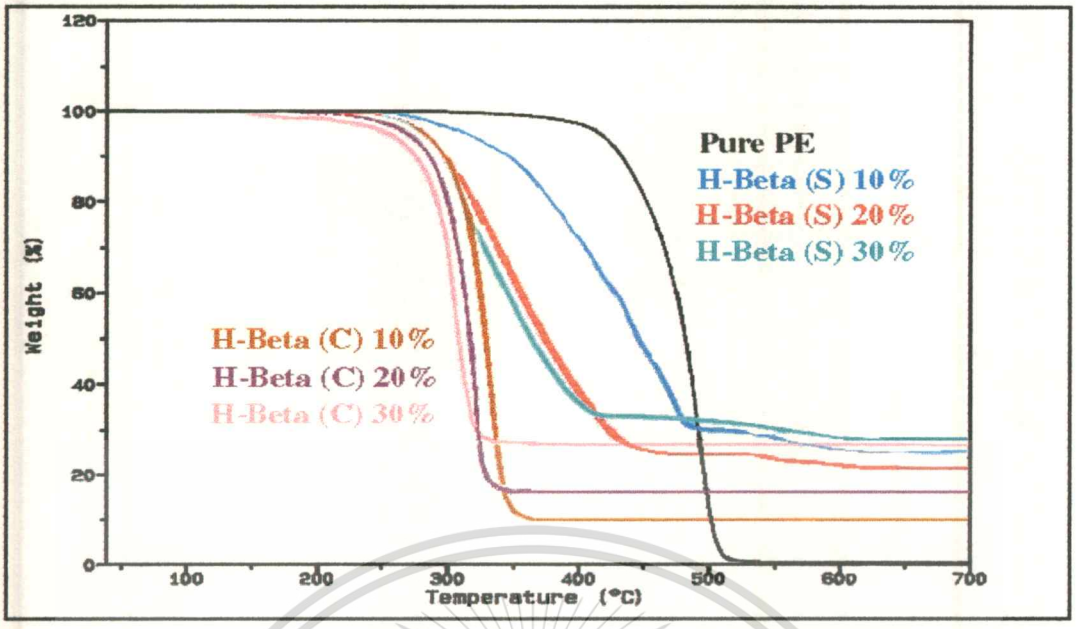

Figure 4.11 Thermogram curves of polyethylene with different H-Beta/polymer ratios as a function of temperature; *Reaction conditions: Temperature, 40-700 °C; Heating rate, 10 °C/min; Catalyst/polymer ratio, 10-30%; Nitrogen, 50 ml/min*

4.2.1.1 Zeolite H-Beta

The results obtained from TGA showed that the initial degradation temperature of pure polyethylene was 445 °C. Figure 4.11 compared the % weight loss obtained from catalytic cracking of polyethylene using zeolite Beta as the catalyst with % weight loss of corresponding thermal cracking. It was remarkable that the initial degradation temperature of polyethylene using zeolite Beta as the catalyst was lower than that of the thermal cracking. These results were in agreement with the fact that the catalytic cracking by strong acid catalysts could catalyze polyethylene into more lighter hydrocarbons than the thermal cracking [10, 39-40]. Over the strong acid catalysts, chain of polyethylene can be protonated and undergoes β-scission to form lighter hydrocarbon. While, the thermal cracking required higher energies for cleavage of carbon-carbon and carbon-hydrogen bonds [29]. Moreover, the reaction using 20% catalyst revealed a lower initial degradation temperature than that using only 10%. It was seen clearly that when catalyst/polymer ratio was increased, a larger number of active sites could amply facilitate protonation, leading to rapid cracking of polyethylene. The mechanism of catalytic cracking can be illustrated as below:

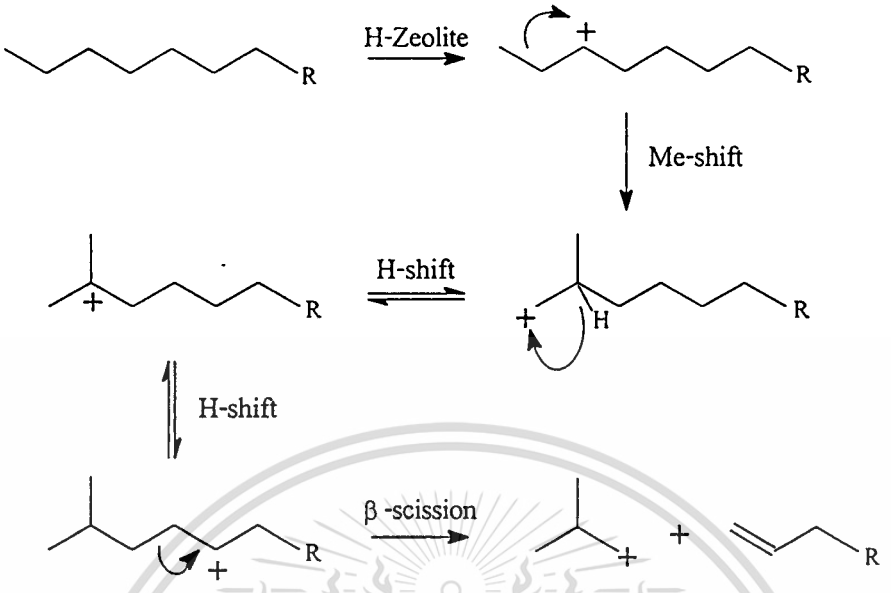

However, in the case of the reaction using catalyst ratio at 30%, the initial degradation temperature was somewhat similar to that using 20%. This was because there was abundance of the acid sites in catalyst/polymer ratio at 30%. The ratio at 20% has sufficient acid sites for cracking of polyethylene. The excess acid sites in catalyst/polymer ratio at 30% would show small effect on the rate of cracking. In other words, the kinetics of the reaction were over saturation at catalyst/polymer ratio of 30%.

The H-Beta (S) showed a slightly higher initial degradation temperature than that of H-Beta (C), while the final degradation temperature was higher than that of H-Beta (C). This can be attributed to the effect of crystal size of the zeolites. H-Beta (C) (Table 4.1) has relatively smaller crystal size (0.2 μm), consequently a higher external surface area is expected. The acid sites located on the external surface of the zeolite crystal may also promote the initial steps of the polyethylene cracking to produce relatively small hydrocarbons [9]. These species can then diffuse into the pore of Beta and undergo further cracking to low molecular hydrocarbons. In addition, the smaller crystal size facilitates the faster diffusion of those hydrocarbon fragments to the acid sites within the zeolite pores. Therefore, rate of cracking can be improved for the small crystal H-Beta (C).

Comparing catalyst efficiency in terms of coke formation, the remaining % weight obtained from H-Beta (C) at 700°C was similar to the % catalyst added. This can clearly indicate that a small amount of coke was formed over this catalyst. This was due to the fast diffusion of

hydrocarbon in the zeolite pore. Whereas, H-Beta (S) showed that the remaining % weight was higher than that of H-Beta (C). This can be explained that there is more coke formation deposited on the acid sites of H-Beta (S). The reaction using H-Beta (S) at 10% catalyst revealed much higher amount of remaining %weight than the original weight. However, when the catalyst content was increased, not only the decrease in the initial degradation temperature was observed but there was also a reduced coke formation. The decreases in the coke formation with the increase in the amount of the catalyst loading was reasonable, because the number of acid sites on the internal and external surface was proportional to the amount of the catalyst loading. The external surface area brings about the increase initial rate of cracking. Therefore, the lower molecular weight hydrocarbon intermediate can easily diffuse into the pore. This leads to an improved diffusion of all hydrocarbon species, therefore, formation of coke is reduced.

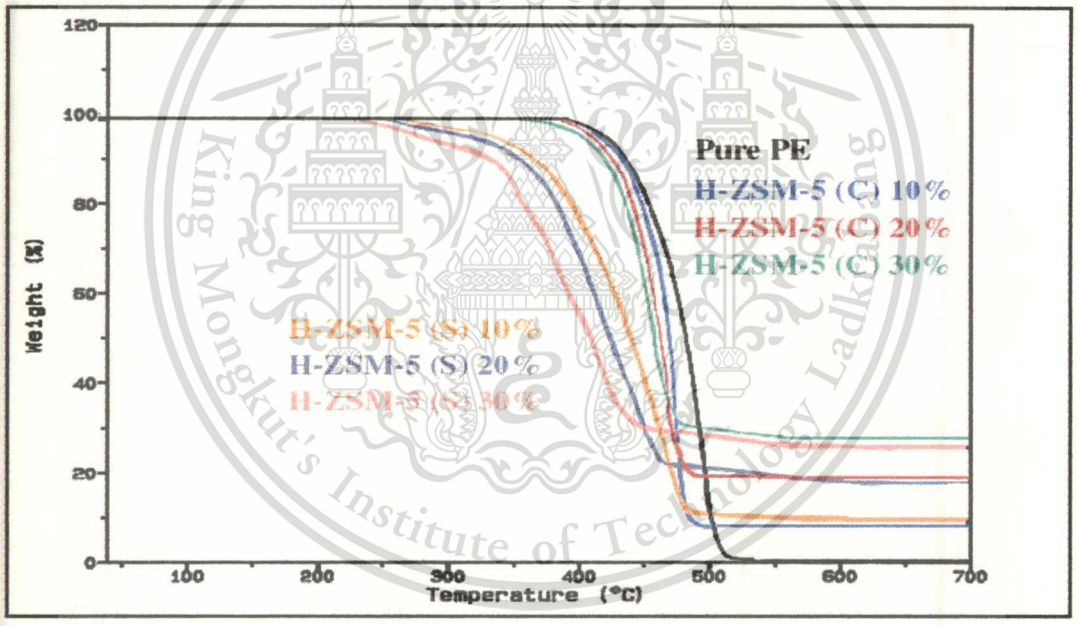

Figure 4.12 Thermogram curves of polyethylene with different H-ZSM-5/polymer ratios as a function of temperature; *Reaction conditions: Temperature, 40-700 °C; Heating rate, 10 °C/min; Catalyst/polymer ratio, 10-30%; Nitrogen, 50 ml/min*

4.2.1.2 Zeolite H-ZSM-5

The thermograms from cracking of polyethylene over both zeolite H-ZSM-5 using different catalyst ratios were shown in Figure 4.12. For both synthesized and commercial, in the case of catalyst ratio at 20%, the initial degradation temperature was lower than in the case of

10% and without catalyst, respectively. While, compared to the case of 20%, the initial degradation temperature of the 30% content was slightly decreased. The results appeared in a similar manner as observed in the case of zeolite H-Beta.

At the same catalyst/polymer ratio, H-ZSM-5 (S) exhibited lower initial degradation temperature than H-ZSM-5 (C) which indicated a higher activity of H-ZSM-5 (S), as compared to H-ZSM-5 (C). This was resulted from the fact that silica/alumina present in H-ZSM-5 (C) possess only weak acid sites. Thus, the proportion of strong acid sites of H-ZSM-5 (C) was relatively low. These results were in agreement with the fact that a higher activity for cracking of polyethylene into lighter hydrocarbons can be obtained from the strong acid catalysis, as compared to the weaker one [32].

The remaining % weight of both H-ZSM-5 (S) and H-ZSM-5 (C) appeared to be the same as the original %weight of the catalyst, although the zeolite content was only 10%. This was due to the effect of pore size and framework structure of ZSM-5. H-ZSM-5 possesses a medium channel structure which allows small coke formation and low deactivation rate. The pore of H-ZSM-5 is restricted to the formation of undesired larger polynucleararomatics [31]. This leads to small coke deposited on the internal surface of catalyst.

It can be clearly seen that the large pore H-Beta showed lower initial degraded temperature than the medium pore H-ZSM-5. This can be accounted for the fact that the diffusion into the larger pore of zeolite was easier than the smaller pore.

4.2.2 Time-dependent activity of the catalyst

At constant temperature (330 $^{\circ}$C), the activity of the catalyst was tested using the 20% catalyst/polymer ratio. The reaction was carried out for 20 minutes. The result was shown in Figure 4.13.

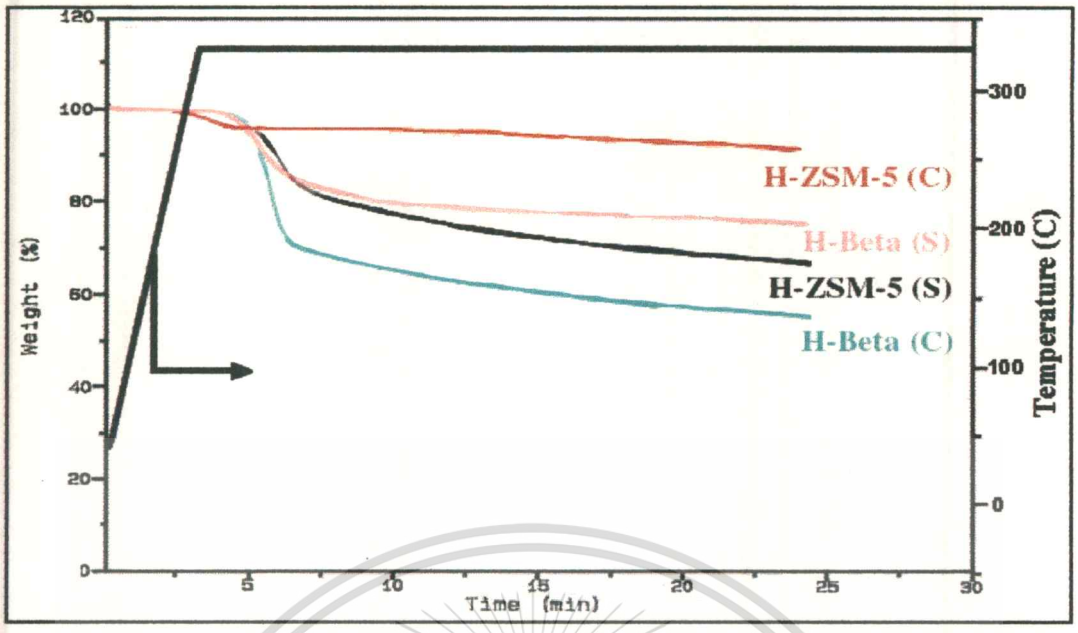

Figure 4.13 Thermogram curves of polyethylene with different zeolites as a function of time; *Reaction conditions: Temperature, 330 ^{o}C; Heating rate, 100 ^{o}C/min; Catalyst/polymer ratio, 20%; Nitrogen, 50 ml/min*

From Figure 4.13, H-ZSM-5 (C) exhibited lowest activity. The rate of decomposition was almost the same as that of the non-catalytic reaction, indicating no catalytic activity of these materials on polymer cracking at this temperature. This can be accounted from the presence of silica/alumina, as discussed earlier. Although, this catalyst possesses both weak and strong acid sites, only the small proportion of strong acid can catalyze the degradation of polyethylene into lighter hydrocarbon. Meanwhile, the large proportion of weak acid sites promotes much less cracking activity.

H-Beta (S) revealed higher activity than H-ZSM-5 (C) but lower than H-ZSM-5 (S) and H-Beta (C), respectively. H-Beta (S) possesses larger crystal size than H-Beta (C). This leads to a slower diffusion into the zeolite pores. Therefore, the activity was declined after 10 minutes reaction time, presumably due to the pore blockage by coking. However, the activity of H-ZSM-5 (S) was higher than H-Beta (S), despite the crystal size of H-Beta (S) is smaller than that of H-ZSM-5 (S). It could be explained that there was a little occasion for the formation of coke precursors on the acid site within the smaller pore and cage of H-ZSM-5. Therefore, the activity was slightly decreased with increasing reaction time due to the lower rate of coke formation.

When cracking reaction was carried out over H-Beta (C), the rate of decomposition of polyethylene was relatively high. While, the activity was gradually dropped even if the pore size is larger than H-ZSM-5 (S). These results were in agreement with the fact that smaller crystal size is responsible for the faster diffusion. Thus, the activity of H-Beta (C) is high due to the faster diffusion and the low rate of catalyst deactivation.

4.3 Study on cracking of polyethylene in a batch reactor

Cracking of polyethylene was investigated in a batch reactor at 430°C for 15 and 30 residence time, using hydrogen or helium as a carrier gas at a flow rate of 100 ml/min. The catalysts employed were described in Table 4.1. The cracked products were classified into 4 groups: gas, liquid, waxy materials, and carbonaceous residues. The waxy materials refer to the hydrocarbon products which are solidified at room temperature. This materials were determined from the weight of waxy materials obtained from washing catalysts and reactor after reaction with pentane. Additionally, small amount of waxy materials remained on the reactor was taken into account by determination of the reactor weight increased. The carbonaceous residues refer to the carbonaceous material depositing on the zeolite catalysts. The carbonaceous residues were determined from the increased catalyst weight after the reaction and washing with pentane. The amount of gaseous products was determined by subtracting the weight of liquid, waxy materials and carbonaceous residues. The gas yield can be defined by the relation;

$$\text{Gas (wt\%)} = 100 - [\text{Liquid (wt\%)} + \text{Wax (wt\%)} + \text{Residues (wt\%)}]$$

Due to the results from TGA, the optimum results can be obtained from the sample with 20% catalyst/polymer ratio. The 20% catalyst/polymer ratio was then used to study the effect of pore size of zeolites, catalyst deactivation, residence time, and carrier gas. Tables G.1-G.4 showed the yields of products from the thermal and catalytic cracking using different zeolites at various conditions.

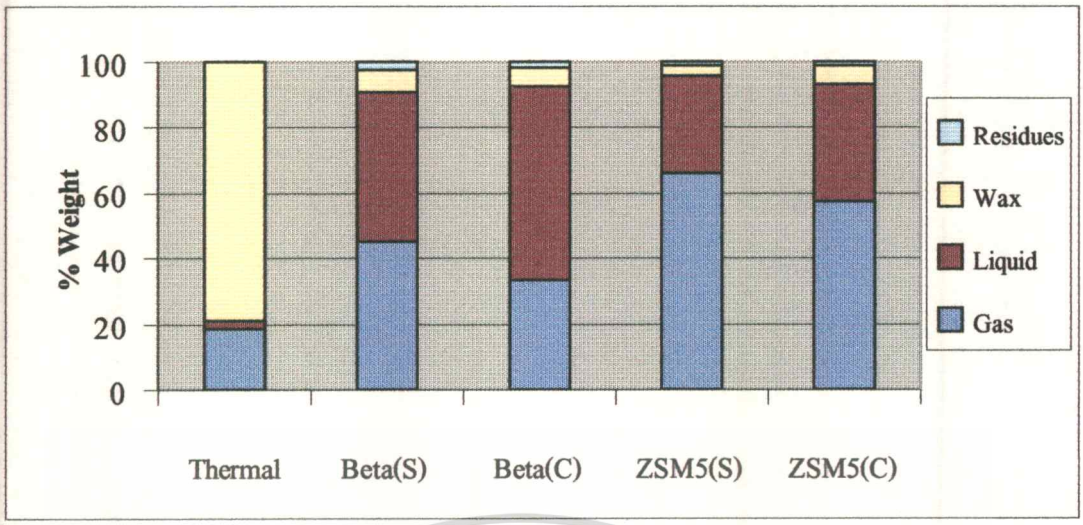

Figure 4.14 Yields of products from thermal and catalytic cracking of polyethylene using H-Beta and H-ZSM-5; *Reaction conditions: Temperature, 430 °C; Catalyst/polymer ratio, 20%; Residence time, 30 min; Catalyst, fresh run; Helium, 100 ml/min*

4.3.1 Effect of pore size of zeolites

The % weight from the thermal and catalytic cracking reaction using H-Beta and H-ZSM-5 were shown in Figure 4.14. Although the thermal cracking of polyethylene using no catalyst was generally initiated at above 400 °C, at 430°C the yield of gaseous product was only 18.66% and that of the liquid product was too small to be measured quantitatively. It was because the thermal cracking occured via a free radical mechanism which a random bond-breaking could be expected. In addition, the pyrolysis process required a high temperature for producing light products. As clearly seen, the catalytic cracking of polyethylene over both H-Beta and H-ZSM-5 produced higher yields of gas and liquid products than those of the thermal cracking. This implied that the degradation of polyethylene was considerably enhanced over both catalysts which lowered the degradation temperature and increased the yield of light product. Catalytic cracking of polyethylene was known to proceed by carbocation mechanism [15-16]. The initial step of the degradation was considered to occur by either the abstraction of the hydride ions by Lewis acid sites or the protonation by BrØnsted acid sites to the C-C bonds of the polyethylene chains [39]. Successive scission of the carbocation intermediate chain take places to produce lower molecular weight fragments. The decomposed fragments can be further cracked or dehydrocyclized in the

subsequent steps to form unsaturate branched hydrocarbons and aromatics, respectively. The formation of aromatics from carbocation fragments can be illustrated as below:

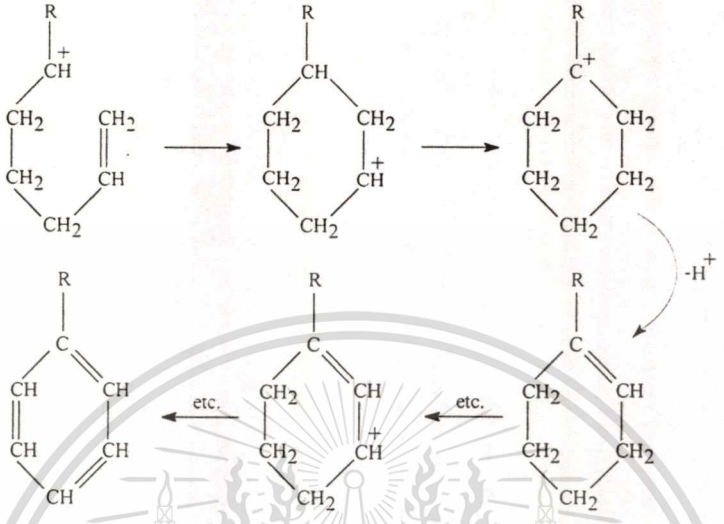

The liquid yields from reaction using H-Beta (S) and H-Beta (C) were higher than those from catalytic reactions over H-ZSM-5 (S) and H-ZSM-5 (C). In contrast, the gas yields from reaction using both H-Beta were lower than those from catalytic reactions over both H-ZSM-5 for all conditions. The fact that the reaction using H-ZSM-5 produces higher yield of gas, can be accounted for the restricted pore of the zeolites with high acid strength. Polyethylene can be protonated and the on-chain carbocation intermediate formed can undergo β-scission, producing low molecular weight hydrocarbons. The medium pore of H-ZSM-5, 0.55 nm, would control the product distribution in a range of (C_3-C_5) (will be discussed in 4.3.2). Whereas, the higher molecular weight hydrocarbons can be formed within the large pore H-Beta. Therefore, the liquid products in the range of (C_5-C_9^-) can be obtained from the reaction using the large pore H-Beta. This clearly showed that product distribution from polyethylene cracking can be controlled by the pore size of the zeolite used.

Regarding to the behavior of the both H-Beta (S) and H-Beta (C), the rate of coke formation observed from H-Beta (S) was higher than that from H-Beta (C). This can be explained by the effect of crystal size, as discussed earlier (section 4.2). While, the rate of coke formation of H-ZSM-5 (S) was low and similar to H-ZSM-5 (C).

Coke formation over in large pore of H-Beta was higher than that of medium pore of H-ZSM-5. This was because the formation of bulky intermediates was sterically hindered within

the 10-ring channel structure (approximately diameter of 0.55×0.51 nm) of H-ZSM-5 and consequently, the catalyst was resistant to coke formation [38]. In contrast, the 12-ring channel of H-Beta (approximately diameter of 0.76×0.64 nm) was less restrictive to the formation of bulky polynucleararomatic intermediates.

4.3.2 Composition of the gaseous products

Tables G.5-G.8 showed the distribution of gaseous products obtained from cracking of polyethylene for 15 and 30 minutes residence time under helium and hydrogen as a carrier gas. As discussed earlier, the gas yields were greatly improved by H-ZSM-5, as compared to thermal reactions (Figure 4.15). The gaseous products from thermal cracking, helium and hydrogen as a carrier gas, were ranged from C_3-C_6^+. For catalytic cracking, on the other hand, selective formation of C_4 can be obtained from H-Beta. While, large amounts of C_3 components were selectively produced on H-ZSM-5. However, the C_5-C_6^+ can be observed from H-ZSM-5 (C) due to the effect of silica/alumina presence in this catalyst. The H-ZSM-5 (C) plus silica/alumina, hybrid catalyst, possess both microporous (ZSM-5) and mesoporous (silica/alumina) materials which can control not only the formation of C_3-C_4 components but also the C_5-C_6^+ components. This was consistant to the above discussion that product distribution could be controlled by the pore size of catalyst. As the reaction using zeolite proceeded via carbocation intermediate within the restricted pore of zeolite, product with certain molecular geometry and size can be obtained. This was not in case for the thermal cracking since the reaction proceeds via free radical intermediates. Therefore, no control of product distribution can be observed.

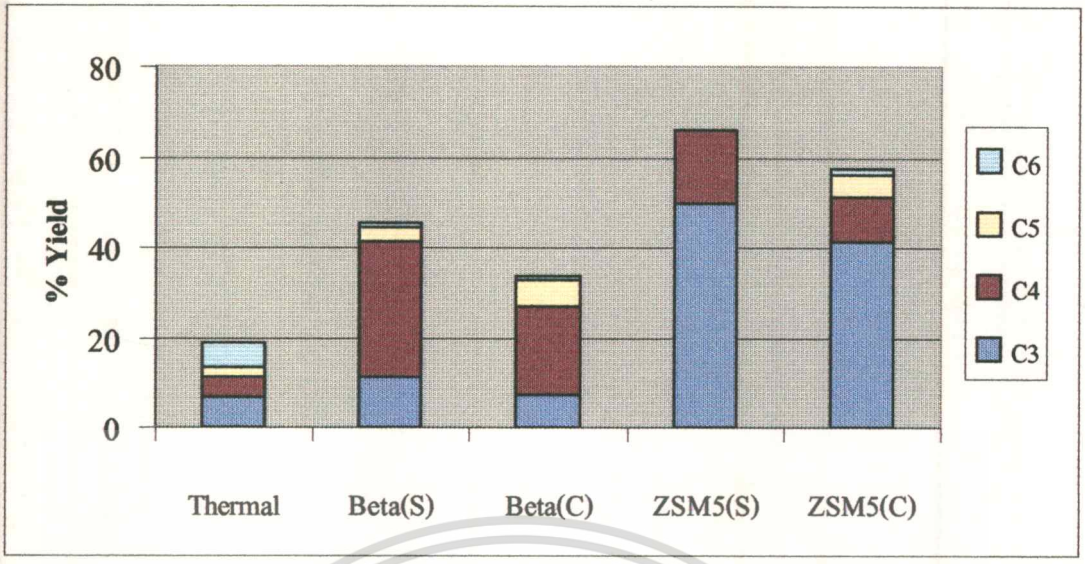

Figure 4.15 Yields of gaseous products from thermal and catalytic cracking of polyethylene using H-Beta and H-ZSM-5; *Reaction conditions: Temperature, 430 °C; Catalyst/polymer ratio, 20%; Residence time, 30 min; Catalyst, fresh run; Helium, 100 ml/min*

4.3.3 Composition of the liquid products

Tables G.9-G.12 showed the products distribution of liquid products obtained from the cracking of polyethylene for 15 and 30 minutes residence time under helium and hydrogen as a carrier gas. For thermal cracking of polyethylene, the liquid products were distributed over a wide range of carbon number, indicating a low selectivity for the cracking of polyethylene. These were typical for the products distribution usually observed in the thermal cracking which proceeds through free radical intermediates. In the case of catalytic cracking, the weight fraction of lighter hydrocarbons (C_5-C_6) was increased and the yield of heavier hydrocarbon (>C_9) was decreased. For H-ZSM-5, larger amounts of C_5 components were produced (Figure 4.16), whilst for H-Beta, larger amounts of C_6-C_7 components were obtained. Again this indicates the effect of pore size on products distribution.

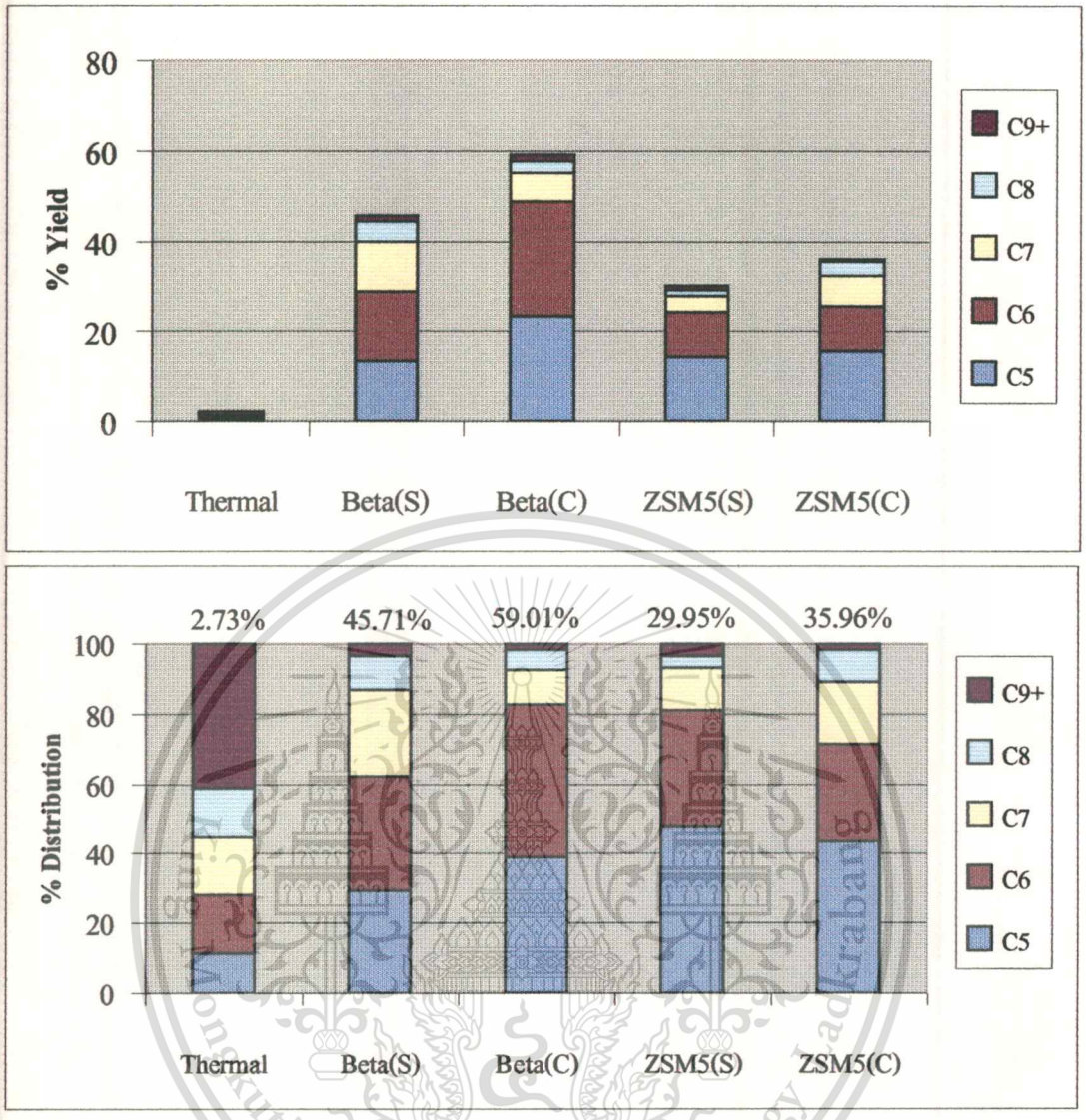

Figure 4.16 Yields and distribution of liquid products from thermal and catalytic cracking of polyethylene using H-Beta and H-ZSM-5; *Reaction conditions: Temperature, 430 ^{o}C; Catalyst/polymer ratio, 20%; Residence time, 30 min; Catalyst, fresh run; Helium, 100 ml/min*

The thermal cracking of polyethylene is very simple in terms of principle and operation, but the high energy cost and the low quality of liquid product as fuels cause the recycling non-attractive efficiency. Alternatively, a large amount of liquid products in the range of gasoline can be obtained from the reaction using zeolite catalyst. Catalytic cracking produces more gasoline with higher octane number than the thermal cracking because gasoline, produced by catalytic

cracking, is richer in branched and unsaturated hydrocarbon. It is expected that the high quality of gasoline production from catalytic cracking of polyethylene can be obtained.

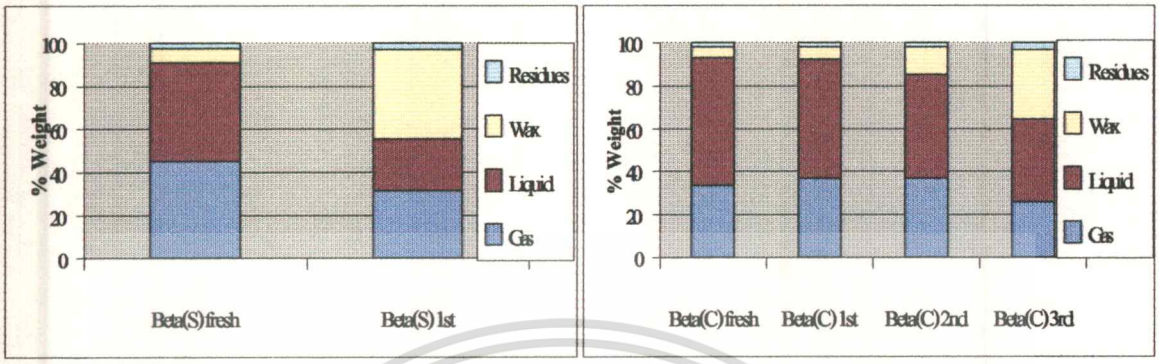

(a) **(b)**

Figure 4.17 Yields of products from catalytic cracking of polyethylene using **(a)** H-Beta (S) and **(b)** H-Beta (C) without regeneration; *Reaction conditions: Temperature, 430 °C; Catalyst/polymer ratio, 20%; Residence time, 30 min; Helium, 100 ml/min*

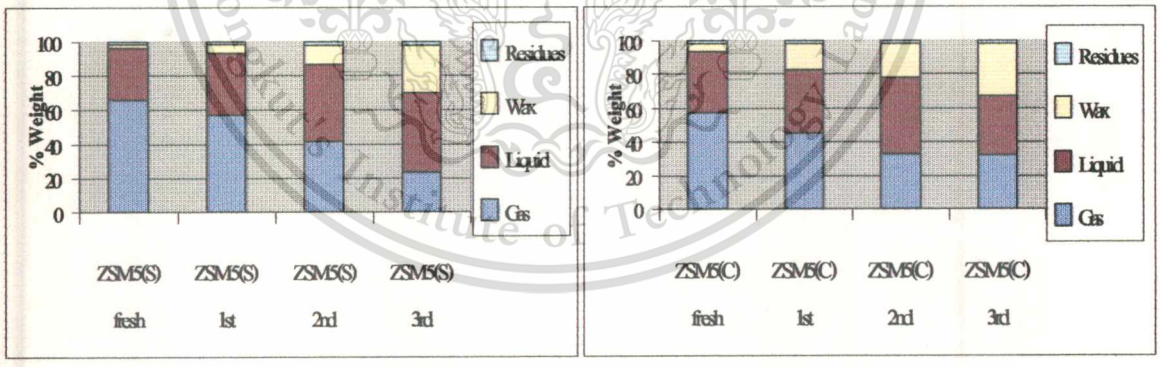

(a) **(b)**

Figure 4.18 Yields of products from catalytic cracking of polyethylene using **(a)** H-ZSM-5 (S) and **(b)** H-ZSM-5 (C) without regeneration; *Reaction conditions: Temperature, 430 °C; Catalyst/polymer ratio, 20%; Residence time, 30 min; Helium, 100 ml/min*

4.3.4 Effect of catalyst deactivation

Tests of catalyst life time for the catalytic cracking of polyethylene were performed by repeating the batch process using the same zeolites without regeneration in three consecutive runs. The process was carried out at 430 °C. From the Figure 4.17, using H-Beta (S), the wax product was dramatically increased from 6.50% to 41.13% in the seconds runs. This might well be derived from a rapid deactivation due to coke formation. H-Beta (S) possessed a large crystal size, causing diffusion difficulty and the higher rate of coke formation. This could be observed from the amount of coke deposition in H-Beta (S) (section 4.2.1). The coke formation can cause the pore blocking, so that the polymeric fragment is unable to diffuse into the zeolite pore. This leads to a decrease in the activity of catalyst and an increase in the waxy products. Whereas, the H-Beta (C) had much less deactivation which can be observed from a gradually increase in the yield of wax from 5.30% to 32.47% within four runs. This can be accounted from the relative smaller crystal sizes. The fast diffusion of polyethylene can be facilitated in the zeolite with smaller crystal size. Thus, little coke formation was observed. The rate of coke formation was slow, so that the activity is slightly reduced and the waxy products were gradually increased.

For gaseous and liquid products, the yields were reduced with increasing the number of runs indicated a reduced activity, as discussed earlier. For H-ZSM-5 (S) and H-ZSM-5 (C) as seen in Figure 4.18, the rate of cracking of polyethylene decreased slowly after repeated use of the catalysts. This indicated a low deactivation of the zeolites due to the smaller pore size. It should be noted that the color of H-ZSM-5 (S) and H-ZSM-5 (C), after the first run, only changed to brown and became darker after the second run. However, the color of H-Beta (S) and H-Beta (C) changed to black after the first run. This resulted from the rapid formation of coke on the catalyst surface.

The distribution of gaseous products from catalytic cracking over used H-Beta and used H-ZSM-5 were almost similar to that from catalytic cracking over fresh zeolite. However, in H-ZSM-5 (C), as the number of reuse was increased, i.e., 4th run (Figure 4.19), the products distribution from catalytic cracking was similar to that from thermal cracking. This result was probably due to the high amount of coke formation, which blocked the pore of catalyst. Therefore, a low product selectivity was observed after repeated use. This implied that the pore of catalyst was no longer able to control the product distribution.

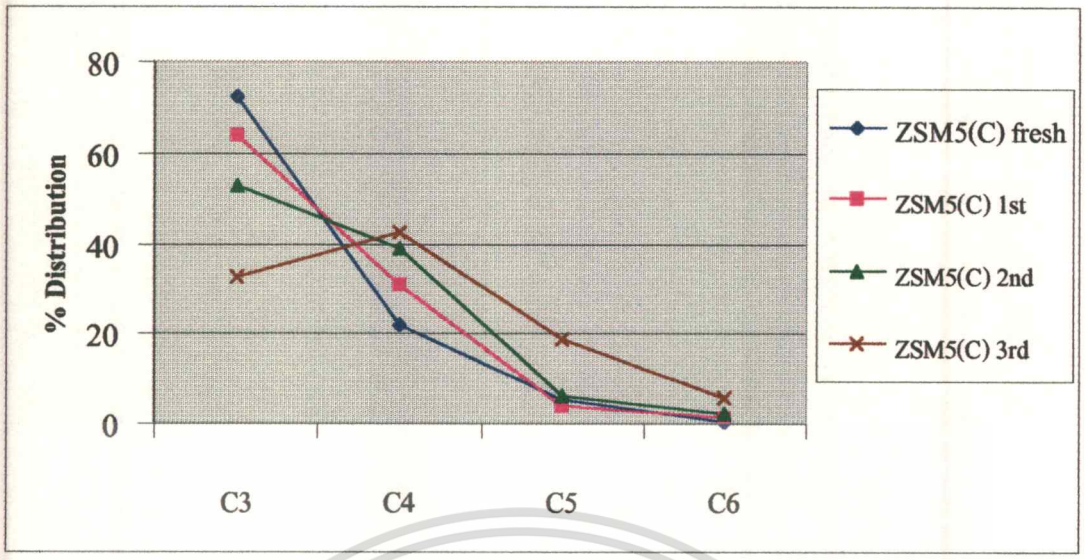

Figure 4.19 Distribution of gaseous products from catalytic cracking of polyethylene using H-ZSM-5 (C) without regeneration; *Reaction conditions: Temperature, 430 ^{o}C; Catalyst/polymer ratio, 20%; Residence time, 15 min; Helium, 100 ml/min*

The loss of product selectivity was more obvious in liquid products. It was found that higher yield of C_9^+ was obtained when the number of runs was increased from the first to the fourth run, while the C_5 and C_6 components decreased (Figure 4.20). This was again due to the decreased activity of the catalyst. The coke formation caused a low selectivity of product. These results appeared in a similar manner as observed on the gaseous products.

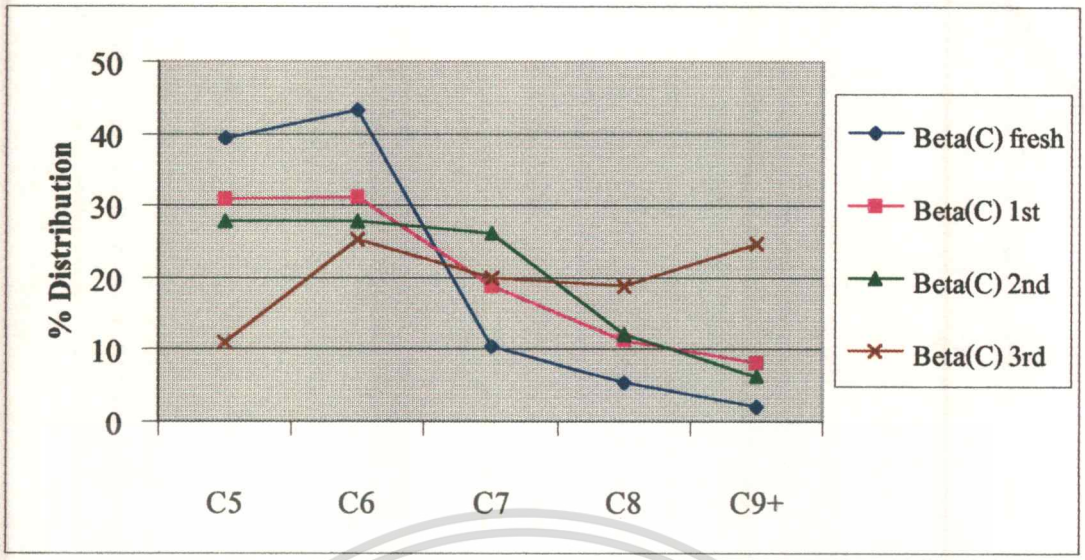

Figure 4.20 Distribution of liquid products from catalytic cracking of polyethylene using H-Beta (C) without regeneration; *Reaction conditions: Temperature, 430 °C; Catalyst/polymer ratio, 20%; Residence time, 30 min; Helium, 100 ml/min*

4.3.5 Effect of residence time

The effect of residence time was investigated for 15 and 30 minutes at 430 °C using helium and hydrogen as carrier gas. The products from the reactions using H-Beta and H-ZSM-5 were shown in Figure 4.21. It was found that the reactions over both H-Beta and H-ZSM-5 for 15 minutes residence time, produced slightly higher wax compounds, as compared with the reactions over 30 minutes residence time. The gaseous and liquid products produced in the reactions with 30 minutes residence time were also similar to that using 15 minutes residence time. However, at the 30 minutes residence time, higher coke formation was observed. It can be suggested that the rate of cracking was so fast and the reaction was nearly completed within 15 minutes residence time. However, with longer residence time, the higher coke could deposite in the pore of zeolite, causing pore blockage. Consequently, no significant increase in activity can be obtained from the reaction with 30 minutes residence time.

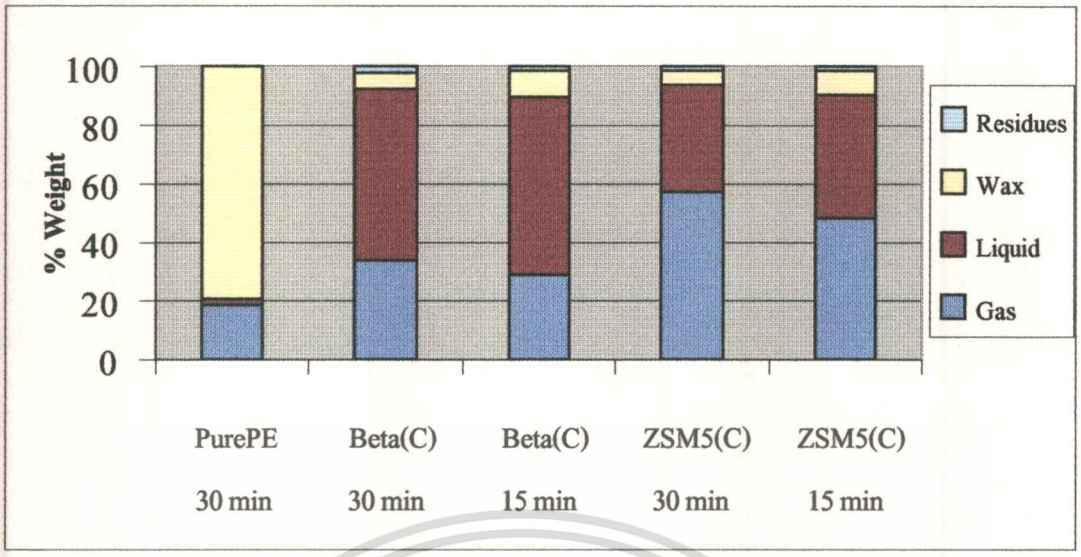

Figure 4.21 Yields of products from thermal and catalytic cracking of polyethylene as a function of residence time; *Reaction conditions: Temperature, 430 °C; Catalyst/polymer ratio, 20%; Residence time, 15 and 30 min; Catalyst, fresh run; Helium, 100 ml/min*

4.3.6 Effect of carrier gas

Catalysis using hydrogen as a carrier gas was compared with that using helium as a carrier gas at a flow rate of 100 ml/min. For the thermal cracking (Figure 4.22), the wax products obtained by the reaction under helium (78.97%), were lower than those obtained in the reactions under hydrogen (87.25%). This indicated that hydrogen might saturate the thermally cracked radicals and prevented them from further cracking.

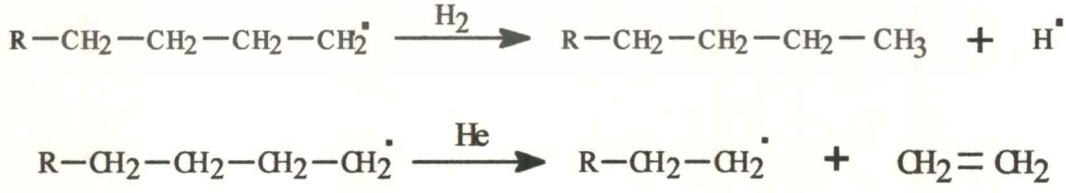

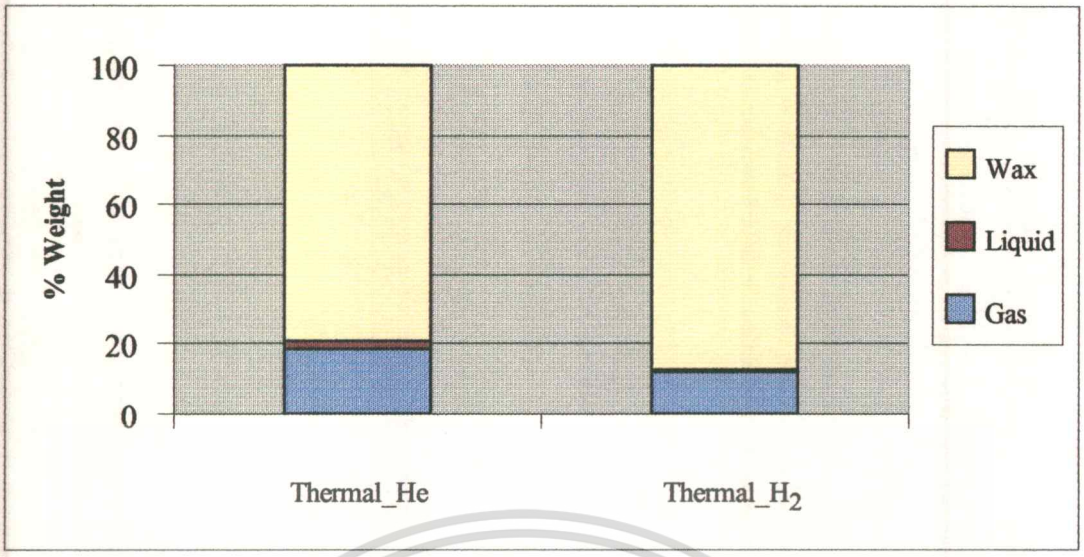

Figure 4.22 Yields of products from thermal cracking of polyethylene as a function of carrier gas; *Reaction conditions: Temperature, 430 °C; Residence time, 30 min; Carrier gas, 100 ml/min*

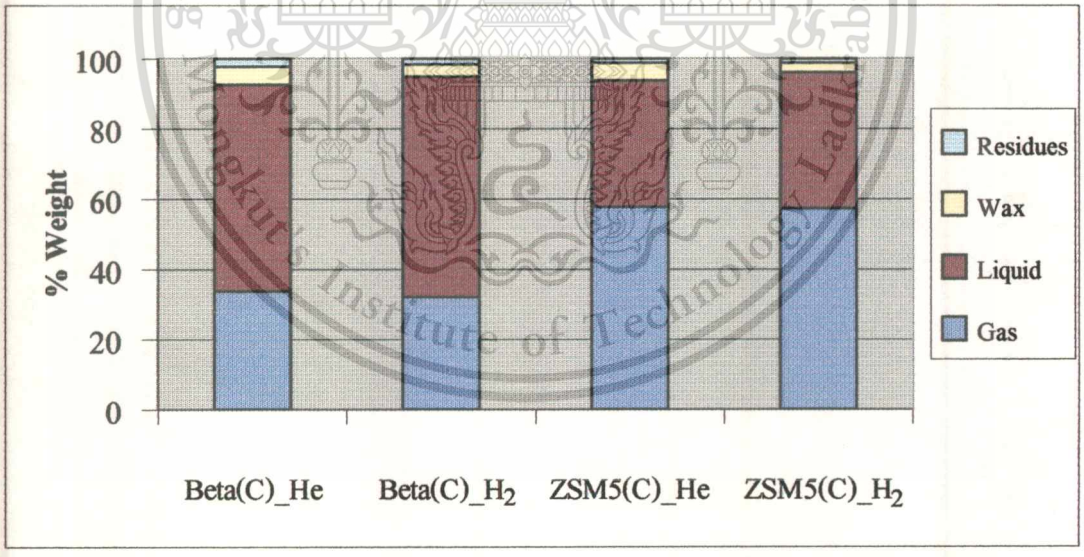

Figure 4.23 Yields of products from catalytic cracking of polyethylene as a function of carrier gas; *Reaction conditions: Temperature, 430 °C; Catalyst/polymer ratio, 20%; Residence time, 30 min; Catalyst, fresh run; Carrier gas, 100 ml/min*

However, in catalytic cracking (Figure 4.23), hydrogen plays role in decreasing coke formation. It can be seen that the coke deposite on zeolite with hydrogen was less than that with helium (Figure 4.24). Moreover, the hydrocracking ability of H-Beta and H-ZSM-5 was reflected, resulting in the lower amount of wax, as compared with those from cracking under helium atmosphere [29]. These results implied that hydrogen could be transferred to the unsaturated species, which were strongly absorbed at the surface of the zeolites, and counteracted coke formation on the acid sites. Therefore, this increased the cracking activity of zeolite when hydrogen was presence as a carrier gas.

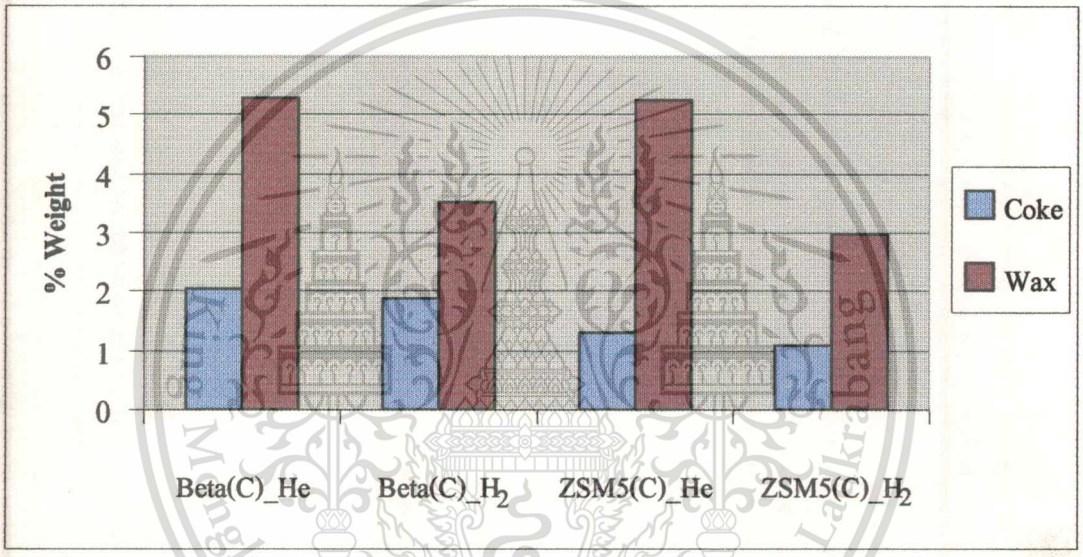

Figure 4.24 Coke formation over H-Beta and H-ZSM-5; *Reaction conditions: Temperature, 430 ^{o}C; Catalyst/polymer ratio, 20%; Residence time, 30 min; Catalyst, fresh run; Carrier gas, 100 ml/min*

4.4 Study on cracking of polyethylene in a continuous system

4.4.1 Continuous flow reaction system

With the public concern that has developed for the environment in recent years, alternatives for the disposal of spent plastic products are being sought. Recycling of thermoplastics from waste products can contribute to solve pollution problems associated with the landfills and incineration of plastics. Therefore, a variety of plastic waste recycling methods have been established and new recycling approach is being developed to avoid placing polymers into landfills. Among the techniques proposed for the recycling of waste polymers, the most attractive method is chemical recycling into the corresponding monomers or raw chemicals. However, the most study has been small-scaled batch processes which cannot separate the used catalyst immediately, resulting in rapid deactivation of catalyst. In this part, instead of batch process, continuous process was particularly designed and constructed to be effective for separating the used catalyst from the cracking reaction. In addition, this system might be used in up-scaling for further cracking of plastic waste in an industrial level. The continuous reactor system comprises a feeder, a reactor chamber and a product collector. The schematic diagram of a designed continuous reactor was shown in Figure 4.25 and the schematic drawing of the extruder, reactor chamber and the product collector were shown in Figures 4.26, 4.31, and 4.40, respectively.

4.4.1.1 Single screw extruder

The single screw extruder is designed for feeding the polymer material to the reactor chamber. It can be divided into three sections [52]. The three geometrically different sections of the screw extruder were shown in Figures 4.26-4.27.

The first section (A), close to the feed hopper, generally has deep flights. The material in this section is mostly in solid state. This section can be referred to as the feeding or conveying section of the screw. The last section (C), close to the die, usually has shallow flights. The material in this section is mostly in molten state. This screw section is referred to as the metering or pumping section. The middle screw section (B) connects between the feeding section and the metering section. This section is called the transition section or compression section. This screw is designed with L/D (length of screw/diameter of screw) ratio of 22. The high 20-30 L/D ratio is usually effective for screw which is designed for a better mixing of polyethylene with catalyst. The outside diameter of the screw is constant whereas the depth of the screw channel (or the

height of the screw flight) is varied according to each zone as shown in Figure 4.28. The flight height is increased from the last part of feeding section towards the beginning of metering section, thus causing a compression of the material in the screw channel.

Powder of polyethylene with or without zeolite was entered the screw from the feed hopper. Generally, the feed material flows by gravity from the feed hopper down into the feeding section of extruder barrel. However, polyethylene can be readily molten and blocked at the exit of the hopper before passing through the feeding section of the extruder. This is due to the effect of heat transfer from barrel to the hopper, causing interrupted flow of polyethylene. The hopper is accordingly designed to overcome this problem by installing a cooling system (Figure 4.29). At the feeding section, the material falls down in the space between the extruder screw and barrel. The material in this section is mostly in the solid state. The rotation of the screw causes frictional forces on the materials with the barrel as well as on the materials with the screw surface. These frictional forces are responsible for transport of the materials towards the next section.

The material at the feeding section is then heated by some heat from frictional force and the heat conducted from the heating mantle which covers the barrel of the extruder. When the temperature of the material exceeds the melting point, a melt film will form at the barrel surface. As the material moves forward to the compression section, the amount of solid material at each flight will be reduced as a result of melting of polyethylene (Figure 4.30). The material in the compression or the transition section is mostly molten. The space volume of screw is subjected to decrease with length, causing compression on the material. Moreover, the air bubble can be inhibited in the pumping section by the back pressure. This is desirable since the air leaking escape into the reactor chamber can cause oxidation reaction and undesired products can be formed. An adequate back pressure generated in pumping section can overcome this unwanted circumstance. The material is compressed and pushed toward to the next section by rotation of the screw. The temperature at the surface of barrel is high and it gradually decline from the barrel to the centre of the screw. Thus, when the channel depth is reduced, the material is not only compressed but also gained a higher heat generated from the frictional force.

When material moves to the metering section, this section accomplishes final melting and mixing. After that, the polymer melt is simply pushed to the die. This die is referred to the pipe at the exit of the screw extruder. The molten polymer is passed through the die and conveyed to the reactor chamber for cracking reaction.

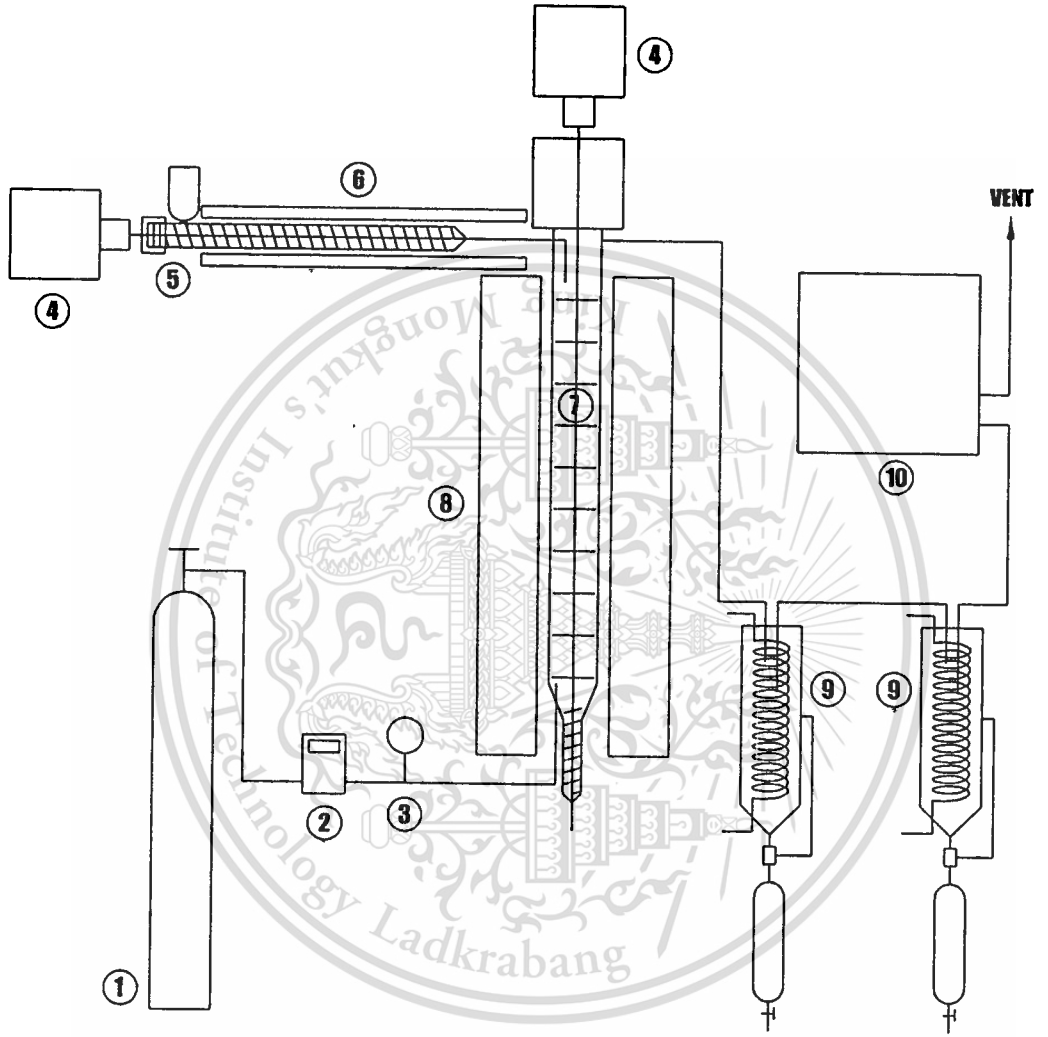

Figure 4.25 Schematic diagram of the continuous cracking apparatus; 1, He cylinder; 2, flow meter; 3, pressure guage; 4, motor; 5, single screw extruder; 6, heating mantle; 7, reactor chamber; 8, furnace; 9, liquid trap condenser; 10, gas chromatograph (GC)

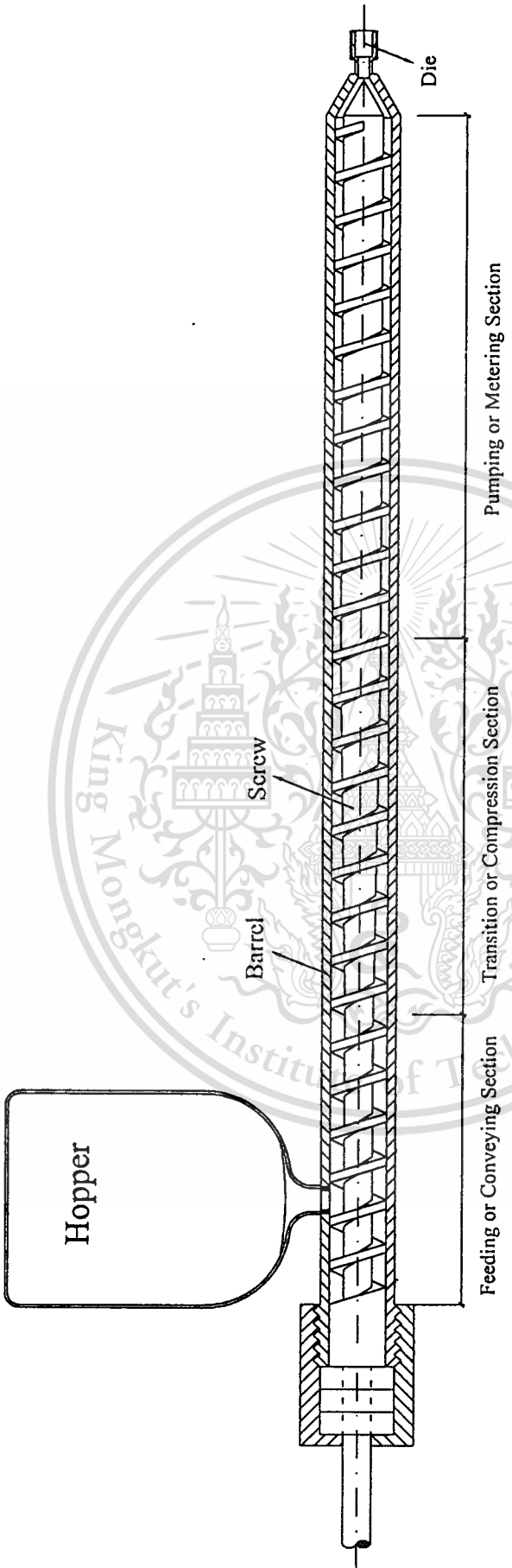

Figure 4.26 Schematic single screw extruder

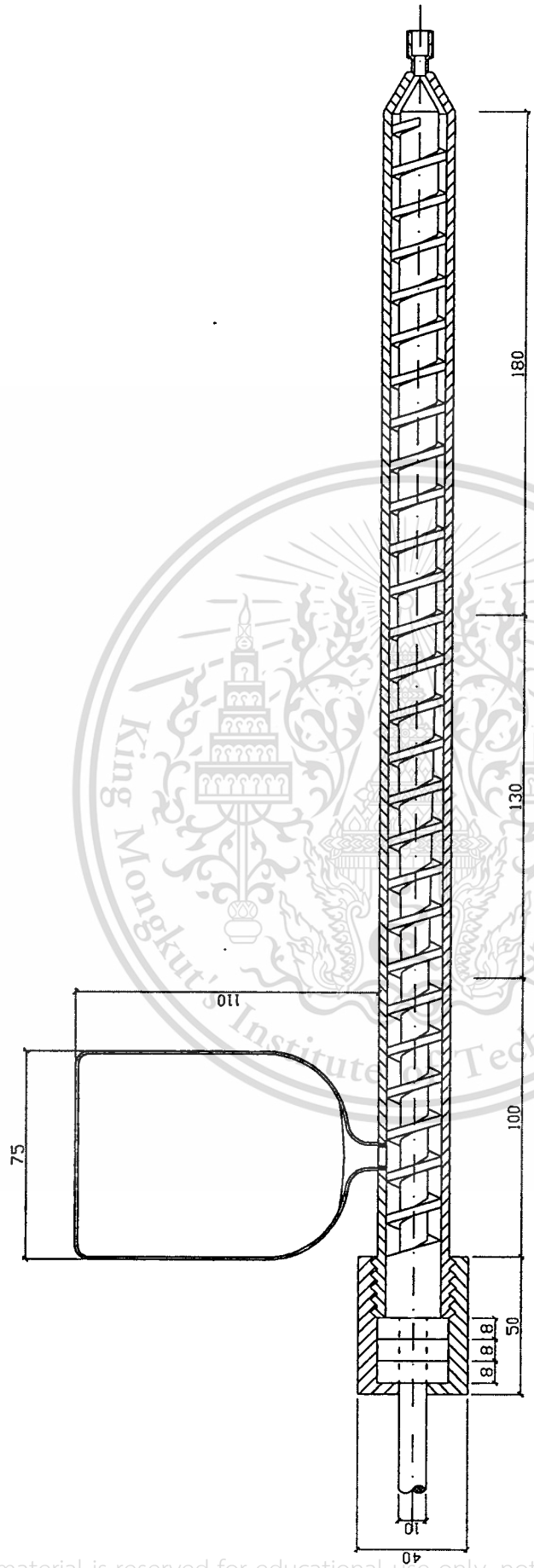

Figure 4.27 Schematic single screw extruder

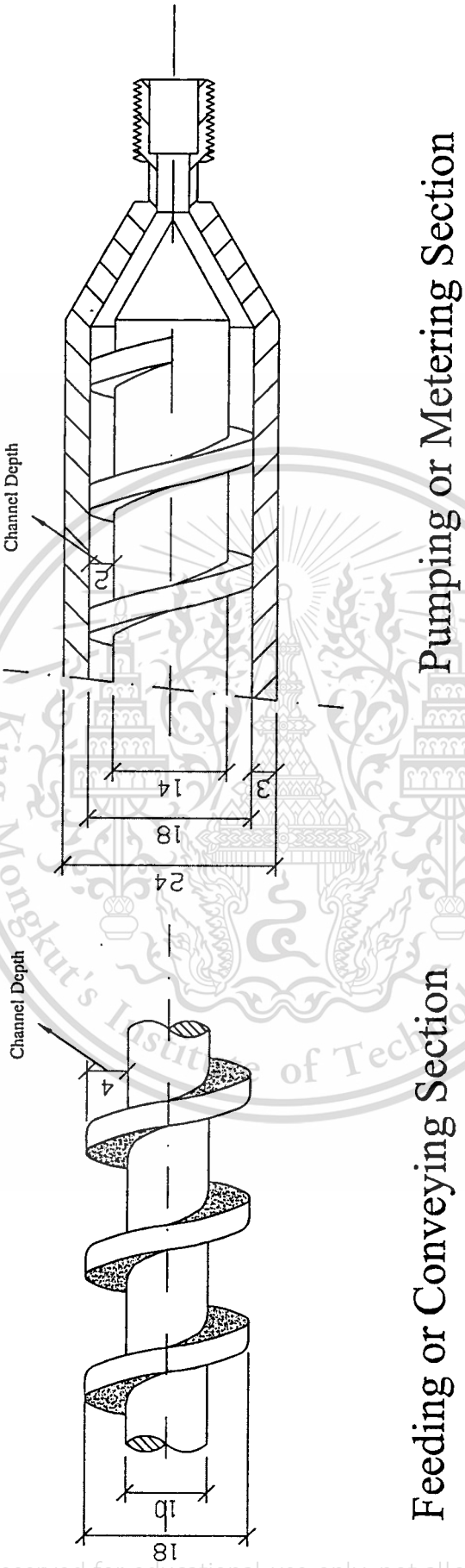

Figure 4.28 Schematic part of single screw extruder

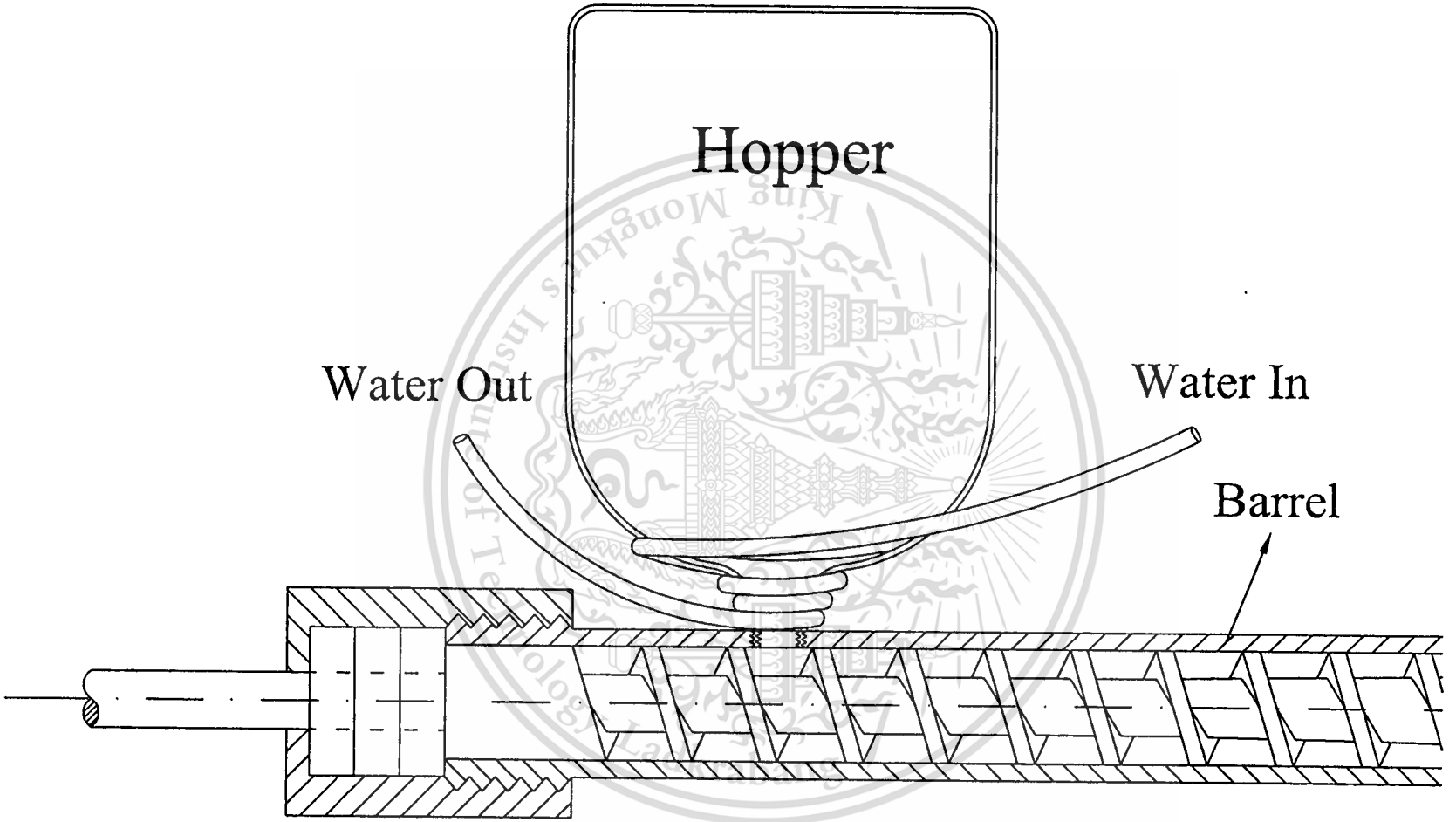

Figure 4.29 Cooling system for feeding polymer

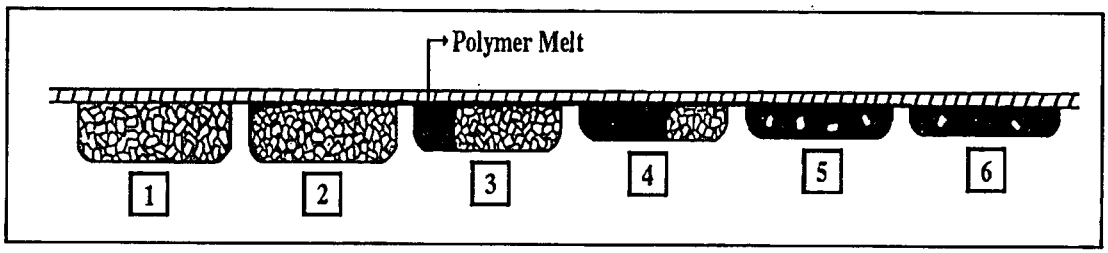

Figure 4.30 Model of melting of polymer at transition section of screw [52]

4.4.1.2 Reactor chamber

The reactor chamber consists of three parts; top section, middle section, and bottom section. The three geometrically different sections of the reactor chamber are shown in Figure 4.31. The top section can be separated into 5 parts as shown in Figures 4.32-4.37.

Part C is the cooling part which is designed for circulating water. Water in this cooling part is flowed in seried after the condensers (20°C). Middle hole in this part can support the axial of rotating shaft. At the contact between part C and part E, a thermal resistant o-ring (F) with a diameter of 6.0 cm is installed for preventing the leakage of gas from the system. Part B is for supporting the axial of rotating shaft in addition to part C. This part is also used to hold the shaft at the time of rotating by sealing with five thermal resistant o-rings (G), diameter of 1.0 cm. The o-rings on both position can be kept from overheated by heat exchanger with cooling part (C). These can prevent the leakage of gas from the system through the contact of C and E and contact of B and C, respectively. Part A and D are used as locking parts. The inside screws (L) lock part B and part C together. The middle screws (M) lock part A and part C. The outside screws (N) are used for pulling part D toward part A which then act as nipping part for part C and E.

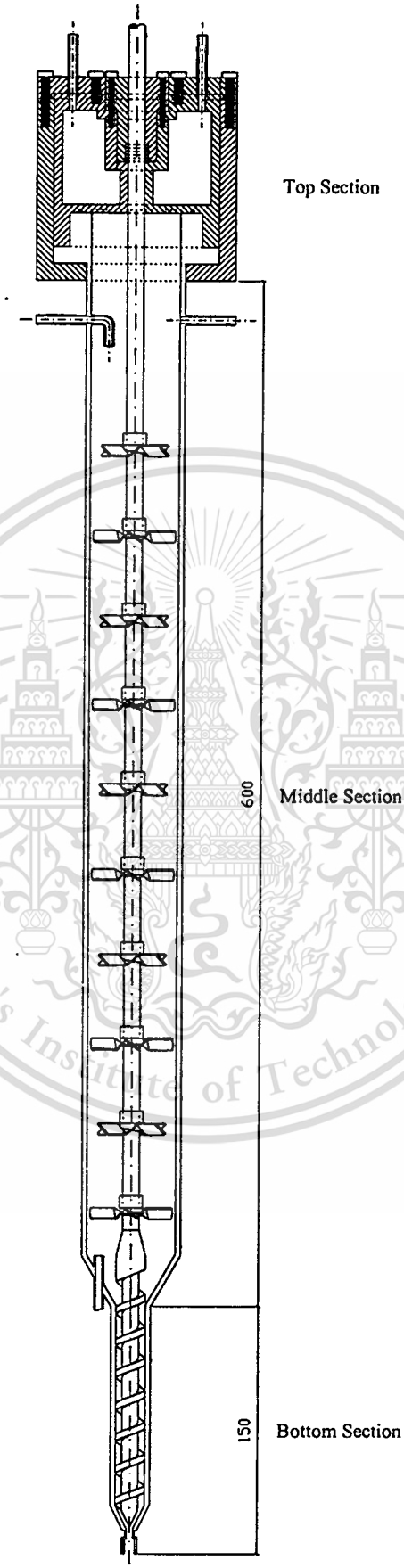

Figure 4.31 Schematic reactor chamber

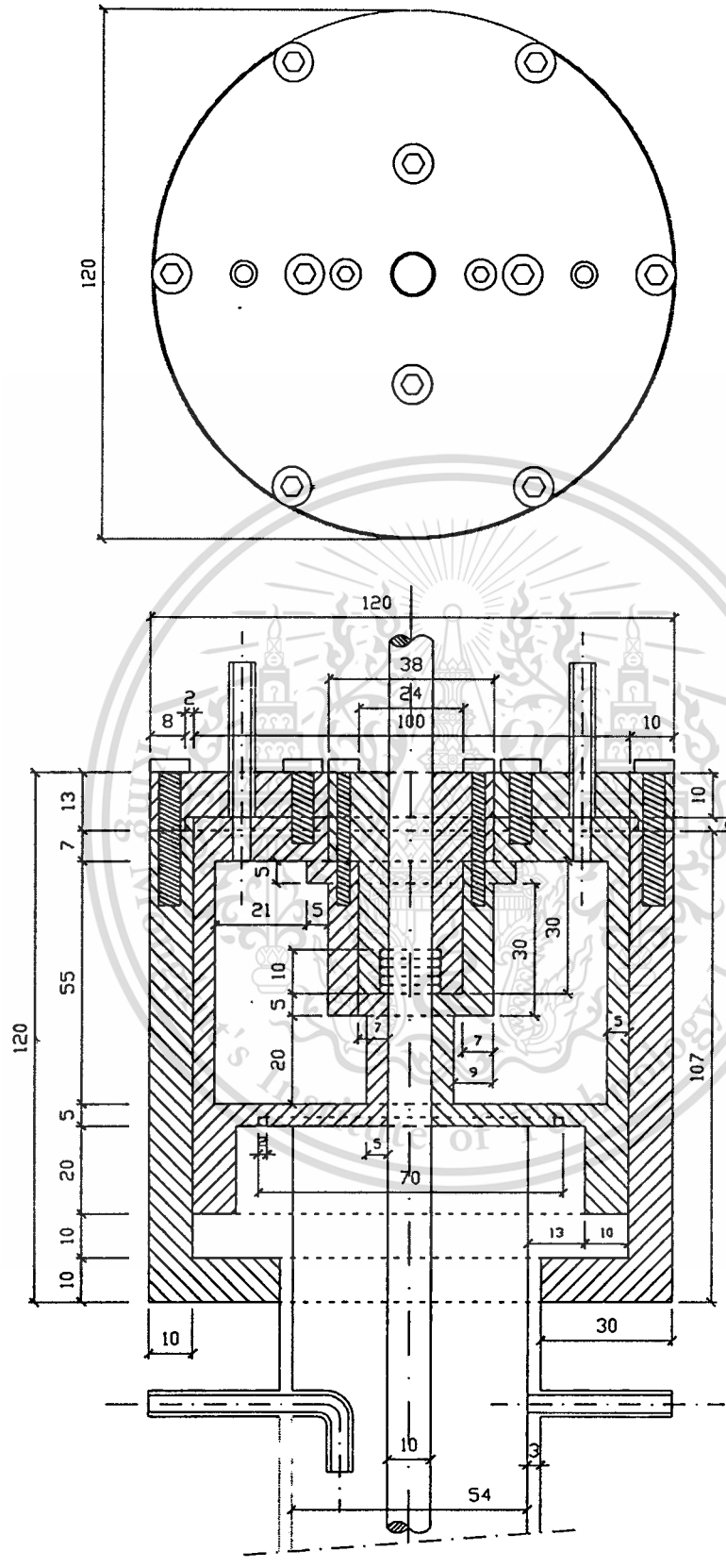

Figure 4.32 Top section of reactor chamber

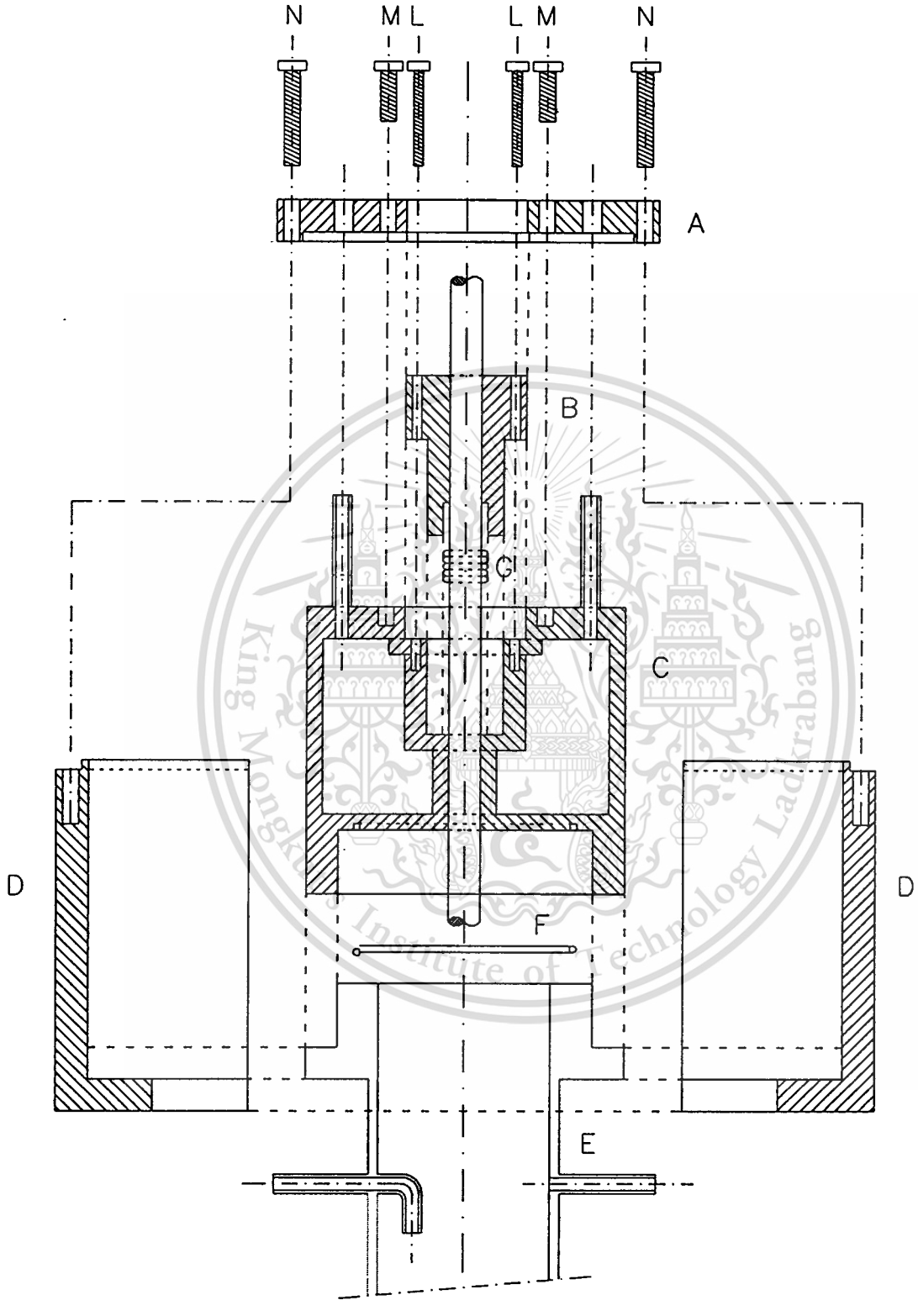

Figure 4.33 Top section of reactor chamber

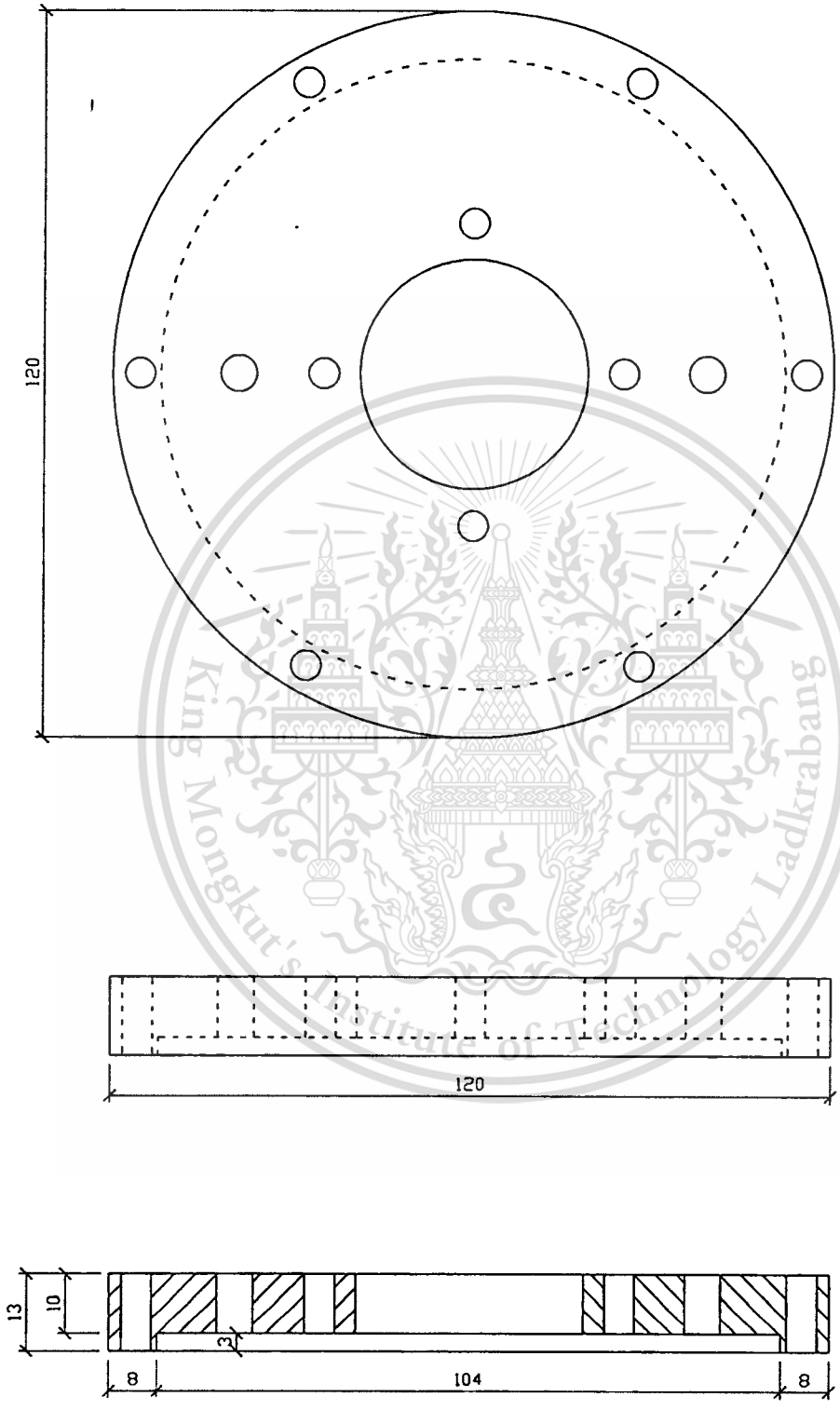

Figure 4.34 Part A of the top section

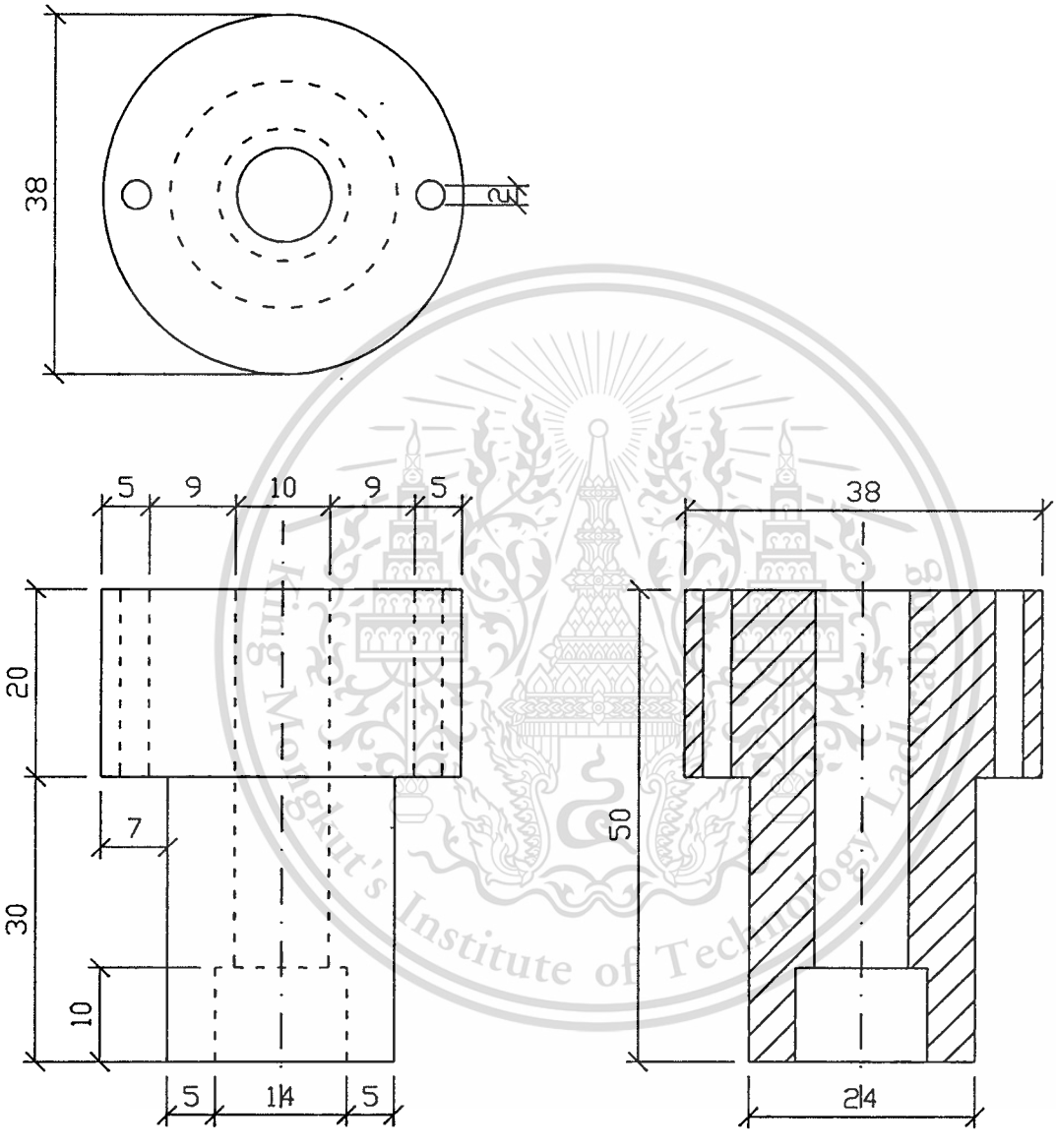

Figure 4.35 Part B of the top section

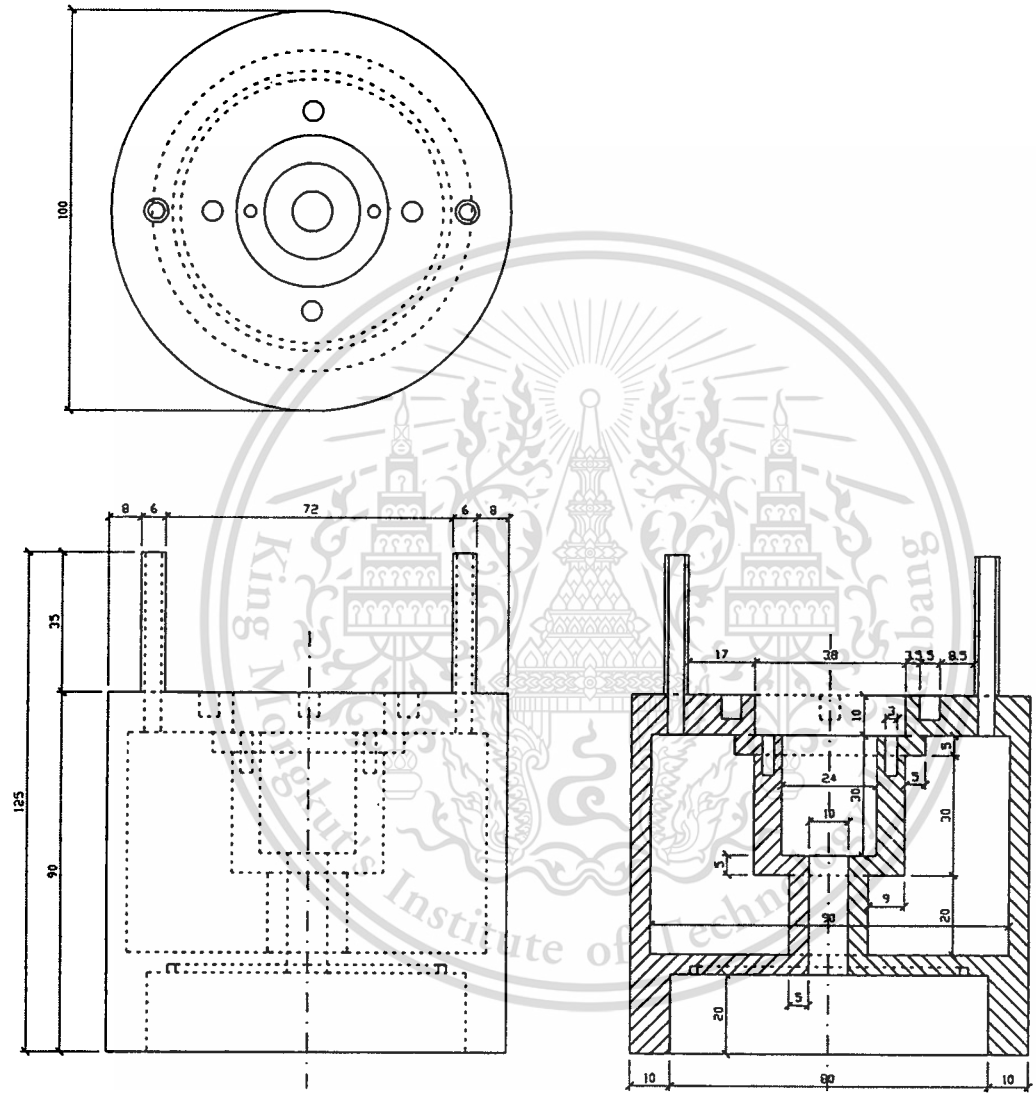

Figure 4.36 Part C of the top section

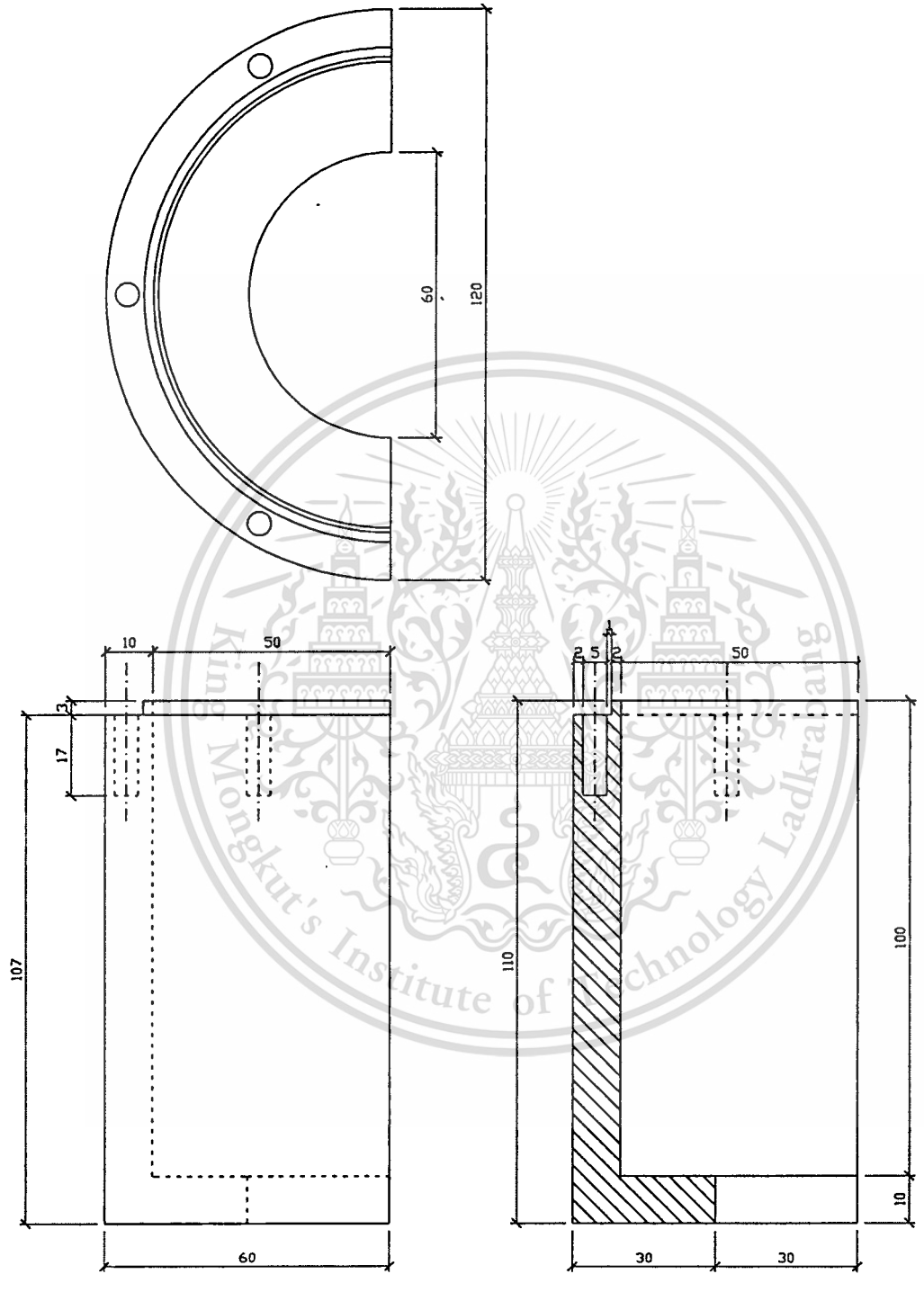

Figure 4.37 Part D of the top section

The middle section is the cracking reaction zone which can be regarded as a trickle bed reactor. It is composed of a power-driven shaft with series of radiating blades, alternately laying down at the angle of 45 degree as shown in Figure 4.38. There are ten blades arranging along the whole length of the reactor (600 mm). These blades were twisted at the angle of 30 degree. Polyethylene is molten in the single screw extruder at about 200^{o}C, and then introduced continuously over 8 hours into the reactor chamber at a constant feeding rate (90 g/h). The feeding point from the extruder is positioned on the top of the middle section. The molten polyethylene can be gradually dropped by gravity from the feeding part to the first blade and further down to the next blade continuously. On rotating, the flow of the material is retarded by these blades, and hence it remains in the reaction zone with a sufficient contact time for cracking reaction. Additionally, these blades can flutter the material to the surface of the reactor. The temperature at the surface of the reactor is high and can facilitate cracking of polyethylene. Whereas, the temperature of the inner reactor is gradually decreased from the surface of reactor. However, the gaseous products having high temperatures can be lifted not only by the blades at the time of rotating but also by the carrier gas. These gaseous products contact and transfer the heat to the new feeding material on the blades and the surface of the reactor, resulting in a high cracking efficiency throughout the reactor. Relatively larger cracked products can be condensed and dropped back to the reaction zone. These can further crack to products with molecular weight low enough to leave the exit of reactor without condensing. The entrance of carrier gas stream is positioned at the bottom of the middle section and the direction of flow is counter-current with the flow of the polyethylene feed. Carrier gas is used for replacing the air in the reactor chamber at the beginning of the process and leading the cracked products to the condenser section during the process. The exit point of the gaseous products is positioned on the top of the middle section across the feeding point.

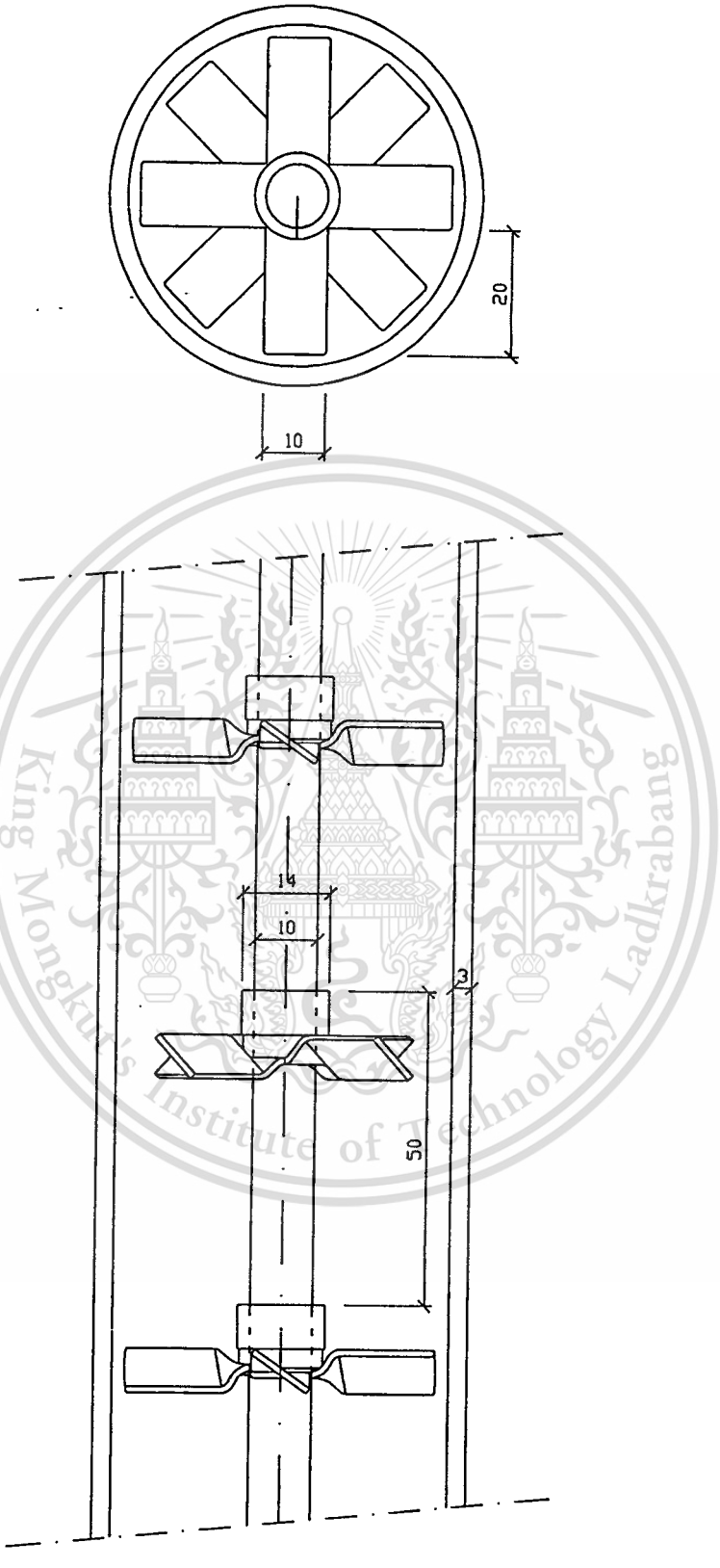

Figure 4.38 Middle section of the reactor chamber

The bottom section, Figure 4.39, consists of a small screw extruder used for discharging waxy materials and spent catalyst. The rotation of the exit screw will lead the waxy materials with spent catalyst to the bottom exit of the reactor chamber. The main concept of this exit screw is only used for conveying the products and reducing the torque of screw rotation, while the mixing quality is unnecessary. When the waxy materials are reduced, the high ratio of used solid catalyst cause the higher torque. The rotation of motor can be retarded due to the overload torque. This problem can be reduced by designing the exit screw which has constant channel depth.

The waxy materials in this section also have an advantage of blocking and preventing the leakage of gas through the bottom exit of the reactor chamber. When the reaction temperature is increased, the output rate of waxy materials is decreased. In addition, the viscosity of waxy materials is reduced due to their low molecular weight when cracking is carried out at high temperatures. Accordingly, the die of the screw is designed to be small (~0.5 mm) for compensating with the small output rate. When the waxy materials are increased, the die can be replaced by those with bigger hole, otherwise the waxy material will accumulate in the reactor and may block the entrance of the carrier gas.

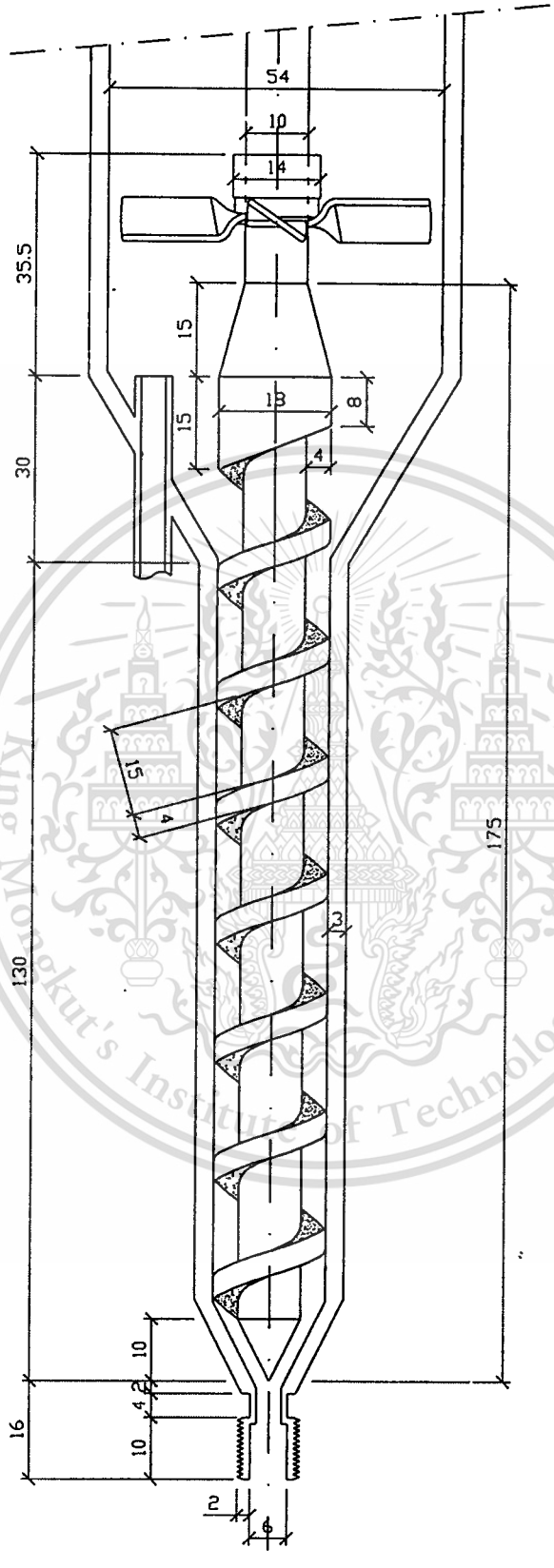

Figure 4.39 Bottom section of the reactor chamber

4.4.1.3 Condenser

Figure 4.40 shows the schematic diagram of condenser designed and used in the present study. There are two units connected in series. When the cracked products enter the first condenser, it will contact with the cooling pipe at 20°C. The relatively high molecular weight hydrocarbon can subsequently condense and drop down to the bottom of the condenser. The three-way connector is used for pressure equallizing, which allows the liquid products to flow into a product collector. The smaller molecular weight products would remain in the gas phase and will leave the 20°C condenser to the chilling condenser (-5°C). Mosts of the light gasoline fraction are collected in this condenser. The remaining gaseous products containing mostly C_3-C_5 are separated from the liquid fraction and then passed through an on-line GC as shown in Figure 3.6.

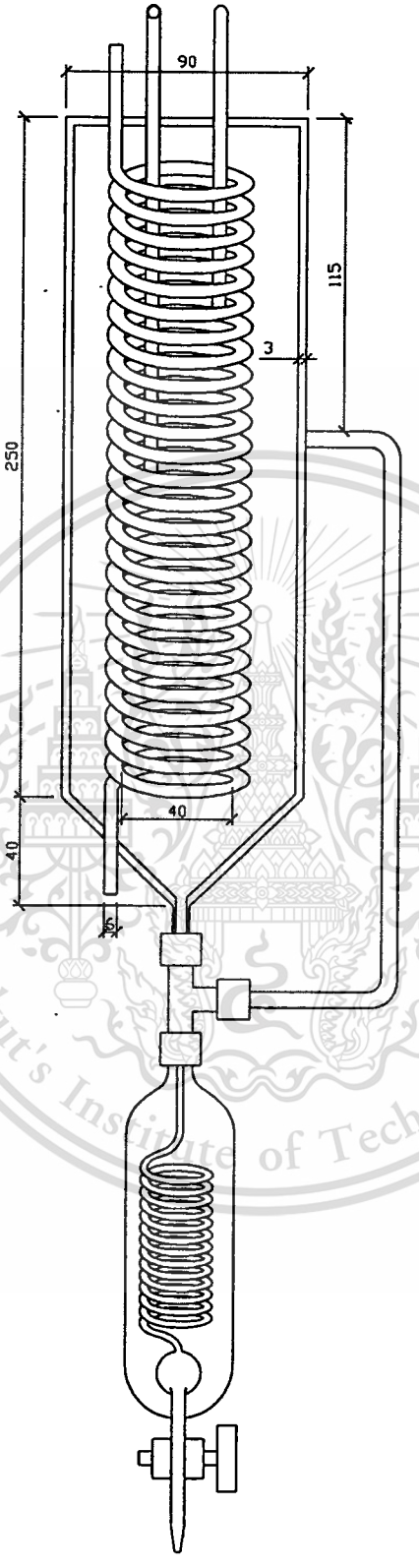

Figure 4.40 Condenser

4.4.2 Continuous catalytic cracking

Cracking of polyethylene was investigated in a continuous system at 350-430°C under helium as a carrier gas with a flow rate of 30 ml/min. Beta (C) was used as the catalyst in this system. The cracked products are classified into 4 groups: gas, light cracked liquid (LCL), heavy cracked liquid (HCL), and waxy materials. Liquid products can be classified into 2 groups: cooling liquid at –5°C (LCL) and 20°C (HCL). The waxy materials are determined from the weight of the output material obtained from the bottom of reactor chamber subtracted the catalyst weight. The amount of each liquid products is determined from the weight of products at 20°C and –5°C, respectively. The amount of gaseous products is determined by subtracting the weight of all of liquids and waxy materials. The gas yield can be defined by the relation;

$$\text{Gas (wt\%)} = 100 - [\,\text{LCL (wt\%)} + \text{HCL (wt\%)} + \text{Wax (wt\%)}\,]$$

Tables H.1-H.2 show the yields of products from the thermal and catalytic cracking using Beta (C) at 350-430°C.

4.4.2.1 Time on stream

Figure 4.41 shows the yields of products from cracking of polyethylene with time on stream. In this reaction, the temperature was set at 400°C. It can be noticed that waxy materials and liquid products at first hour were relatively low and gradually increased to a constant % weight after 4 hours on stream. On the other hand, the amount of gaseous products was high at the first hour and slowly decreased during the 2-4 hours on stream. From the above results, it can be explained that at the begining of the reaction the entering molar flow rate (material input) was higher than the exit molar flow rate (material output) because the waxy materials still accumulated in the reactor. However, after 4 hours, the waxy materials and used catalyst reached the bottom of the reactor and could be removed by the designed exit screw (section 4.4.1.2). The material input was then balanced with the material output. This indicated that the reaction approached a steady state. Additionally, catalyst deactivation was not observed because the coking catalyst can be continuously removed and replaced by newly fed catalyst.

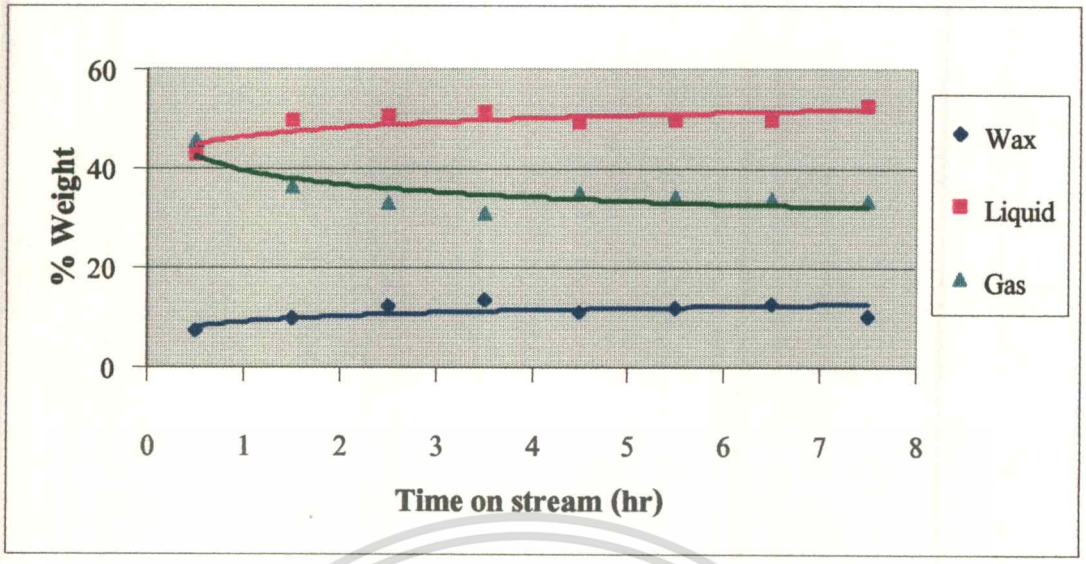

Figure 4.41 Yields of products from catalytic cracking of polyethylene using H-Beta (C) as a function of time on stream; *Reaction conditions: Temperature, 400 °C; Polyethylene with catalyst, 90 g/h; Catalyst/polymer ratio, 2%; Helium 30 ml/min*

4.4.2.2 Effect of reaction temperature

The effect of reaction temperature on the yields of products was investigated at temperatures range between 350°C and 430°C with and without catalyst. The average % weight from the thermal cracking reaction is shown in Figure 4.42. For thermal reaction, the amount of waxy materials was extremely large over the range of reaction temperatures studied. The liquid products could not be obtained at 350°C due to the low temperatures allow only the cleavage of polyethylene chain ends to give gaseous products. When the temperature was increased, the total of liquid products increased slightly and could be obtained only about 20% by weight at 430°C. When comparing the liquid products, the yield of light cracked liquid products was extremely small, as compared to that of the heavy cracked liquid products for the temperature range from 375°C to 430°C. These results again suggested that the thermal cracking of polyethylene took place via a free radical mechanism, causing random scission of polymer chains as discussed earlier in the batch process (section 4.3.1).

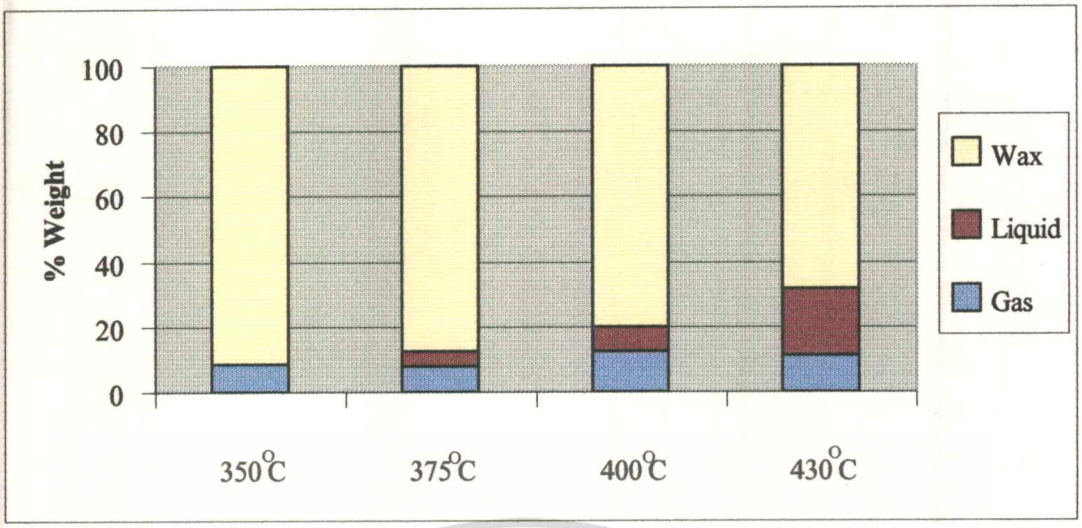

Figure 4.42 Yields of products from thermal cracking of polyethylene at reaction temperature between 350°C and 430°C; *Reaction conditions: Polyethylene, 90 g/h; Helium, 30 ml/min*

The average % weight from the catalytic cracking reaction is shown in Figure 4.43. With the addition of Beta (C) ratio at 5%, the waxy materials decreased significantly as compared with those of thermal cracking. However, the amount of waxy materials obtained from catalytic cracking at 350°C was similar to that of thermal cracking. This result indicated that there is no significant catalytic activity at this temperature, presumably due to an insufficient activation energy for the formation of carbocation intermediate on the polyethylene chains. In addition, it was probably due to the reduced mobility of polyethylene chains to diffuse into zeolite pore at low temperatures. Surprisingly, when temperature reached at 375°C, the waxy materials were rapidly decreased from 84.93% to 19.81%. On the other hand, the gaseous and total liquid products were amply increased. This indicated that H-Beta (C) was effective for the cracking of polyethylene at the reaction temperature above 375°C.

As mentioned earlier (section 4.3.1), the products obtained from Beta (C) at temperature from 375°C to 430°C were mainly liquid products due to the large pore sizes of Beta which allows formation of hydrocarbons contain C_5-C_9.

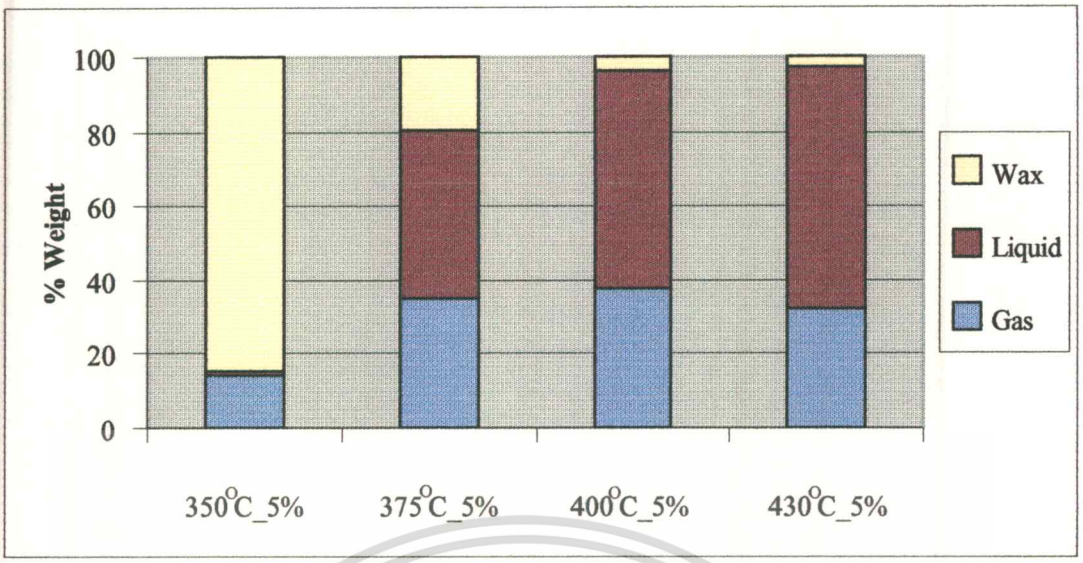

Figure 4.43 Yields of products from catalytic cracking of polyethylene using H-Beta (C) at reaction temperature between 350°C and 430°C; *Reaction conditions: Polyethylene with catalyst, 90 g/h; Catalyst/polymer ratio, 5%; Helium, 30 ml/min*

The effect of reaction temperature as a function of time on stream is shown in Figure 4.44. It can be observed that the higher yield of liquid products was obtained at higher temperatures. The amount of liquid products was almost constant at 430°C during the all of reaction times. However, at 375° and 400°C, amounts of liquid products were gradually increased and remained constant after 4 hours on stream. It can be explained that the higher temperatures accelerated the cracking reaction [10], and a steady state could be reached rather rapidly. This was because a high amount of gaseous products can be produced and less waxy products were accumulated. Additionally, the high amount of gaseous products which flew counter-current with the new feeding material, would transfer a larger amount of heat to these polymers melt. As a result, the high efficiency of cracking and a rapid steady state can be observed.

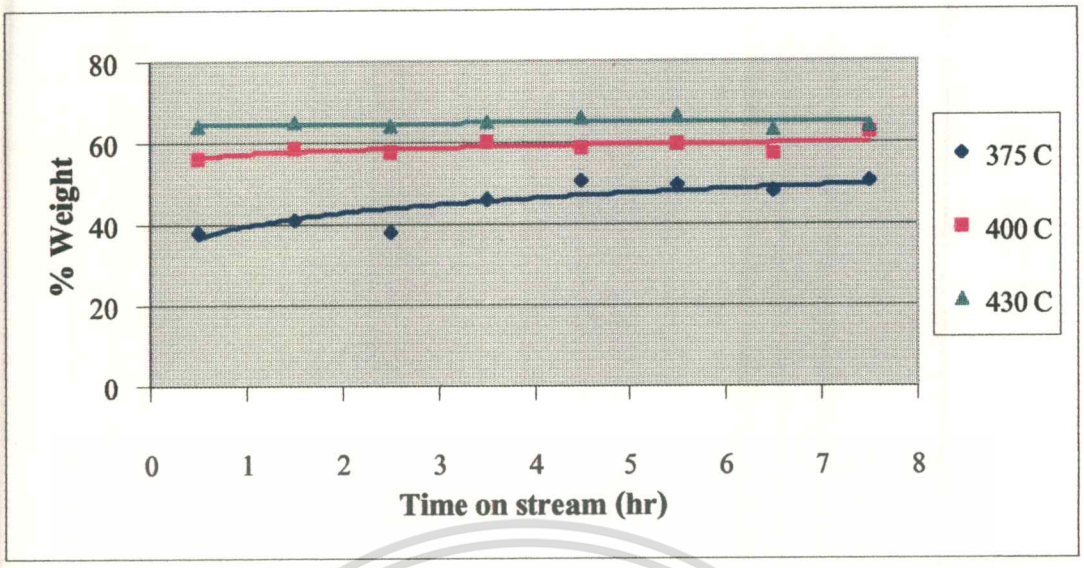

Figure 4.44 Effect of reaction temperature on the yields of total liquid products obtained over H-Beta (C) as a function of time on stream; *Reaction conditions: Temperature, 375-430 ^{o}C; Polyethylene with catalyst, 90 g/h; Catalyst/polymer ratio, 5%; Helium, 30 ml/min*

4.4.2.3 Effect of catalyst/polymer ratio

The catalytic cracking of polyethylene as a function of catalyst/polymer ratio is shown in Figure 4.45. It was found that the reaction using catalyst ratio at 5% produced higher amount of liquid products than catalyst ratio at 2% and with no catalyst, respectively. In contrast, the waxy materials were lower. It was suggested that the yield of liquid products (aromatic, aliphatic) increased with catalyst/polymer ratio because a higher contact time with the catalyst would promote further cracking of waxy materials, resulting in an increase in the yield of lighter products. However, no significant change was observed for the amount of gaseous products. This was because the increase in contact time accelerated secondary reactions of the hydrocarbon fragments such as isomerization, aromatization. More aromatic products were presumed to be formed from the primary products [29]. The cracking of aromatic products in liquid fractions to gaseous products seemed unlikely to occur. This was because the cleavage of the aromatic rings would be difficult because of its great stability [35]. In addition, the gaseous products, especially C_3 and C_4, could be also converted to aromatics. However, the large pore zeolite Beta can control the products in the range of liquids as discussed previously in section 4.3.1. From the above discussion, it can be concluded that, the shape selectivity of zeolites is an important factor for

controlling the yields of products because the obtained aromatic yields were relatively low (as further discussion in section 4.4.3).

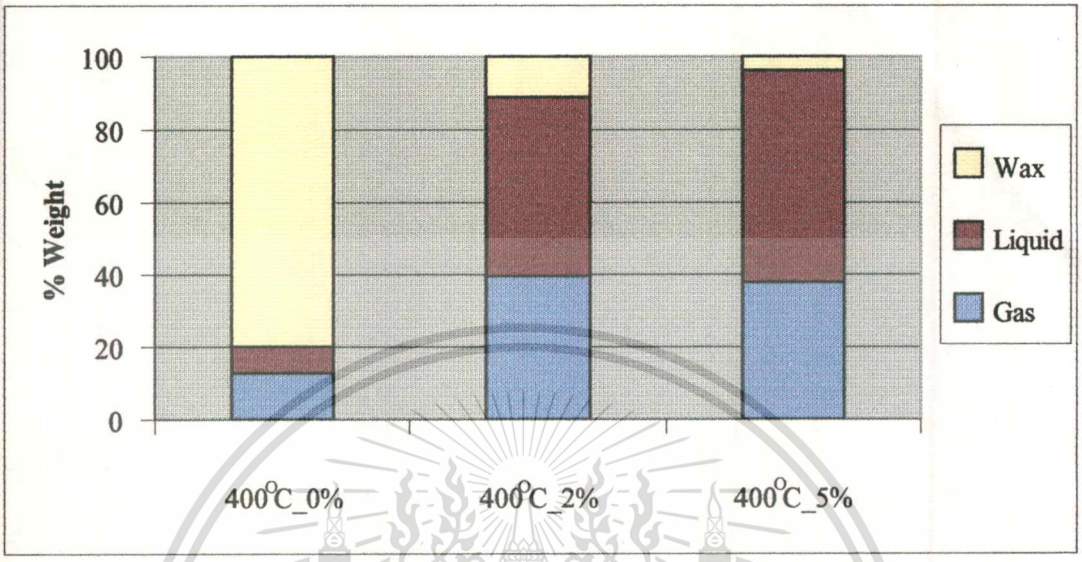

Figure 4.45 Yields of products from catalytic cracking of polyethylene using H-Beta (C) at catalyst/polymer ratio of 0-5%; *Reaction conditions: Temperature, 400 °C; Polyethylene with catalyst, 90 g/h; Helium, 30 ml/min*

In the case of catalyst/polymer ratio as a function of time on stream (Figure 4.46), the amount of liquid products obtained from thermal cracking was extremely small, as compared with catalytic cracking. Whereas, a similar trend of the effect of catalyst/polymer ratio could be observed in the reaction using catalyst/polymer ratios of 2% and 5%. However, the ratio of 5% accelerated the cracking reaction than ratio of 2% and a rapid steady state could be observed. The same reason could be applied as in the case of temperature.

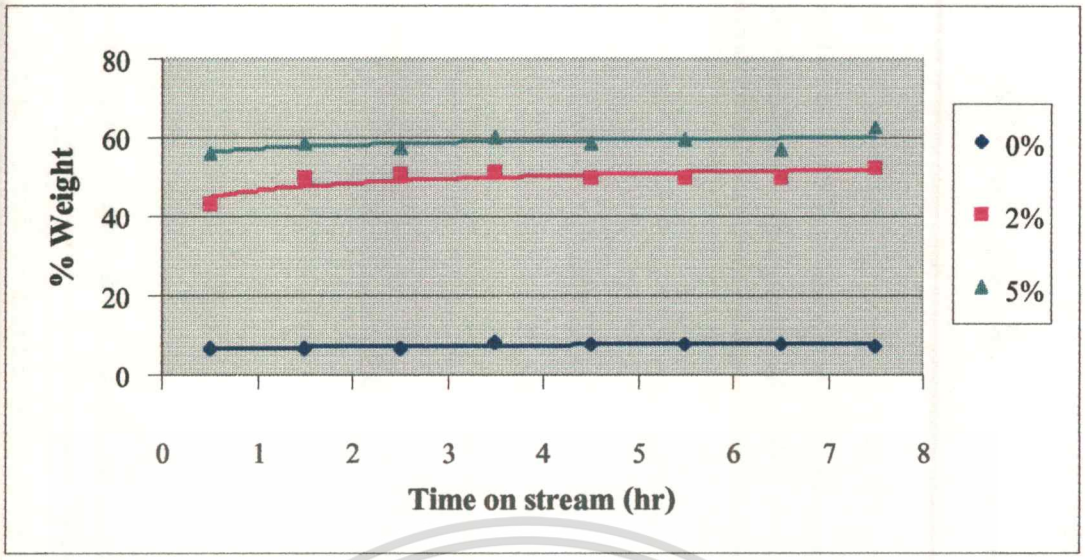

Figure 4.46 Effect of catalyst/polymer ratios on the yields of total liquid products obtained over H-Beta (C) as a function of time on stream; *Reaction conditions: Temperature, 400 °C; Polyethylene with catalyst, 90 g/h; Catalyst/polymer ratio, 0-5 %, Helium, 30 ml/min*

4.4.2.4 Composition of the gaseous products

Product distribution of the gaseous products from cracking of polyethylene at 350-430°C in continuous process is shown in Table H.5. For thermal cracking at 350°C (Figure 4.47), it is shown that the gaseous products were distributed in a wide range of carbon number from C_3 to C_6^+. When the temperature was increased, the yielding of C_6^+ components decreased. It can be presumably attributed to the fact that, at high temperatures, the high molecular weight hydrocarbons could further crack into smaller hydrocarbons, which were thermodynamically favored for free radical intermediate mechanism.

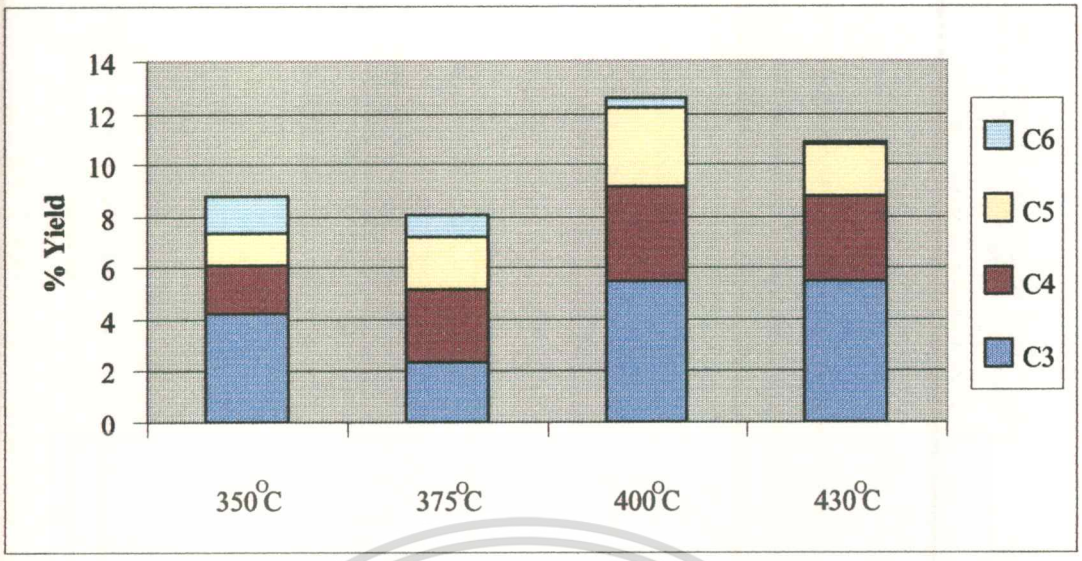

Figure 4.47 Distribution of gaseous products from thermal cracking of polyethylene at reaction temperature between 350°C and 430°C; *Reaction conditions: Polyethylene, 90 g/h; Helium, 30 ml/min*

In catalytic cracking over Beta (C), 350°C, the product distribution was similar to thermal cracking products as shown in Figure 4.48. In a similar manner, the yielding of C_6^+ component decreased and C_3, C_4 and C_5 components increased when the reaction temperature was increased.

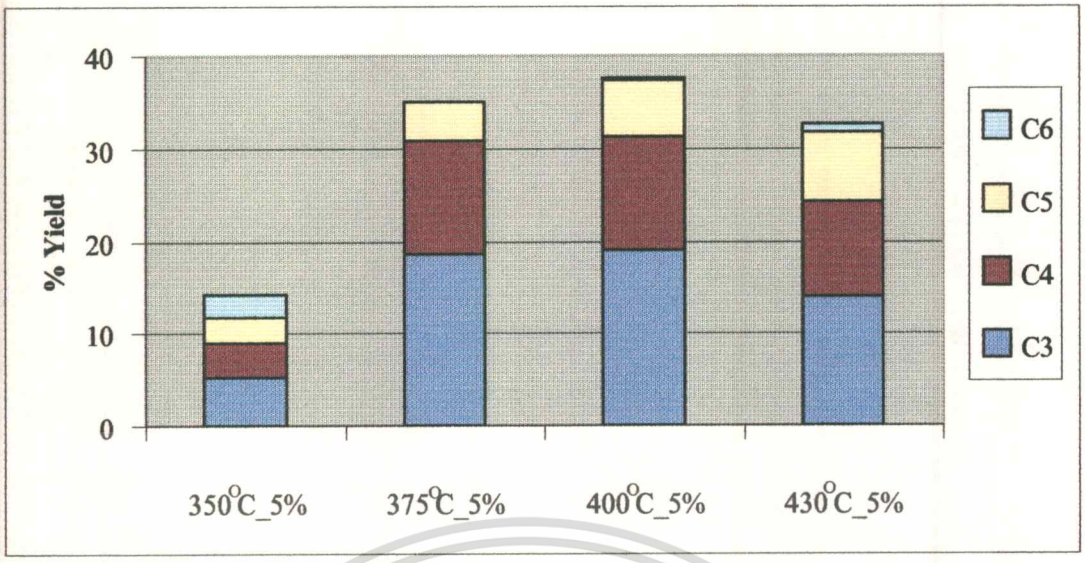

Figure 4.48 Distribution of gaseous products from catalytic cracking of polyethylene using H-Beta (C) at reaction temperature between 350°C and 430°C; *Reaction conditions: Polyethylene with catalyst, 90 g/h; Catalyst/polymer ratio, 5 %; Helium, 30 ml/min*

4.4.2.5 Composition of the liquid products

Tables H.6-H.8 show the product distribution of total liquid from cracking of polyethylene at 350-430°C in continuous process. In the case of thermal cracking (Figure 4.49), the liquid products could not be obtained at 350°C. As the temperature of reaction was increased, the liquid products were similarly distributed over a wide range of carbon number at each temperature. This supported the earlier discussion (section 4.3.3) that the control of product distribution cannot be observed since the reaction proceed via free radical intermediates.

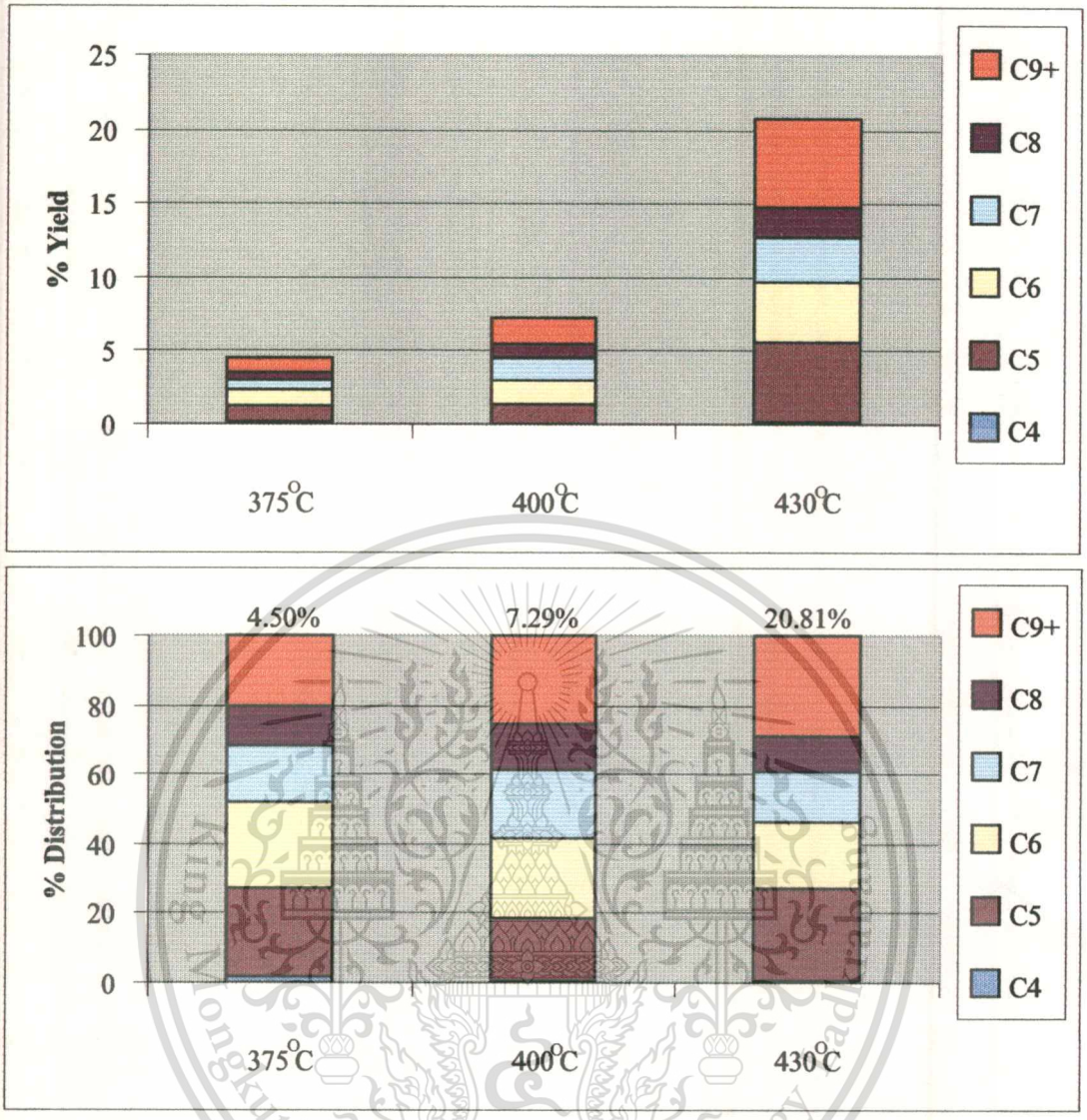

Figure 4.49 Yields and distribution of liquid products from thermal cracking of polyethylene at reaction temperature between 350°C and 430°C; *Reaction conditions: Polyethylene, 90 g/h; Helium, 30 ml/min*

In the case of catalytic cracking over Beta (C), Figure 4.50, the major components of liquid products at 350°C are C_9^+ hydrocarbon. This can be attributed to the effect of low mobility of polyethylene into the zeolite pores. At this temperature, the polymeric fragments had high viscosity, therefore, the diffusion into the pore was difficult. Since the large chain molecules could not penetrate the pore of zeolite, the cracking reaction should be occurred only on the external surfaces of the zeolite. When increasing the reaction temperature, the distribution of liquid products became narrow. The component of C_5 was increased and that of heavier

hydrocarbons (C_9^+) was decreased. As discussed earlier in the batch process, the liquid products in the range of (C_5-C_9^+) can be selectively obtained when using zeolite Beta as the catalyst.

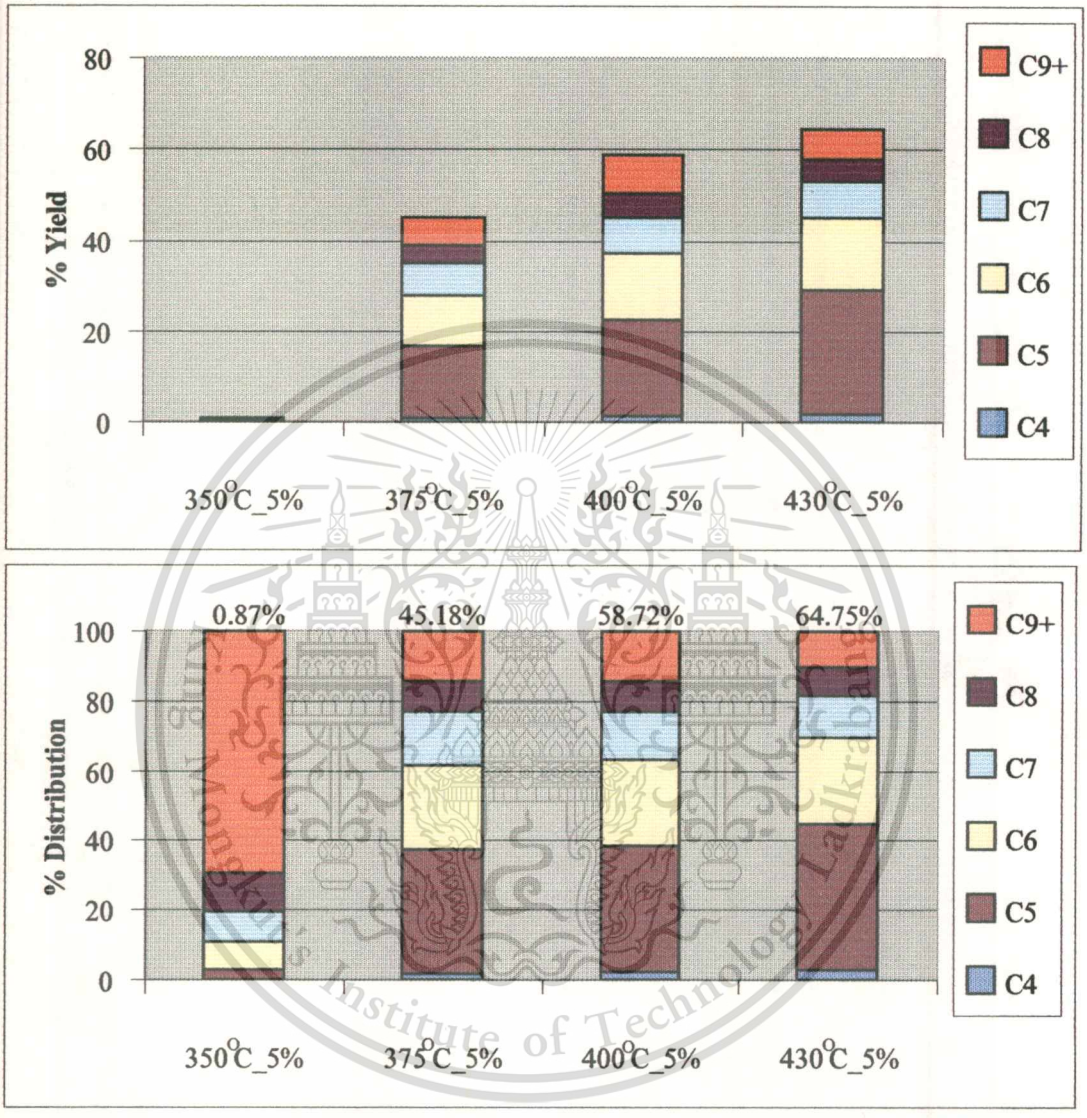

Figure 4.50 Yields and distribution of liquid products from catalytic cracking of polyethylene using H-Beta (C) at reaction temperature between 350°C and 430°C; *Reaction conditions:Polyethylene with catalyst, 90 g/h; Catalyst/polymer ratio, 5%; Helium, 30 ml/min*

4.4.3 NMR results

A nuclear magnetic resonance (NMR) technique has been developed for determining the octane number from the composition of gasoline. Since the determination of gasoline octane number using the ASTM test engine required large quantities of the samples. The NMR technique can be used for limited amounts of samples. These measurements are performed using a Bruker AVANCE DPX300 NMR spectrometer with 300-MHz proton resonance frequency. A typical NMR spectrum of a gasoline fraction is shown in Figure 4.51.

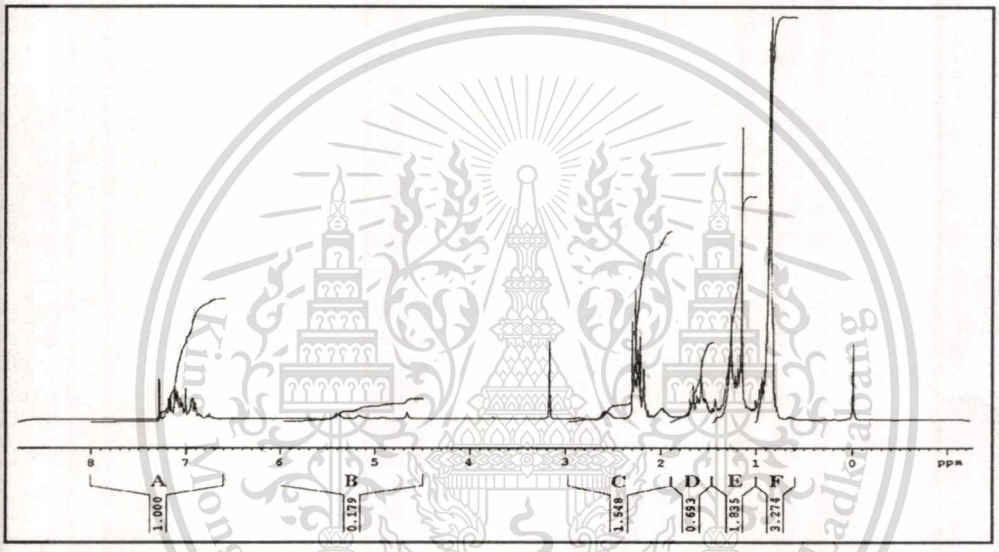

Figure 4.51 NMR spectrum of a gasoline sample

The hydrocarbon species including aromatics, paraffins and olefins which are major components of petroleum products are estimated using literature correlations developed by Myers *et at.* [50]. In these equations, the chemical shift scale is divided into 6 regions (Figure 4.51), marked as A to F. A, B, C, D, E and F representing the integrated area of the spectral regions are used for the octane number prediction as shown in Table 4.3.

Table 4.3 NMR spectral regions

Agent	Proton type	Chemical shift region (ppm)
A	Ring aromatics	6.6-8.0
B	Olefin	4.5-6.0
C	α-methyl	2.0-3.0
D	Methine (paraffins)	1.5-2.0
E	Methylene (paraffins)	1.0-1.5
F	Methyl (paraffins)	0.6-1.0

These equations include correction factors for the varying densities of the different hydrocarbon types which can be defined by the relations:

$$\text{Aromatics, vol.\%} = \left[\frac{0.97\left(A + \frac{C}{3}\right) \times 100}{0.97\left(A + \frac{C}{3}\right) + 1.02\left(D - 2B + \frac{E}{2} + \frac{F}{3}\right) + 3.33B} \right] \quad \text{-------(4.1)}$$

$$\text{Paraffins, vol.\%} = \left[\frac{1.02\left(D - 2B + \frac{E}{2} + \frac{F}{3}\right) \times 100}{0.97\left(A + \frac{C}{3}\right) + 1.02\left(D - 2B + \frac{E}{2} + \frac{F}{3}\right) + 3.33B} \right] \quad \text{--------(4.2)}$$

$$\text{Olefins, vol.\%} = \left[\frac{3.33B \times 100}{0.97\left(A + \frac{C}{3}\right) + 1.02\left(D - 2B + \frac{E}{2} + \frac{F}{3}\right) + 3.33B} \right] \quad \text{--------(4.3)}$$

In addition, Myers *et al.* [51] also developed correlations for an 'isoparaffin index', and octane number. The isoparaffin index represents the estimated yields of branching which are the measured ratios of CH_3/CH_2 in the paraffins. The CH_3/CH_2 ratio is thus taken as a principal entry in an equation to calculate the octane number. The octane rating of gasoline (sample) is primarily arised from its isoparaffin and aromatic contents. By increasing the aromatic content, the blender can increase the octane quality to the required level. Aromatics are used because their individual octane ratings tend to be high. Another possible contributor to the high octane number would be

the olefins. However, among the three hydrocarbon types (paraffins, aromatics, and olefins), olefin concentration is usually low (~10%) in petroleum fraction, which is fortunate because the olefin groups are determined with the least precision. Thus, olefin concentration is ignored in the linear regression analysis. A multiple linear equation is developed to express the octane number as a linear combination of the isoparaffin index, the aromatic content (vol%), the lead content (g/gal), and the sulfur content (wt%)

Isoparaffin index = CH_3/CH_2 = (F/3) / (E/2) --------**(4.4)**

RON = 80.2 + 8.9(isoparaffin index) + 0.107aromatics(vol.%)
+ 2.93lead(g/gal) –13.4sulfur(wt%) --------**(4.5)**

MON = 70.8 + 10.0(isoparaffin index) + 0.101aromatics(vol.%)
+ 3.27lead(g/gal) – 11.1sulfur(wt%) --------**(4.6)**

In the case of cracking of polyethylene, lead and sulfur contents are assumed to be negligible in the final gasoline range products. Therefore, equations (4.5) and (4.6) can be rewritten as:

RON = 80.2 + 8.9(isoparaffin index) + 0.107aromatics(vol.%) --------**(4.7)**

MON = 70.8 + 10.0(isoparaffin index) + 0.101aromatics(vol.%) --------**(4.8)**

4.4.3.1 Hydrocarbon types and gasoline quality

Tables J.1-J.2 show hydrocarbon species and the octane number of the gasoline fraction from catalytic cracking of polyethylene using Beta (C) as the catalyst which are determined by NMR analysis. Similar trends in hydrocarbon types of the light cracked liquid products are observed in the reaction at temperatures ranging from 375-430°C. These liquid products contained large amounts of isoparaffin and olefin, with a small amount of aromatics. Paraffins and olefins are the predominant species of 40-50% mol with some aromatics of 4-6% mol. The high content of isoparaffin and olefin in product indicated a high progress of catalytic cracking reaction. One main indication of gasoline quality is the degree of branching in the paraffins, since the isoparaffins have much greater octane numbers than their normal counterparts. This is becoming more important due to the recently mandated reduction of aromatics content in the gasoline.

The RON and MON values are used as an index for the quality of the liquid products. The higher the octane number, the higher the efficiency for antiknocking in mobile engine [35]. The light cracked liquid products possess an estimated octane number about 110-140 which can be readily used to blend with the lower octane number products to obtain a required octane level. The high isoparaffin index causes high octane number products which can be calculated from Equations (4.7) and (4.8).

For the heavy cracked liquid products (HCL, cooled at 20°C), the amount of aromatics was higher than the light cracked liquid products (LCL, cooled at -5°C), while the amounts of olefins and isoparaffin were lower. However, aromatic content was much lower than the commercial gasoline as shown in Figure 4.52.

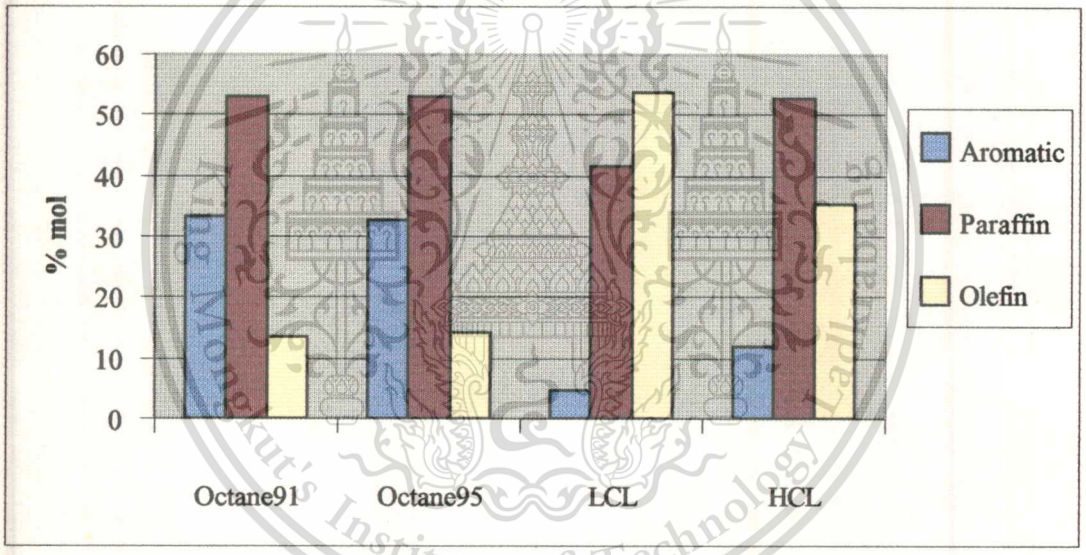

Figure 4.52 Hydrocarbon types of commercial gasoline and liquid products using H-Beta (C);
Reaction conditions: Temperature, 430 °C; Catalyst/polymer ratio, 5%;
Octane 91 and 95 products obtained from Petroleum Authority of Thailand

The product selectivity of the heavy cracked liquid products obtained from catalytic cracking over H-Beta (C) as a function of temperature is shown in Figure 4.53.

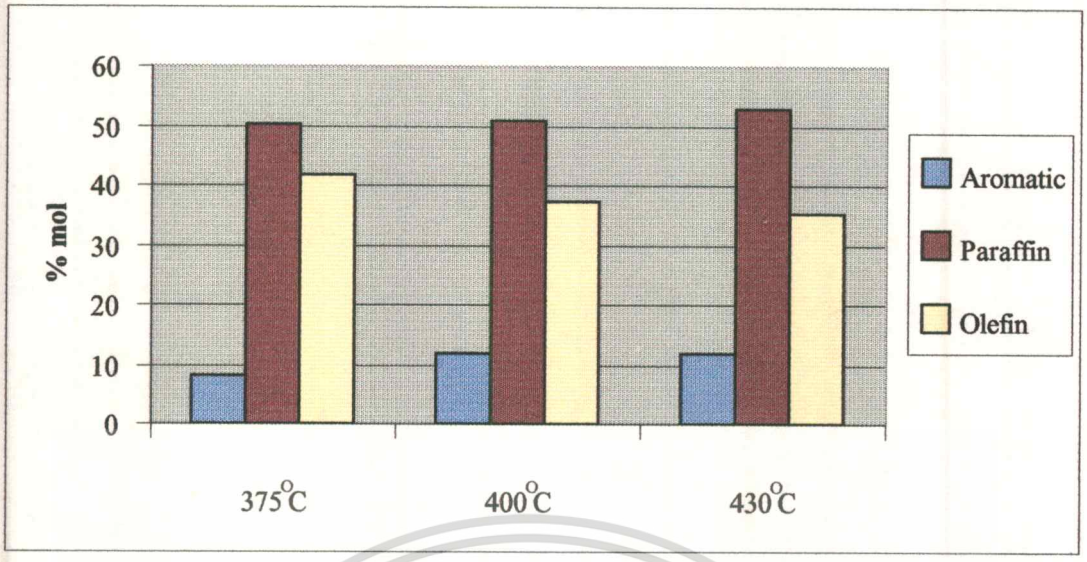

Figure 4.53 Hydrocarbon types of heavy cracked liquid products using H-Beta (C) at different temperatures; *Reaction conditions: Temperature, 375-430 °C; Polyethylene with catalyst, 90 g/h; Catalyst/polymer ratio, 5%; Helium, 30 ml/min*

When the reaction temperature was increased, more aromatics were produced, whereas the yields of the olefins decreased. The increase in the aromatic composition indicated that the C_4, C_5, and C_6^+ aliphatics formed in the cracking of polyethylene could further react to give aromatic hydrocarbons. The aromatics could be formed from the direct dehydrocyclization of C_6^+ aliphatics such as mono- and di-methyl alkane and their unsaturated derivatives and also from the oligomerization subsequent aromatization of the C_3 and C_4 hydrocarbons. In addition, hydrogen transfer from the aromatization might be consumed by the hydrogenation of olefins, resulting in an increased paraffin contents. However, regarding to the proportion of branched to normal paraffins, it was shown that the light cracked liquid products (LCL) had higher isoparaffin index than heavy cracked liquid products (HCL), possibly due to the decreased yielding of higher molecular weight hydrocarbon chains.

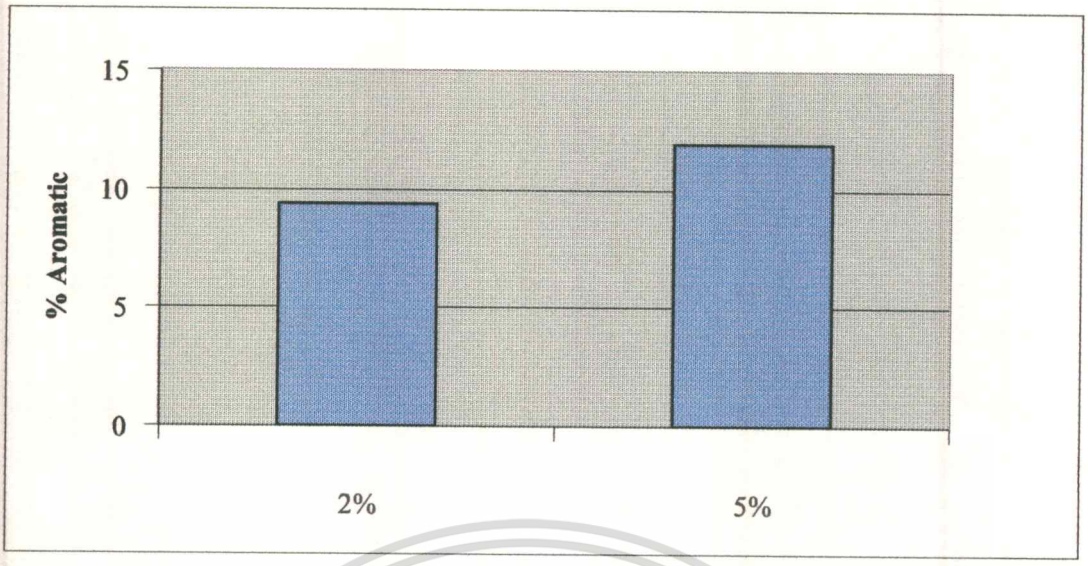

Figure 4.54 Aromatic selectivity of heavy cracked liquid products using H-Beta (C) at different catalyst/polymer ratios (or contact times); *Reaction conditions: Temperature, 400 °C; Polyethylene with catalyst, 90 g/h; Catalyst/polymer ratio, 2-5%; Helium 30 ml/min*

In HCL, the products obtained from reaction using 2% Beta contain lower aromatics than that using 5% Beta (Figure 4.54). The relative yield of aromatic fractions increased with catalyst/polymer ratio, because the longer contact time promoted the secondary reaction for the cracked products. These results indicated that isomerization and aromatization to form aromatics were important secondary reactions. Once the aromatics were formed, cracking of aromatic fractions was limited. However, these gasoline fractions possessed an environmentally favorable qualities, due to the lower aromatic content.

CHAPTER 5

CONCLUSIONS AND SUGGESTION

5.1 Conclusions

In this thesis, the cracking of polyethylene was studied in a batch process, compared with a continuous process using commercial and synthesized zeolites to control the product distribution and enhance high octane products. The main results and general conclusions obtained were reviewed as follows:

1. The significant dependence of the cracking extent on the crystal size of zeolite revealed that the small crystal size caused an increase in the acid sites located on the external surface and also result in fast diffusion of the polymeric chains into zeolite pores. The high acid sites located on the external surface brought about the increase initial rate of cracking. The initial cracked products could easily diffuse into the pores and then cracked in the pores of zeolites. This leaded to an improved diffusion of all hydrocarbon species, resulting in small coke formation. However, the larger crystal size of H-ZSM-5 still showed high activity due to the effect of restricted pore size and structure.

2. The strong acid sites of zeolites were more effective in converting polyethylene to volatile hydrocarbons than the weak acid sites. Alkane was relatively less reactive, therefore, the hydrocarbon chains can be difficultly protonated by the weak acid sites.

3. When the catalyst/polymer ratio was increased, not only the increase in the initial rate of cracking was observed, but also reduced the coke formation. The catalyst/polymer ratio at 20% was suitable for cracking of polyethylene in a batch process.

4. The study on the effect of pore size of zeolites showed that a larger amount of gaseous products in a range of C_3-C_5 was produced over the medium pores of ZSM-5, while mainly liquid products in a range of C_5-C_9^+ were obtained over the large pores of Beta. This clearly showed that product distribution from polyethylene cracking can be controlled by the pore sizes of the zeolites used. The large pore size also caused the higher rate of coke formation than the medium pore size.

5. The rate of cracking over both H-Beta and H-ZSM-5 was so fast and the reaction was nearly completed within 15 minutes residence time. The yield of gas and liquid products could be increased to a considerable extent by operating under helium for thermal cracking reaction and under hydrogen for catalytic cracking reaction.

6. For the continuous process, the continuous flow reactor system comprises a feeder, a reactor chamber, and product collectors. High L/D ratio of the extruder in the range of 20-30 indicated good mixing and good melting capabilities. The reactor chamber designed allows high cracking efficiency together with the separation of waxy materials and spent catalyst. When the waxy materials were reduced, the die of screw at the bottom of reactor chamber was designed to be small (~0.5 mm) for compensating with the small output rate. However, the high ratio of solid catalyst/waxy materials causes the higher torque. The problem of overload torque can be reduced by designing the screw with a constant channel depth.

7. The study on effect of temperature showed that the liquid yield from the reaction over H-Beta increased with rise in temperature. While, in thermal cracking, there was no significant increase in activity over the whole range of reaction temperature studied. In catalytic cracking, the higher temperature accelerated the cracking reaction and more aromatics were produced. In addition, a steady state could be reached rather rapidly. The reaction temperature at 400°C with catalyst/polymer ratio at 2% was preferable because the appropriate waxy materials and low aromatic products were obtained. The light cracked liquid products (LCL) possessed an estimate octane number about 110-140 and contained a large amount of isoparaffins and olefins, with a small amount of aromatics. For the heavy cracked liquid products (HCL), the amount of aromatics was higher, while the amount of olefins and isoparaffin were lower.

8. The reaction pathway for the cracking of polyethylene can be concluded and postulated as followed:

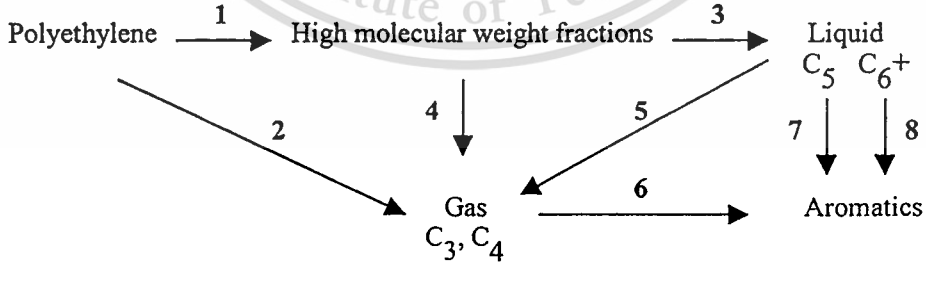

The cracking of polyethylene can be initiated by scission of polymer chains (steps 1 and 2). The resulting fractions of high molecular weights were cracked catalytically to give liquid and gaseous products (steps 3, 4 and 5). The C_6^+ liquid components can be converted into aromatics through the dehydrocyclization (step 8). At higher temperature, the aromatization of C_3/C_4 (step 6) and subsequent dehydrocyclization of C_5 fractions (step 7) could also take place, contributing higher yield of aromatics.

The gasoline products from the investigation were found to be more environmentally favorable (more isoparaffins and less aromatics) than a typical commercial gasoline. This is because, although the aromatics in gasoline have high octane numbers, they are undesirable from an environmental point of views because of the formation of toxic hydrocarbon emissions. Moreover, the high octane products can be readily used to blend with the lower octane products to obtain a required octane level.

5.2 Suggestion for future studies

1. The screw at the bottom section of reactor chamber was designed for only separation. The channel depth is high and constant (0.4 mm). If the amount of waxy materials is relative low, there is not enough material to block the gas stream at the exit of the screw. Therefore, the screw concept should be designed not only for fast separation but also for blocking the gas leakage.

2. Due to the problem of low torque motor, if the viscosity of polyethylene is high, the rotation of screw will be then retarded and the motor will probably slow down. Accordingly, the various feed rates of materials cannot be controlled. For a future study, the various feed rates should be investigated when the high torque motor can be applied.

3. An efficient condenser should be added to improve the separation of liquid products and refine the gasoline fraction. Nevertheless, the large amount of gaseous products was difficult to collect. Accordingly, the gas stream outlet should be designed for simultaneous use of LPG for heating elements.

REFERENCES

[1] Scherzer J., Gruia A.J. **Hydrocracking Science and Technology.** 10th Ed. New York : Marcel Dekker, Inc. 1996.

[2] Dyer A. **An Introduction to Zeolite Molecular Sieves.** New York : John Wiley & Sons, Inc. 1998.

[3] Gates B.C. **Catalytic Chemistry.** New York : John Wiley & Sons, Inc. 1992.

[4] Jacob P.A., Ballmoss R.V. " Framework Hydroxyl Groups of H-ZSM-5 Zeolites." J. Phys. Chem., vol. 86, no. 15, 1982. pp. 3050-3052.

[5] Kim W.J., Lee M.C. and Hayhurst D.T. " Synthesis of ZSM-5 at Low Temperature and Atmospheric Pressure in a Pilot-scale Batch Reactor." Microporous and Mesoporous Materials, vol. 26, 1998. pp. 133-141.

[6] Machado F.J., Lopez C.M., Centeno M.A. and Urbina C. " Template-free Synthesis and Catalytic Behaviour of Aluminium-rich MFI-type Zeolites." Applied Catalysis A : General, vol. 181, 1999. pp. 29-38.

[7] Kokotailo G.T. " Structure of Synthetic Zeolite ZSM-5." [Online]. Available : http://www.iza-sc.ethz.ch/IZA-SC/Atlas/data/models/MFI_mod.html. 1999.

[8] Shamshoum E.S. " Modified Zeolite Beta Method of Preparation." U.S patent no. 5256392, October 1993.

[9] Aguado J., Serrano D.P., Escola J.M., Garagorri E. and Fernandez J.A. " Catalytic Conversion of Polyolefins into Fuels over Zeolite Beta." Polymer Degradation and Stability, vol. 69, 2000. pp. 11-16.

[10] Newsam J.M. " Structural Characterization of Zeolite Beta." [Online]. Available : http://www.iza-sc.ethz.ch/IZA-SC/Atlas/data/models/BEA_mod.html. 1999.

[11] Sachanen A.N., Tikcheyev M.D. **Chemistry and Technology of Cracking.** Translated by Bochtlingk A.A., Brown D.F. and Steik K.T. New York : J.J. Little and Iver Company, Inc. 1932.

[12] Speight J.G. **The Chemistry and Technology of Petroleum.** 2nd Ed. New York : Marcel Dekker, Inc. 1991.

[13] Olah G.A., Molnar A. **Hydrocarbon Chemistry.** New York : John Wiley& Sons, Inc. 1995.

[14] Matar S., Hatch L.F. **Chemistry of Petrochemical Processes.** Houston : Gulf. 1994.

[15] Satterfield C.N. **Heterogeneous Catalysis in Practice.** New York : McGraw-Hill, Inc. 1980.

[16] Gates B.C. **Chemistry of Catalytic Processes.** New York : McGraw-Hill, Inc. 1979.

[17] Maxwell I.E., Stork W.H.J. " Introduction to Zeolite Science and Practice." Stud. Surf. Sci. catal., vol. 58, 1991. pp. 571-579.

[18] Mills M.J. **Plastics : Microstructure, Properties and Applications.** London : English Language Book Society. 1986.

[19] Sinclair K.B. " For Polyolefins : Estimate Gas Phase Production Costs." Hydrocarbon Processing, vol. 64, no. 7, 1985. pp 81-83.

[20] Deanin R.D. **Polymer Structure, Properties and Applications.** Pennsylvania : Cahners Publishing. 1972.

[21] Sack W. " Packaging Container." Chemtech, vol. 18, no. 8, 1988. pp 480-483.

[22] Sodero S.F., Berruti F. and Behie L.A. " Ultrapyrolytic Cracking of Polyethylene-A High Yield Recycling Method." Chemical Engineering Science, vol. 51, no. 11, 1996. pp 2805-2810.

[23] Kaminsky W., Schlesselmann B. and Simon C. " Olefins from Polyolefins and Mixed Plastics by Pyrolysis." Journal of Analytical and Applied Pyrolysis, vol. 32, 1995. pp. 19-27.

[24] Williams E.A., Williams P.T. " The Pyrolysis of Individual Plastics and a Plastic Mixture in a Fixed Bed Reactor." J. Chem. Tech. Biotechnol., vol. 70, 1997. pp. 9-20.

[25] Kaminsky W. " Thermal Recycling of Polymers." Journal of Analytical and Applied Pyrolysis, vol. 8, 1995. pp. 439-448.

[26] Wampler T.P. " Thermometric Behaviour of Polyolefins." Journal of Analytical and Applied Pyrolysis, vol. 5, 1989. pp. 187-195.

[27] Sakata Y., Uddin M.A., Koizumi K. and Murata K. " Thermal Degradation of Polyethylene Mixed with Poly(vinyl chloride) and Poly(ethyleneterephthalate)." Polymer Degradation and Stability, vol. 53, 1996. pp. 111-117.

[28] Uddin M.A., Koizumi K., Murata K. and Sakata Y. " Thermal and Catalytic Degradation of Structurally Different Types of Polyethylene into Fuel Oil." Polymer Degradation and Stability vol. 56, 1997. pp. 37-44.

[29] Ding W., Liang J. and Anderson L.L. " Thermal and Catalytic Degradation of High Density Polyethylene and Commingled Post-consumer Plastic Waste." Fuel Processing Technology, vol. 51, 1997. pp. 47-62.

[30] Liu K., Meuzelaar H.L.C. " Catalytic Reactions in Waste Plastics, HDPE and Coal Studied by High-Pressure Thermogravimetry with On-line GC/MS." Fuel Processing Technology, vol. 49, 1996. pp. 1-15.

[31] Uemichi Y., Ayame A., Kashiwaya Y. and Kanoh H. " Gas Chromatographic Determination of the Products of Degradation of Polyethylene over a Silica-Alumina Catalyst." Journal of Chromatography, vol. 259, 1983. pp. 69-77.

[32] Uddin M.A., Sakata Y., Muto A., Shiraga Y., Koizumi K., Kanada Y. and Murata K. " Catalytic Degradation of Polyethylene and Polypropylene into Liquid Hydrocarbons with Mesoporous Silica." Microporous and Mesoporous Materials, vol. 21, 1998. pp. 557-564.

[33] Negelein D.L., Lin R. and White R.L. " Effects of Catalyst Acidity and HZSM-5 Channel Volume on Polypropylene Cracking." Journal of Applied Polymer Science, vol. 67, 1998. pp. 341-348.

[34] Aguado J., Serrano D.P., Romero M.D. and Escola J.M. " Catalytic Conversion of Polyethylene into Fuels over Mesoporous MCM-41." Chem. Commun., 1996. pp. 725-726.

[35] Takuma K., Uemichi Y. and Ayame A. " Product Distribution from Catalytic Degradation of Polyethylene over H-Gallosilicate." Applied Catalysis A : General, vol. 192, 2000. pp. 273-280.

[36] Arandes J.M., Abajo I., Fernandez I., Azkoiti M.J., Olazar M. and Bilbao J. " Transformation of Several Plastic Wastes into Fuels by Catalytic Cracking." Ind. Eng. Chem. Res., vol. 36, 1997. pp. 4523-4529.

[37] Mordi R.C., Fields R. and Dwyer J. " Gasoline Range Chemicals from Zeolite-catalysed Thermal Degradation of Polypropylene." J. Chem. Soc., Chem. Commun., 1992. pp. 374-375.

[38] Garforth A.A., Lin Y.H., Sharratt P.N. and Dwyer J. " Production of Hydrocarbons by Catalytic Degradation of High Density Polyethylene in a Laboratory Fluidised-bed Reactor." Applied Catalysis A : General, vol. 169, 1998. pp. 331-342.

[39] Park D.W., Hwang E.Y., Kim J.R., Choi J.K., Kim Y.A. and Woo H.C. " Catalytic Degradation of Polyethylene over Solid Acid Catalysts." Polymer Degradation and Stability, vol. 65, 1999. pp. 193-198.

[40] You Y.S., Kim J.H. and Seo G. " Liquid-phase Catalytic Degradation of Polyethylene Wax over MFI Zeolites with Different Particle Sizes." Polymer Degradation and Stability, vol. 70, 2000. pp. 365-371.

[41] บรรจง เลิศโรจน์ชูสิทธิ์, วินิดา อัศวชัยพงษ์ และเอกรินทร์ วรุตบางกูร " ผลของโครงสร้างทางโทโปโลยีของตัวเร่งปฏิกิริยาซีโอไลต์ต่อการสลายตัวด้วยความร้อนของพอลิเอทิลีนชนิดความหนาแน่นสูง." โครงงานพิเศษวิทยาศาสตรบัณฑิต สาขาเคมีอุตสาหกรรม คณะวิทยาศาสตร์, สถาบันเทคโนโลยีพระจอมเกล้าเจ้าคุณทหารลาดกระบัง. 2540.

[42] สิรินทร ศรีธาดาวุฒิ, สุรีย์พร อุตเจริญ และอภิชัย ชาญพาณิชย์การ " การสลายตัวทางความร้อนของพอลิเอทิลีนชนิดความหนาแน่นสูงโดยใช้ซีโอไลต์เป็นตัวเร่งปฏิกิริยา." โครงงานพิเศษวิทยาศาสตรบัณฑิต สาขาเคมีอุตสาหกรรม คณะวิทยาศาสตร์, สถาบันเทคโนโลยีพระจอมเกล้าเจ้าคุณทหารลาดกระบัง. 2541.

[43] Buchanan J.S. " The Chemistry of Olefins Productions by ZSM-5 addition to Catalytic Cracking Units." Catalysis Today, vol. 55, 2000. pp. 207.212.

[44] Buchanan J.S. " Gasoline Selective ZSM-5 FCC Additives: Model Reactions of C_6-C_{10} Olefins over Steamed 55:1 and 450:1 ZSM-5." Applied Catalysis A : General, vol. 171, 1998. pp. 57-64.

[45] Stephen H. " Polymer Cracking." E.P patent no.567292A1, October 1993.

[46] Parrillo D.J., Gorte R.J. J. Phys. Chem., vol. 97, 1993. pp. 8786-8792.

[47] Smirniotis P.G., Ruckenstein E. " Comparison of the Performance of ZSM-5, β Zeolite, Y, USY, and their Composites in the Catalytic Cracking of n-Octane, 2,2,4-Trimethylpentane, and 1-Octene." Ind. Eng. Chem. Res., vol. 33, 1994. pp. 800-813.

[48] Kongsakpisal A. **Instrumental Analysis.** Ladkrabang : n.p. 1994.

[49] Fries J., Getrost H. **Organic Reagents for Trace Analysis.** E. Merk. Darmstadt. 1977.

[50] Myer M.E., Stollsteimer J. and Wims A.M. " Determination of Hydrocarbon-Type Distribution and Hydrogen/Carbon Ratio of Gasolines by Nuclear Magnetic Resonance Spectrometry." Analytical Chemistry, vol. 47, no. 12, Oct. 1975. pp. 2010-2015.

[51] Myer M.E., Stollsteimer J. and Wims A.M. " Determination of Gasoline Octane Numbers from Chemical Composition." Analytical Chemistry, vol. 47, no. 13, Nov. 1975. pp. 2301-2304.

[52] สมศักดิ์ วรมงคลชัย. **เทคโนโลยีพอลิเมอร์ 1.** พิมพ์ครั้งที่ 2. กรุงเทพฯ : สถาบันเทคโนโลยีพระจอมเกล้าเจ้าคุณทหารลาดกระบัง. 2543.

APPENDICES

APPENDIX A

SYNTHESIS OF ZEOLITES

A.1 Zeolite ZSM-5

The zeolite ZSM-5 employed in this thesis was synthesized hydrothermally from an aluminosilicate gel with a nominal composition of

$$40\ SiO_2 : Al_2O_3 : 4\ Na_2O : 2\ TPABr : 1200\ H_2O$$

From this gel composition, the 100 grams of water is basis of calculation. Therefore, the mole composition is adjusted to

$$0.1850\ SiO_2 : 0.0046\ Al_2O_3 : 0.0185\ Na_2O : 0.0093\ TPABr : 5.5509\ H_2O$$

Therefore, the weight of materials is summerized in Table A.1.

Table A.1 Material weight of zeolite ZSM-5 (S)

Materials	Mole composition	Weight (grams)
SiO_2	0.1850	11.1156
Al_2O_3	0.0046	0.4716
Na_2O	0.0185	1.1468
TPABr	0.0093	2.4633
H_2O	5.5509	100.0000

Calculation of SiO_2

Ludox (40%SiO_2, w/w)

SiO_2 40 grams prepared from Ludox solution 100 grams

SiO_2 11.1156 grams prepared from Ludox solution (100/40)×11.1156

= 27.7890 grams

Ludox solution 27.7890 grams consists of water = 27.7890-11.1156

= 16.6734 grams

Calculation of Al_2O_3 and Na_2O

$Na_2Al_2O_4$ consists of Na_2O = 37.57 % (w/w)

Al_2O_3 = 59.54 % (w/w)

Therefore,

Al_2O_3 59.54 grams prepared from $Na_2Al_2O_4$ 100 grams

Al_2O_3 0.4716 grams prepared from $Na_2Al_2O_4$ (100/59.54)×0.4716

= 0.7921 grams

$Na_2Al_2O_4$ 100 grams consists of Na_2O 37.37 grams

$Na_2Al_2O_4$ 0.7921 grams consists of Na_2O (37.37/100)×0.7921

= 0.2960 grams

Thus, it requires Na_2O = 1.1468-0.2960

= 0.8508 grams = 0.0137 mole

$$2NaOH \longrightarrow Na_2O + H_2O$$

Na_2O 1 mole prepared from NaOH 2 mole

Na_2O 0.0137 mole prepared from NaOH (2/1)×0.0137

= 0.0274 mole

= 1.0976 grams

NaOH 2 mole produced H_2O 1 mole

NaOH 0.0274 mole produced H_2O (1/2)×0.0274

= 0.0137 mole

= 0.2468 grams

Calculation of H_2O

The total H_2O = 100.0000 grams

There is water from other solution = 16.6734+0.2468

= 16.9202 grams

The water is added = 100.0000-16.9202

= 83.0798 grams

From above calculation, the materials required are summarized in Table A.2.

Table A.2 Summarized of required chemical reagents amount for synthesis zeolite ZSM-5 (S)

Material sources	SiO_2 (g)	Al_2O_3 (g)	Na_2O (g)	TPABr (g)	H_2O (g)
0.7921 g of $Na_2Al_2O_4$ (37.57% wt Na_2O, 59.54 % wt Al_2O_3)	-	0.4716	0.2960	-	-
1.0976 g of NaOH	-	-	0.8508	-	0.2468
27.7890 g of Ludox (40%SiO_2, w/w)	11.1156	-	-	-	16.6734
2.4633 g of TPABr	-	-	-	2.4633	-
83.0798 g of H_2O	-	-	-	-	83.0798
Total	**11.1156**	**0.4716**	**1.1468**	**2.4633**	**100.0000**

A.2 Zeolite Beta

The zeolite Beta employed in this thesis was synthesized hydrothermally from an aluminosilicate gel with a nominal composition of

30 SiO_2 : Al_2O_3 : 0.9 Na_2O : 6 TEAOH : 290 H_2O

From this gel composition, the 35 grams of water is basis of calculation. Therefore, the mole composition is adjusted to

0.2010 SiO_2 : 0.0067 Al_2O_3 : 0.0060 Na_2O : 0.0402 TEAOH : 1.9428 H_2O

Therefore, the weight of materials is summerized in Table A.3.

Table A.3 Material weight of zeolite Beta (S)

Materials	Mole composition	Weight (grams)
SiO_2	0.2010	12.0769
Al_2O_3	0.0067	0.6831
Na_2O	0.0060	0.3737
TEAOH	0.0402	5.9199
H_2O	1.9428	35.0000

Calculation of SiO_2

Ludox (40%SiO_2, w/w)

SiO_2	40	grams prepared from Ludox solution	100	grams	
SiO_2	12.0769	grams prepared from Ludox solution	(100/40)×12.0769		
			= 30.1923	grams	
Ludox solution	30.1923	grams consists of water	= 30.1923-12.0769		
			= 18.1154	grams	

Calculation of Al_2O_3 and Na_2O

$Na_2Al_2O_4$ consists of Na_2O = 37.57 % (w/w)

Al_2O_3 = 59.54 % (w/w)

Therefore,

Na_2O	37.57	grams prepared from $Na_2Al_2O_4$	100	grams
Na_2O	0.3737	grams prepared from $Na_2Al_2O_4$	(100/37.57)×0.3737	
			= 0.9947	grams
$Na_2Al_2O_4$	100	grams consists of Al_2O_3	59.54	grams
$Na_2Al_2O_4$	0.9947	grams consists of Al_2O_3	(59.54/100)×0.9947	
			= 0.5922	grams

Thus, it requires Al_2O_3 = 0.6831-0.5922

= 0.0909 grams = 8.9152×10^{-4} mole

$$2Al(OC_2H_5)_3 + 3H_2O \longrightarrow Al_2O_3 + 3C_2H_5OH$$

Al_2O_3	1	mole prepared from $Al(OC_2H_5)_3$	2	mole
Al_2O_3	8.9152×10^{-4}	mole prepared from $Al(OC_2H_5)_3$	(2/1)×8.9152×10^{-4}	
			= 1.7830×10^{-3}	mole
			= 0.2891	grams

Al_2O_3	1	mole prepared from H_2O	3	mole
Al_2O_3	8.9152×10^{-4}	mole prepared from H_2O	(3/1)× 8.9152×10^{-4}	
		=	2.6746×10^{-3}	mole
		=	0.0482	grams

Calculation of TEAOH

TEAOH (40%, w/w)

TEAOH 40 grams prepared from TEAOH solution 100 grams

TEAOH 5.9199 grams prepared from TEAOH solution (100/40)×5.9199

= 14.7998 grams

TEAOH solution 14.7998 grams consists of water = 14.7998 - 5.9199

= 8.8799 grams

Calculation of H_2O

The total H_2O = 35.0000+0.0482 = 35.0482 grams

There is water from other solution = 18.1154+8.8799

= 26.9953 grams

The water is added = 35.0482-26.9953

= 8.0529 grams

From above calculation, the materials required are summarized in Table A.4.

Table A.4 Summarized of required chemical reagents amount for synthesis zeolite Beta (S)

Material sources	SiO_2 (g)	Al_2O_3 (g)	Na_2O (g)	TEAOH (g)	H_2O (g)
0.9947 g of $Na_2Al_2O_4$ (37.57% wt Na_2O, 59.54 % wt Al_2O_3)	-	0.5922	0.3737	-	-
0.2891 g of $Al(OC_2H_5)_3$	-	0.0909	-	-	-
30.1923 g of Ludox (40%SiO_2, w/w)	12.0769	-	-	-	18.1154
14.7998 g of TEAOH (40%, w/w)	-	-	-	5.9199	8.8799
8.0529 g of H_2O	-	-	-	-	8.0529
Total	**12.0769**	**0.6831**	**0.3737**	**5.9199**	**35.0482**

APPENDIX B

X-RAY DIFFRACTION OF STANDARD PATTERN

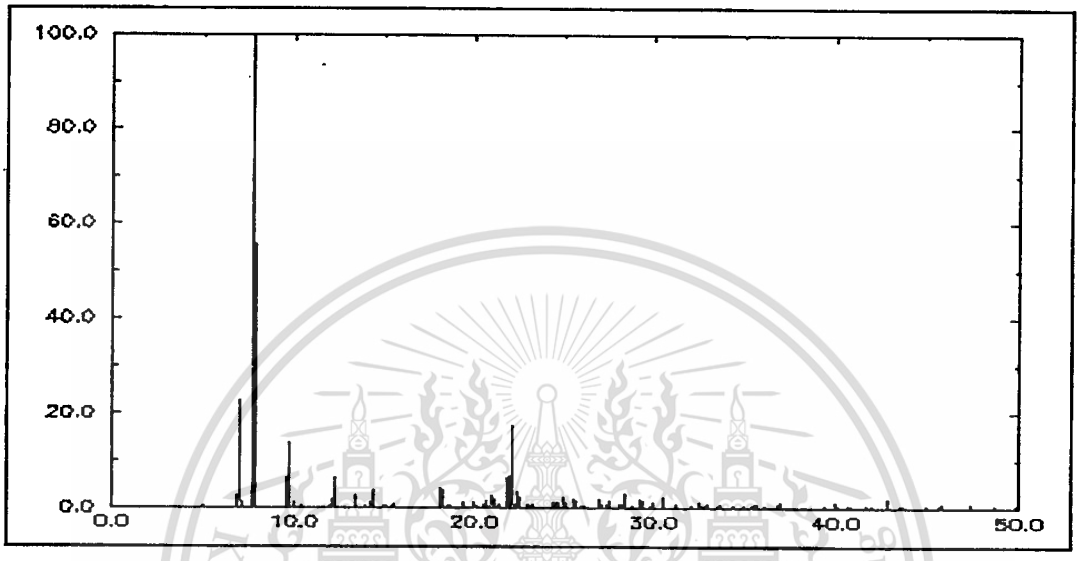

Figure B.1 X-ray diffraction pattern of standard Beta

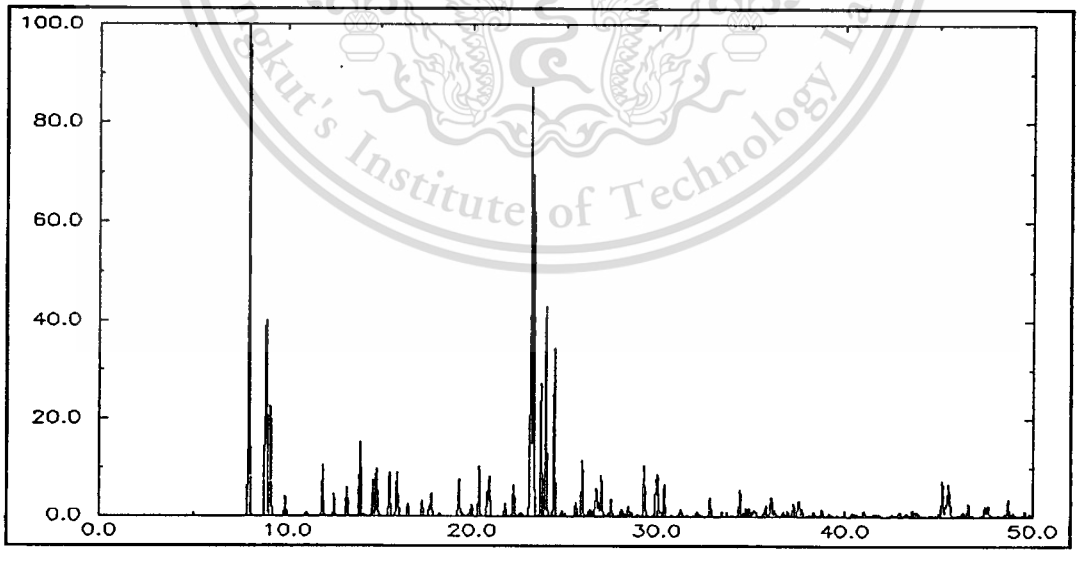

Figure B.2 X-ray diffraction pattern of standard ZSM-5

APPENDIX C

CALCULATION OF ACIDITY OF ZEOLITES

The acidity of zeolites was determined by potentiometric titration. The accurate concentration of standard solution (sodium tetraborate) which was diluted to 100 mL with distilled water can be calculated by:

$$\left[\frac{g}{Mw}\right] = \left[\frac{CV}{1000}\right]$$

$$C_{Na_2B_4O_7} = \left[\frac{g \times 1000}{Mw \times V}\right]$$

$$= \left[\frac{1.9068 \times 1000}{381.24 \times 100}\right]$$

$$= 0.0500 \text{ mol/l}$$

Then, the accurate concentration of sodium tetraborate was used as a titrant for determining the accurate concentration of hydrochloric acid. The $\Delta pH/\Delta V$ versus the volume of added solution was plotted and determined the equivalent point.

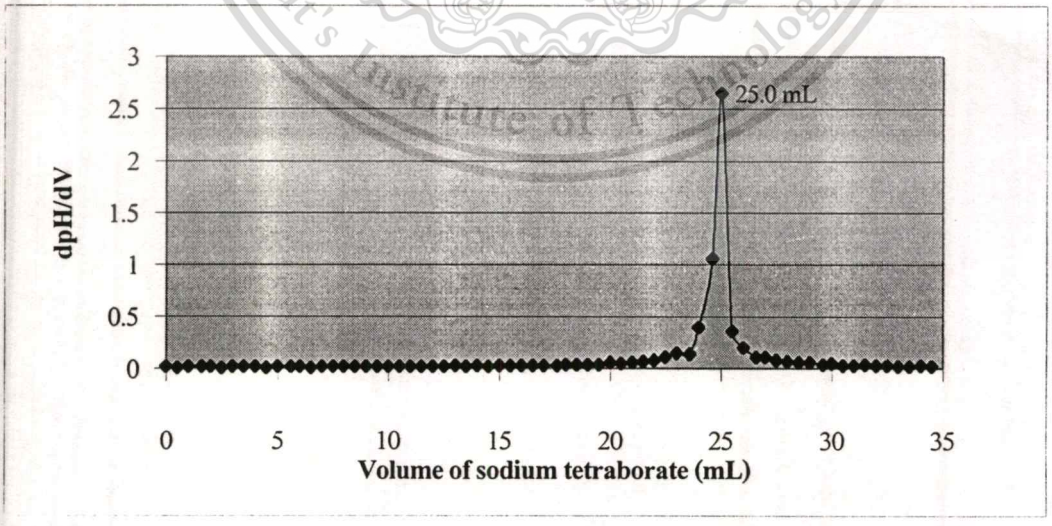

Figure C.1 The titration curve of sodium tetraborate with hydrochloric acid (the first titration)

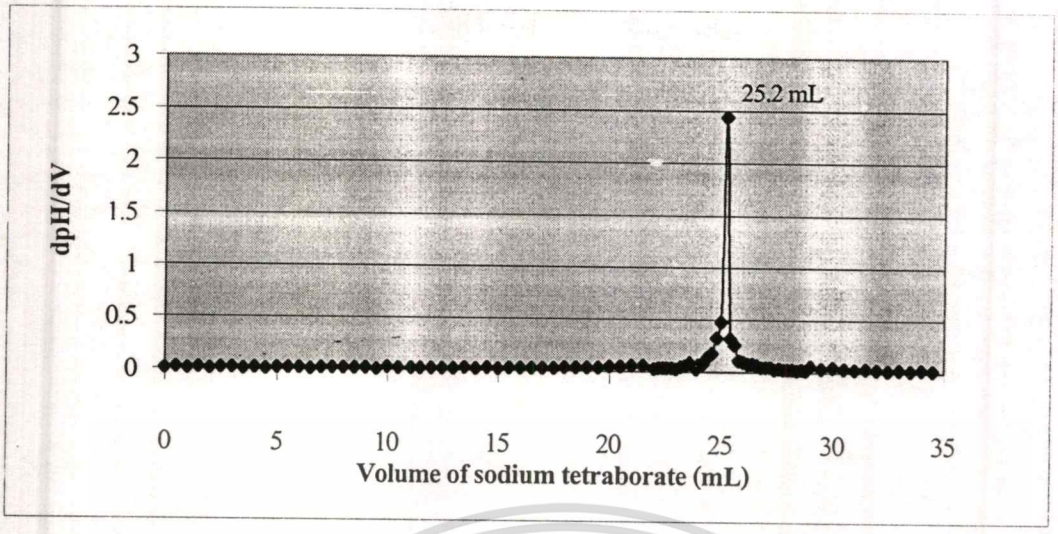

Figure C.2 The titration curve of sodium tetraborate with hydrochloric acid (the second titration)

From the titration curve (Figures C.1-C.2), average Ve, the average volume of sodium tetraborate solution belonging to the equivalent point is 25.1. The sodium tetraborate solution was titrated with 25 mL of hydrochloric acid Therefore, the accurate concentration of hydrochloric acid, C_{HCl}, is

$$\left[\frac{\text{mol } Na_2B_4O_7}{\text{mol HCl}}\right] = \frac{1}{2}$$

$$C_{HCl} = \left[\frac{2 \times 0.05 \times 25.1}{25}\right]$$

$$= 0.1004 \text{ mol/l}$$

Similar determination was used in the case of ammonium hydroxide concentration.

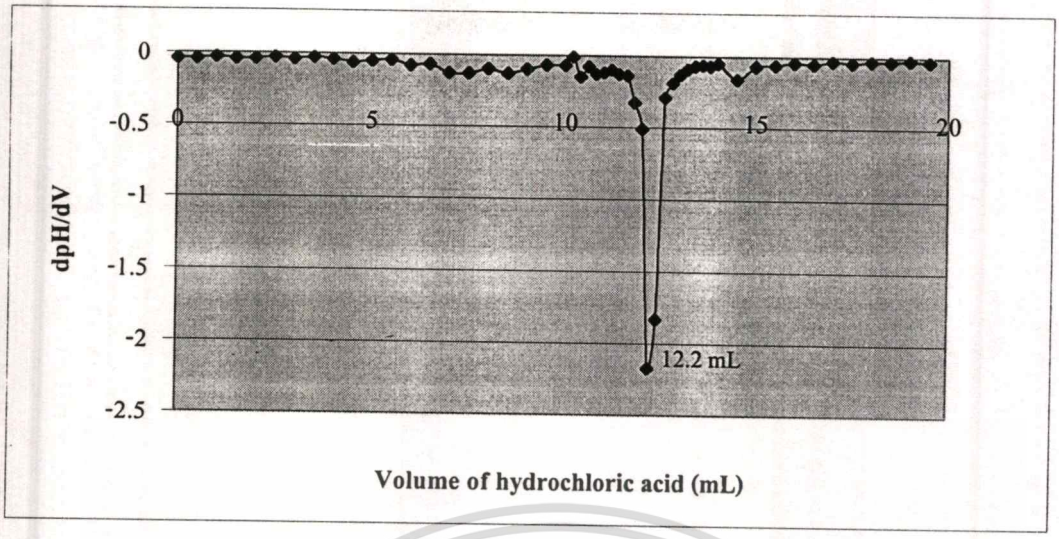

Figure C.3 The titration curve of hydrochloric acid with ammonium hydroxide (the first titration)

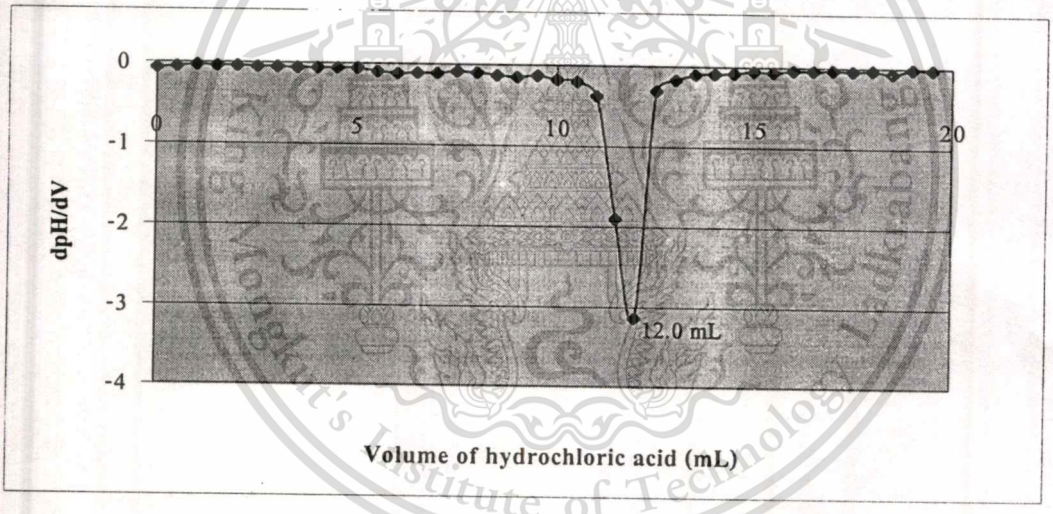

Figure C.4 The titration curve of hydrochloric acid with ammonium hydroxide (the second titration)

From the curve of ammonium hydroxide-hydrochloric acid titration (Figures C.3-C.4), average Ve of hydrochloric acid is 12.1. The hydrochloric acid was titrated with 25 mL of ammonium hydroxide. Therefore, the accurate concentration of ammonium hydroxide, C_{NH4OH}, is

$$\left[\frac{\text{mol HCl}}{\text{mol } NH_4OH}\right] = \frac{1}{1}$$

$$C_{NH_4OH} = \left[\frac{0.1004 \times 12.1}{25}\right]$$
$$= 0.0486 \text{ mol/l}$$

From the above results, the acid amount of H-Beta (S) was determined by using back titration techniques.

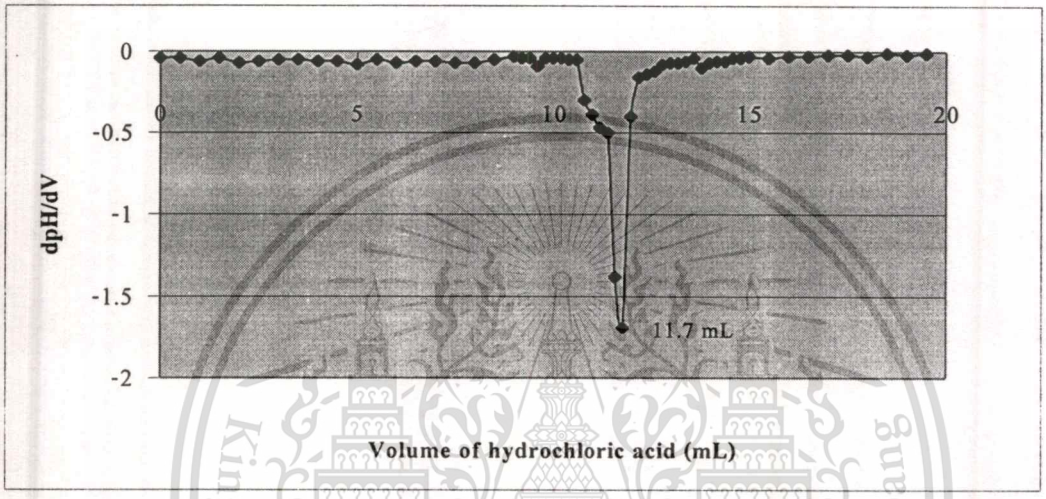

Figure C.5 The titration curve of hydrochloric acid with residual ammonium hydroxide (the first titration)

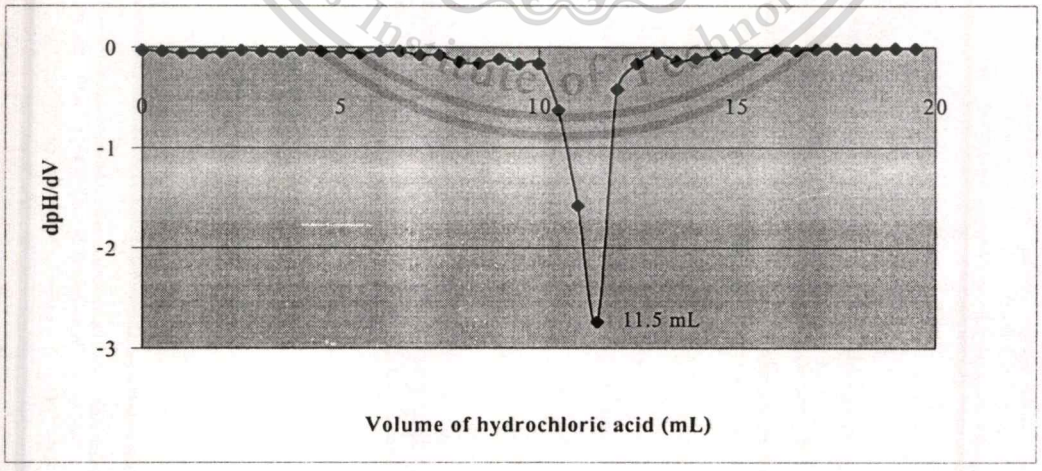

Figure C.6 The titration curve of hydrochloric acid with residual ammonium hydroxide (the second titration)

It was found that the curve of residual ammonium hydroxide-hydrochloric acid titration obtains average Ve = 11.6 by using initially 25 mL of ammonium hydroxide solution and 0.0740 grams of H-Beta (S). Therefore, the concentration of residual ammonium hydroxide is

$$\left[\frac{\text{mol HCl}}{\text{mol } NH_4OH}\right] = \frac{1}{1}$$

$$C_{NH_4OH} = \left[\frac{0.1004 \times 11.6}{25}\right]$$

$$= 0.0466 \text{ mol/l}$$

The concentration of acid site of 0.0740 grams of H-Beta (S) is calculated by using the initially added mole of ammonium hydroxide minus the residual mole of ammonium hydroxide.

$$\text{mol}\left(NH_4OH\right)_i - \text{mol}\left(NH_4OH\right)_f = \left[\frac{\left(0.0486 - 0.0466\right) \times 25}{1000}\right]$$

$$= 0.05 \text{ mmol}$$

Therefore, the acidity of H-Beta (S) is 0.68 mmol/g of zeolite (0.05 mmol/0.0740 grams of zeolite). Similar determination was used in the case of other zeolites.

APPENDIX D

ELEMENTAL ANALYSIS FROM UV-VIS SPECTROPHOTOMETER

D.1 Determination of silicon

The standard curve was plotted between concentration and absorbance as linear curve. The silicon concentration of zeolites can be calculated by comparing with the standard calibration curve. The concentration and absorbance of standard and sample are shown in Table D.1.

Table D.1 The concentration and absorbance of silicon determined by UV-Vis Spectrophotometer

Material	Concentration (ppm)	Absorbance (815 nm)
Standard of silicon	0.231	0.073
	0.462	0.238
	0.693	0.400
	0.924	0.552
Beta (S)	-	0.533
ZSM-5 (S)	-	0.521

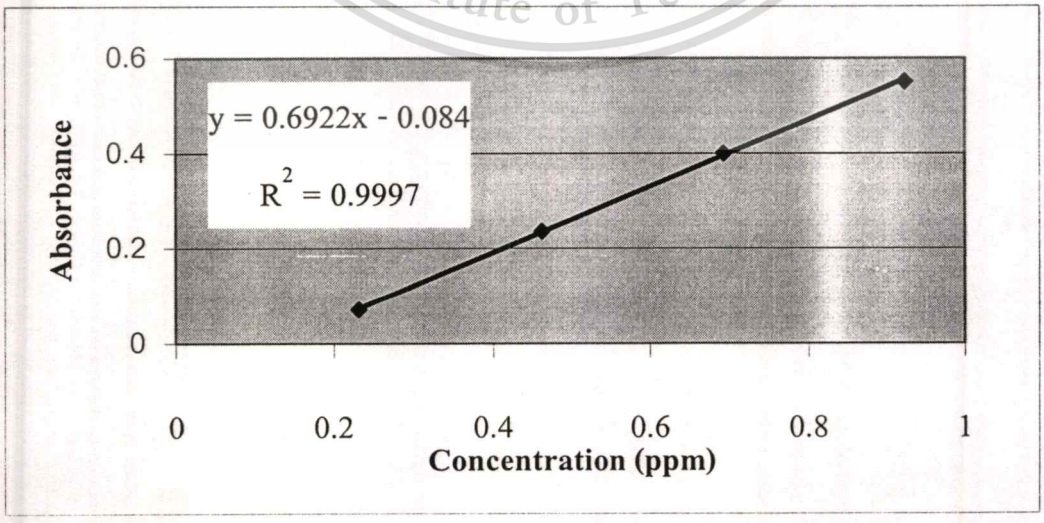

Figure D.1 Calibration curve and equation related between concentration and absorbance

From the curve, relation between concentration and absorbance can be determined by:

$$Y = 0.6922\,[X] - 0.0840$$

Where, X = silicon concentration (ppm)

Y = absorbance

From the experiment, this sample solution was diluted 100 times as follows:

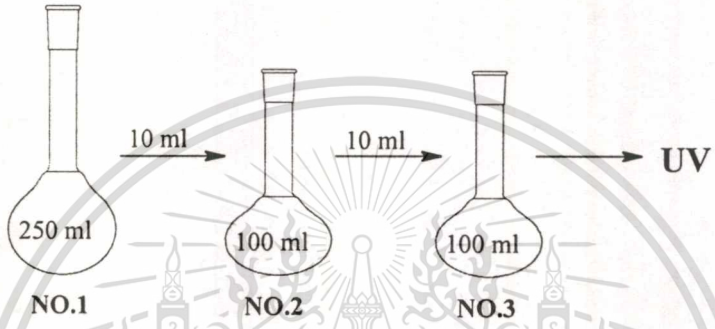

This equation is used for calculation silicon of zeolite sample. For example, the absorbance of Beta (S), No.3, is 0.533 then:

$$Y = 0.6922\,[Si]_{Beta\ (S)} - 0.0840$$

$$[Si] = 0.8910 \text{ ppm}$$

The accurate silicon concentration of the flask NO.1 is 89.10 ppm (or 22.28 mg/250 ml). Therefore, the mole of silicon is 22.29/28 = 0.7960.

D.2 Determination of aluminium

The standard curve was plotted between concentration and absorbance as a linear curve. The aluminium concentration of zeolites can be calculated by comparing with the standard calibration curve. The concentration and absorbance of standard and samples are shown in Table D.2.

Table D.2 The concentration and absorbance of aluminium determined by UV-Vis Spectrophotometer

Material	Concentration (ppm)	Absorbance (410 nm)
Standard of aluminium	0.502	0.087
	1.004	0.209
	1.506	0.332
	2.008	0.456
Beta (S)	-	0.080
ZSM-5 (S)	-	0.075

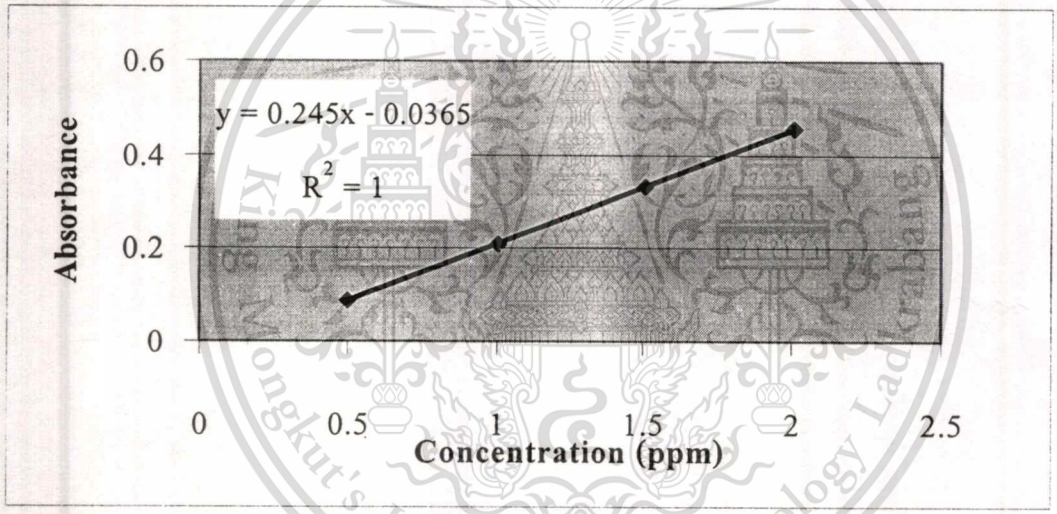

Figure D.2 Calibration curve and equation related between concentration and absorbance

From the curve, relation between concentration and absorbance can be determined by:

$$Y = 0.2450\,[X] - 0.0365$$

Where, X = aluminium concentration (ppm)

Y = absorbance

From the experiment, this sample solution was diluted 10 times as follows:

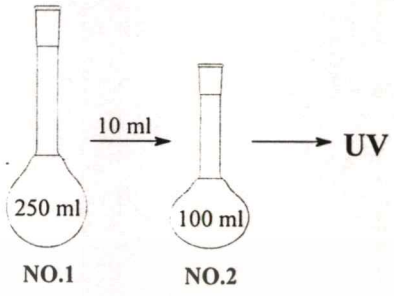

This equation is used for calculation aluminium of zeolite sample. For example, the absorbance of Beta (S), NO.2, is 0.080 then:

$$Y = 0.2450\,[Al]_{Beta\,(S)} - 0.0365$$

$$[Al] = 0.4760 \text{ ppm}$$

The accurate aluminium concentration of the flask NO.1 is 4.76 ppm (or 1.19 mg/250 ml). Therefore, the mole of aluminium is 1.19/27 = 0.0440.

From the above results, the silicon/aluminium ratio is calculated as follows:

$$\frac{\text{Mol of silicon}}{\text{Mol of aluminium}} = \frac{[Si]}{[Al]}$$

$$= \frac{0.7960}{0.0440} = 18.1$$

- Beta (C), Si/Al = 27 (obtained from data information of Tosoh corporation)
- ZSM-5 (C) Si/Al cannot be certainly evaluated due to the presence of silica/alumina

APPENDIX E

CALCULATION OF % MOL OF CARBON FROM GAS CHROMATOGRAPH

From the chromatogram, the peak of hydrocarbon sample is identified using reference standard for comparison. The peak area of hydrocarbon which possesses the equal number of carbon is summarized. The summarized peak area data which obtained from chromatogram of a mixture hydrocarbon product (Figure E.1) is shown in Table E.1.

Figure E.1 Chromatogram of hydrocarbons product

Table E.1 The summarized peak area of a mixture hydrocarbon products

Number of carbon	% Summarized area
C_3	32.5701
C_4	30.5786
C_5	29.6000
C_6	7.2511
Total	100

In the normalization method, the areas of all eluted peak are computed; after correcting these areas for differences in the detector response to different compounds. In this study, the flame ionization detector (FID) is used because for hydrocarbon it responded proportionally to the number of carbon atoms in the molecule entering the detector per unit time. After correcting % areas, the mole fraction of the sample is obtained from the ratio of its area to the total area of all peaks. The corrected area for normalization of the equaled carbon can be calculated as follows:

$$\text{Corrected area of } C_n = \left[\frac{\% \text{ area of } C_n}{n} \right]$$

Where n is the response factor of the analytic C_n hydrocarbons which is equaled to number of carbon atom in the hydrocarbon molecule.

For example;

$$\text{Corrected area of } C_3 = \left[\frac{32.5701}{3} \right] = 10.8567$$

$$\text{Corrected area of } C_4 = \left[\frac{30.5786}{4} \right] = 7.6447$$

$$\text{Corrected area of } C_5 = \left[\frac{29.6000}{5} \right] = 5.9200$$

$$\text{Corrected area of } C_6 = \left[\frac{7.2511}{6} \right] = 1.2085$$

The % mol of each component of the sample can be calculated as follows:

$$\%\text{ mol of } C_n = \left[\frac{\text{corrected area of } C_n}{\text{total corrected area}} \right] \times 100$$

For example;

$$\%\text{ mol of } C_3 = \left[\frac{10.8567}{25.6299} \right] \times 100 = 42.3595$$

$$\%\text{ mol of } C_4 = \left[\frac{7.6447}{25.6299} \right] \times 100 = 29.8273$$

$$\%\text{ mol of } C_5 = \left[\frac{5.9200}{25.6299} \right] \times 100 = 23.0980$$

$$\% \text{ mol of } C_6 = \left[\frac{1.2085}{25.6299}\right] \times 100 = 4.7152$$

The % mol of each product which is obtained from the above calculation is shown in Table E.2.

Table E.2 % Mol of carbon derived by normalization method

Number of Carbon	% Area	Corrected area	% Mol
C_3	32.5701	10.8567	42.3595
C_4	30.5786	7.6447	29.8273
C_5	29.6000	5.9200	23.0980
C_6	7.2511	1.2085	4.7152
Total	100	25.6299	100

Reaction conditions: Temperature, 400 °C; Catalyst/polymer ratio, 2 %; 1 hour on stream; Helium, 30 ml/min

APPENDIX F

GAS CHROMATOGRAPH CONDITION

F.1 Condition for gaseous and liquid products from batch process and heavy cracked liquid products from continuous process

Column parameter

Type	:	VA-1 capillary column
Length (meters)	:	15
I.D. (mm)	:	0.53
Film thickness (μm)	:	1.5

Carrier gas	:	Helium
Linear velocity	:	12.3 cm/sec
Injector temperature	:	220°C
FID detector temperature	:	220°C

Column oven condition for gaseous products from batch process

Temp (°C)	Rate (°C/min)	Hold (min)	Total (min)
30	-	5.0	5.0
200	5.0	26.0	65.0

Column oven condition for liquid products from batch process and heavy cracked liquid products from continuous process

Temp (°C)	Rate (°C/min)	Hold (min)	Total (min)
30	-	5.0	5.0
220	5.0	22.0	65.0

F.2 Condition for gaseous products and light cracked liquid products from continuous process

Column parameter

Type	:	HP-Plot capillary column
Length (meters)	:	30
I.D. (mm)	:	0.53
Film thickness (μm)	:	15.0

Carrier gas	:	Helium
Linear velocity	:	53.6 cm/sec
Injector temperature	:	200°C
FID detector temperature	:	250°C

Column oven condition for gaseous products and light cracked liquid products from continuous process

Temp (°C)	Rate (°C/min)	Hold (min)	Total (min)
100	-	10.0	10.0
190	1.0	10.0	110.0

APPENDIX G

BATCH PROCESS DATA

Table G.1 Yields of products from cracking of polyethylene in batch reactor at 430°C under helium for 30 minutes residence time

Reaction System (He, 30 min) PE + Zeolite (20%w/w)	Repeated Number	Yields (wt%)			
		Gas	Liquid	Wax	Residues
PE	-	18.66	2.37	78.97	-
PE + H-Beta (S)	Fresh	45.30	45.71	6.50	2.49
PE + H-Beta (S)	1st	31.78	23.74	41.13	3.35
PE + H-Beta (S)	2 nd	-	-	-	-
PE + H-Beta (S)	3 rd	-	-	-	-
PE + H-Beta (C)	Fresh	33.64	59.01	5.30	2.05
PE + H-Beta (C)	1st	37.27	55.01	5.82	1.90
PE + H-Beta (C)	2 nd	37.11	47.66	13.27	1.96
PE + H-Beta (C)	3 rd	25.99	38.04	32.47	3.50
PE + H-ZSM-5 (S)	Fresh	65.89	29.95	2.96	1.20
PE + H-ZSM-5 (S)	1st	57.11	35.34	5.75	1.80
PE + H-ZSM-5 (S)	2 nd	41.53	45.02	11.22	2.23
PE + H-ZSM-5 (S)	3 rd	22.88	46.48	28.56	2.08
PE + H-ZSM-5 (C)	Fresh	57.51	35.96	5.24	1.29
PE + H-ZSM-5 (C)	1st	44.98	37.62	15.67	1.73
PE + H-ZSM-5 (C)	2 nd	32.54	45.12	20.33	2.01
PE + H-ZSM-5 (C)	3 rd	31.98	35.22	30.88	1.92

Table G.2 Yields of products from cracking of polyethylene in batch reactor at 430°C under hydrogen for 30 minutes residence time

Reaction System (H_2, 30 min) PE + Zeolite (20%w/w)	Repeated Number	Yields (wt%)			
		Gas	Liquid	Wax	Residues
PE	-	12.09	0.65	87.26	-
PE + H-Beta (C)	Fresh	32.11	62.49	3.51	1.89
PE + H-Beta (C)	1st	38.86	55.28	4.33	1.53
PE + H-Beta (C)	2 nd	34.72	48.72	14.94	1.62
PE + H-Beta (C)	3 rd	33.95	37.02	26.61	2.42
PE + H-ZSM-5 (C)	Fresh	57.28	38.65	2.97	1.10
PE + H-ZSM-5 (C)	1st	56.11	31.42	11.33	1.14
PE + H-ZSM-5 (C)	2 nd	50.25	29.58	18.19	1.98
PE + H-ZSM-5 (C)	3 rd	48.63	32.40	17.61	1.36

Table G.3 Yields of products from cracking of polyethylene in batch reactor at 430°C under helium for 15 minutes residence time

Reaction System (He, 15 min) PE + Zeolite (20%w/w)	Repeated Number	Yields (wt%)			
		Gas	Liquid	Wax	Residues
PE + H-Beta (C)	Fresh	29.04	60.92	8.78	1.26
PE + H-Beta (C)	1st	24.40	60.07	13.75	1.78
PE + H-Beta (C)	2 nd	28.42	54.73	14.98	1.87
PE + H-Beta (C)	3 rd	23.43	38.33	36.22	2.02
PE + H-ZSM-5 (C)	Fresh	48.17	42.08	8.66	1.09
PE + H-ZSM-5 (C)	1st	36.59	43.32	18.84	1.25
PE + H-ZSM-5 (C)	2 nd	25.05	40.74	32.25	1.96
PE + H-ZSM-5 (C)	3 rd	22.40	39.53	36.56	1.51

Table G.4 Yields of products from cracking of polyethylene in batch reactor at 430°C under hydrogen for 15 minutes residence time

Reaction System (H_2, 15 min) PE + Zeolite (20%w/w)	Repeated Number	Yields (wt%)			
		Gas	Liquid	Wax	Residues
PE + H-Beta (C)	Fresh	28.79	65.79	3.52	1.90
PE + H-Beta (C)	1st	31.82	59.80	7.29	1.09
PE + H-Beta (C)	2 nd	37.56	42.89	17.90	1.65
PE + H-Beta (C)	3 rd	39.34	35.13	23.97	1.56
PE + H-ZSM-5 (C)	Fresh	46.61	45.93	6.55	0.91
PE + H-ZSM-5 (C)	1st	45.38	38.91	14.55	1.16
PE + H-ZSM-5 (C)	2 nd	35.42	36.78	26.22	1.58
PE + H-ZSM-5 (C)	3 rd	33.39	37.93	27.28	1.40

Table G.5 Distribution of gaseous products from cracking of polyethylene at 430°C under helium for 30 minutes residence time

Reaction System (He, 30 min) PE + Zeolite (20%w/w)	Repeated Number	Product Distribution (%)			
		C_3	C_4	C_5	C_6
PE	-	35.00	24.72	11.62	28.66
PE + H-Beta (S)	Fresh	25.14	66.32	7.00	1.53
PE + H-Beta (S)	1st	23.72	44.61	24.51	7.16
PE + H-Beta (S)	2 nd	-	-	-	-
PE + H-Beta (S)	3 rd	-	-	-	-
PE + H-Beta (C)	Fresh	21.65	58.60	16.73	3.02
PE + H-Beta (C)	1st	36.68	47.35	14.13	1.84
PE + H-Beta (C)	2 nd	29.02	54.42	14.26	2.29
PE + H-Beta (C)	3 rd	22.81	52.09	21.68	3.41
PE + H-ZSM-5 (S)	Fresh	75.83	24.16	-	-
PE + H-ZSM-5 (S)	1st	51.66	32.32	13.53	2.49
PE + H-ZSM-5 (S)	2 nd	49.03	41.17	8.02	1.77
PE + H-ZSM-5 (S)	3 rd	50.39	35.31	12.08	2.23
PE + H-ZSM-5 (C)	Fresh	71.57	17.56	8.45	2.41
PE + H-ZSM-5 (C)	1st	57.04	33.48	7.72	1.77
PE + H-ZSM-5 (C)	2 nd	40.00	38.36	16.78	4.86
PE + H-ZSM-5 (C)	3 rd	40.97	41.02	15.29	2.72

Table G.6 Distribution of gaseous products from cracking of polyethylene at 430°C under hydrogen for 30 minutes residence time

Reaction System (H_2, 30 min) PE + Zeolite (20%w/w)	Repeated Number	Product Distribution (%)			
		C_3	C_4	C_5	C_6
PE	-	33.71	27.94	11.55	26.80
PE + H-Beta (C)	Fresh	22.59	64.87	10.63	1.92
PE + H-Beta (C)	1st	20.70	64.75	12.14	2.41
PE + H-Beta (C)	2 nd	21.60	58.36	16.96	3.08
PE + H-Beta (C)	3 rd	27.50	50.58	17.27	4.65
PE + H-ZSM-5 (C)	Fresh	74.68	25.32	-	-
PE + H-ZSM-5 (C)	1st	54.14	37.63	6.33	1.89
PE + H-ZSM-5 (C)	2 nd	56.95	33.20	7.73	2.13
PE + H-ZSM-5 (C)	3 rd	40.32	47.37	10.30	2.01

Table G.7 Distribution of gaseous products from cracking of polyethylene at 430°C under helium for 15 minutes residence time

Reaction System (He, 15 min) PE + Zeolite (20%w/w)	Repeated Number	Product Distribution (%)			
		C_3	C_4	C_5	C_6
PE + H-Beta (C)	Fresh	17.15	63.87	14.89	4.09
PE + H-Beta (C)	1st	19.74	64.71	13.54	2.02
PE + H-Beta (C)	2 nd	25.47	60.64	10.34	3.55
PE + H-Beta (C)	3 rd	23.73	58.17	14.28	3.82
PE + H-ZSM-5 (C)	Fresh	72.25	22.01	5.14	0.60
PE + H-ZSM-5 (C)	1st	63.85	30.99	3.81	1.35
PE + H-ZSM-5 (C)	2 nd	52.58	39.09	6.20	2.14
PE + H-ZSM-5 (C)	3 rd	32.83	42.54	18.61	6.02

Table G.8 Distribution of gaseous products from cracking of polyethylene at 430°C under hydrogen for 15 minutes residence time

Reaction System (H_2, 15 min) PE + Zeolite (20%w/w)	**Repeated Number**	**Product Distribution (%)**			
		C_3	**C_4**	**C_5**	**C_6**
PE + H-Beta (C)	Fresh	33.54	55.15	8.56	2.75
PE + H-Beta (C)	1st	22.76	62.92	11.55	2.77
PE + H-Beta (C)	2 nd	26.44	57.21	14.22	2.13
PE + H-Beta (C)	3 rd	19.76	61.42	14.98	3.84
PE + H-ZSM-5 (C)	Fresh	74.38	17.72	6.03	1.87
PE + H-ZSM-5 (C)	1st	63.33	29.82	5.57	1.27
PE + H-ZSM-5 (C)	2 nd	50.38	34.05	13.11	2.46
PE + H-ZSM-5 (C)	3 rd	55.67	34.62	7.50	2.22

Table G.9 Distribution of liquid products from cracking of polyethylene at 430°C under helium for 30 minutes residence time

Reaction System (He, 30 min) PE + Zeolite (20%w/w)	Repeated Number	Product Distribution (%)				
		C_5	C_6	C_7	C_8	C_9^+
PE	-	11.77	16.40	16.59	13.95	41.29
PE + H-Beta (S)	Fresh	29.37	32.90	24.38	9.87	3.49
PE + H-Beta (S)	1st	4.48	11.87	19.48	26.22	37.95
PE + H-Beta (S)	2 nd	-	-	-	-	-
PE + H-Beta (S)	3 rd	-	-	-	-	-
PE + H-Beta (C)	Fresh	39.33	43.20	10.26	5.29	1.92
PE + H-Beta (C)	1st	30.88	31.18	18.72	11.16	8.06
PE + H-Beta (C)	2 nd	27.87	27.90	26.23	11.94	6.06
PE + H-Beta (C)	3 rd	11.02	25.32	20.03	18.93	24.71
PE + H-ZSM-5 (S)	Fresh	47.82	33.05	12.24	3.18	3.71
PE + H-ZSM-5 (S)	1st	33.96	30.74	19.10	10.34	5.85
PE + H-ZSM-5 (S)	2 nd	36.00	26.25	15.01	10.66	12.08
PE + H-ZSM-5 (S)	3 rd	35.58	24.05	15.86	11.58	12.92
PE + H-ZSM-5 (C)	Fresh	43.54	27.47	18.05	9.05	1.89
PE + H-ZSM-5 (C)	1st	35.99	31.98	15.52	8.95	7.57
PE + H-ZSM-5 (C)	2 nd	32.78	24.75	18.92	12.66	10.89
PE + H-ZSM-5 (C)	3 rd	31.89	24.08	16.11	11.70	16.22

Table G.10 Distribution of liquid products from cracking of polyethylene at 430°C under hydrogen for 30 minutes residence time

Reaction System (H_2, 30 min) PE + Zeolite (20%w/w)	Repeated Number	Product Distribution (%)				
		C_5	C_6	C_7	C_8	C_9^+
PE	-	10.05	14.93	15.36	13.35	46.32
PE + H-Beta (C)	Fresh	36.93	38.29	14.68	7.95	2.15
PE + H-Beta (C)	1 st	28.76	35.06	17.43	11.99	6.75
PE + H-Beta (C)	2 nd	27.18	28.27	27.90	11.60	5.05
PE + H-Beta (C)	3 rd	22.03	23.40	28.94	13.86	11.77
PE + H-ZSM-5 (C)	Fresh	49.98	33.00	8.11	4.86	4.06
PE + H-ZSM-5 (C)	1 st	39.00	34.34	14.63	7.67	4.37
PE + H-ZSM-5 (C)	2 nd	32.81	28.48	18.06	11.35	9.30
PE + H-ZSM-5 (C)	3 rd	30.18	26.09	18.00	13.68	12.04

Table G.11 Distribution of liquid products from cracking of polyethylene at 430°C under helium for 15 minutes residence time

Reaction System (He, 15 min) PE + Zeolite (20%w/w)	Repeated Number	Product Distribution (%)				
		C_5	C_6	C_7	C_8	C_9^+
PE + H-Beta (C)	Fresh	26.56	38.89	10.33	17.59	6.63
PE + H-Beta (C)	1 st	29.82	37.81	15.61	10.41	6.34
PE + H-Beta (C)	2 nd	31.28	35.51	15.49	9.35	8.37
PE + H-Beta (C)	3 rd	1.92	3.14	18.43	28.01	48.50
PE + H-ZSM-5 (C)	Fresh	43.53	25.88	16.40	11.71	2.48
PE + H-ZSM-5 (C)	1 st	36.94	35.90	14.89	8.10	4.16
PE + H-ZSM-5 (C)	2 nd	38.47	26.48	16.78	9.33	8.94
PE + H-ZSM-5 (C)	3 rd	29.48	23.17	15.83	12.56	18.96

Table G.12 Distribution of liquid products from cracking of polyethylene at 430°C under hydrogen for 15 minutes residence time

Reaction System (H_2, 15 min) PE + Zeolite (20%w/w)	Repeated Number	Product Distribution (%)				
		C_5	C_6	C_7	C_8	C_9^+
PE + H-Beta (C)	Fresh	23.02	45.67	17.14	7.62	6.54
PE + H-Beta (C)	1 st	22.77	37.10	18.01	12.29	9.83
PE + H-Beta (C)	2 nd	30.55	38.42	14.63	9.70	6.70
PE + H-Beta (C)	3 rd	19.73	35.52	16.92	11.03	16.80
PE + H-ZSM-5 (C)	Fresh	40.29	36.21	15.64	4.68	3.18
PE + H-ZSM-5 (C)	1 st	37.75	28.05	20.32	10.21	3.68
PE + H-ZSM-5 (C)	2 nd	31.41	24.95	18.41	12.55	12.68
PE + H-ZSM-5 (C)	3 rd	30.82	25.20	17.32	12.70	13.95

APPENDIX H

CONTINUOUS PROCESS DATA

Table H.1 Yields of products from thermal cracking of polyethylene in continuous reactor at temperatures range between 375°C and 430°C

Pure PE	Gas %	Liquid %			Wax %
T (°C)		Cool –5°C	Cool 20°C	Total	
350	8.73	-	-	-	91.27
375	8.08	0.93	3.57	4.50	87.42
400	12.61	0.95	6.34	7.29	80.10
430	11.11	1.19	19.62	20.81	68.08

Table H.2 Yields of products from catalytic cracking of polyethylene in continuous reactor at temperatures range between 375°C and 430°C using H-Beta (C) as a catalyst

Beta/PE		Gas %	Liquid %			Wax %
T (°C)	Ratio		Cool –5°C	Cool 20°C	Total	
350	5%	14.20	-	0.87	0.87	84.93
375	5%	35.01	5.68	39.50	45.18	19.81
400	5%	37.65	12.16	46.56	58.72	3.64
430	5%	32.46	12.25	52.50	64.75	2.79
400	2%	39.30	8.14	41.37	49.51	11.10

Table H.3 Yields of products from thermal cracking of polyethylene in continuous reactor as a function of time on stream at temperatures range between 375°C and 430°C

Pure PE		**Time (hours)**							
T = 375°C		**1**	**2**	**3**	**4**	**5**	**6**	**7**	**8**
Cool at	g	2.85	3.68	4.14	3.42	3.10	2.78	2.70	3.00
20°C	%	3.17	4.09	4.60	3.80	3.44	3.09	3.00	3.33
Cool at	g	1.21	1.03	0.89	0.72	0.64	0.77	0.70	0.77
-5°C	%	1.34	1.14	0.99	0.80	0.72	0.86	0.78	0.85
Total	g	4.06	4.71	5.03	4.14	3.74	3.55	3.40	3.77
	%	4.51	5.24	5.59	4.60	4.16	3.95	3.78	4.19
Pure PE		**Time (hours)**							
T = 400°C		**1**	**2**	**3**	**4**	**5**	**6**	**7**	**8**
Cool at	g	4.84	5.23	4.99	6.65	6.11	5.99	6.10	5.73
20°C	%	5.38	5.82	5.54	7.38	6.79	6.66	6.78	6.37
Cool at	g	0.99	0.86	0.92	0.83	0.81	0.84	0.76	0.82
-5°C	%	1.10	0.96	1.02	0.92	0.90	0.94	0.85	0.91
Total	g	5.83	6.09	5.91	7.48	6.92	6.83	6.86	6.55
	%	6.49	6.77	6.57	8.30	7.70	7.60	7.63	7.28
Pure PE		**Time (hours)**							
T = 430°C		**1**	**2**	**3**	**4**	**5**	**6**	**7**	**8**
Cool at	g	24.37	20.44	14.95	15.00	19.53	14.47	13.72	18.75
20°C	%	27.08	22.71	16.62	16.67	21.71	16.08	15.25	20.83
Cool at	g	1.55	1.38	1.27	1.05	0.76	1.00	0.64	0.92
-5°C	%	1.72	1.53	1.41	1.17	0.85	1.11	0.71	1.03
Total	g	25.92	21.82	16.22	16.05	20.29	15.47	14.36	19.67
	%	28.80	24.24	18.03	17.84	22.55	17.19	15.96	21.85

Table H.4 Yields of products from catalytic cracking of polyethylene in continuous reactor as a function of time on stream at temperatures range between 350°C and 430°C

PE/Beta 5%		**Time (hours)**							
T = 350°C		**1**	**2**	**3**	**4**	**5**	**6**	**7**	**8**
Cool at	g	0.33	0.69	0.76	0.61	0.84	0.93	0.87	0.87
20°C	%	0.38	0.81	0.89	0.71	0.98	1.08	1.04	1.04
Cool at	g	-	-	-	-	-	-	-	-
–5°C	%	-	-	-	-	-	-	-	-
Total	g	0.33	0.69	0.76	0.61	0.84	0.93	0.87	0.87
	%	0.38	0.81	0.89	0.71	0.98	1.08	1.04	1.04
PE/Beta 5%		**Time (hours)**							
T = 375°C		**1**	**2**	**3**	**4**	**5**	**6**	**7**	**8**
Cool at	g	30.22	31.99	29.71	34.95	36.91	35.95	34.03	36.43
20°C	%	35.34	37.41	34.75	40.87	43.17	42.05	39.80	42.61
Cool at	g	2.45	3.28	2.82	4.28	6.05	6.27	7.07	6.63
–5°C	%	2.87	3.83	3.29	5.01	7.08	7.33	8.27	7.75
Total	g	32.67	35.27	32.53	39.23	42.96	42.22	41.10	43.06
	%	38.21	41.25	38.04	45.88	50.26	49.38	48.07	50.37
PE/Beta 5%		**Time (hours)**							
T = 400°C		**1**	**2**	**3**	**4**	**5**	**6**	**7**	**8**
Cool at	g	40.91	38.80	39.06	41.13	39.48	40.55	38.16	40.40
20°C	%	47.85	45.38	45.68	48.10	46.17	47.43	44.63	47.25
Cool at	g	7.03	11.04	10.18	10.35	10.65	10.16	10.66	13.08
–5°C	%	8.22	12.91	11.91	12.10	12.46	11.88	12.47	15.30
Total	g	47.94	49.84	49.24	51.48	50.13	50.71	48.82	53.48
	%	56.07	58.29	57.59	60.20	58.63	59.31	57.10	62.55

Table H.4 (continued)

PE/Beta 5%		**Time (hours)**							
T = 430°C		**1**	**2**	**3**	**4**	**5**	**6**	**7**	**8**
Cool at	g	45.43	43.16	43.83	45.06	45.97	45.47	45.59	44.59
20°C	%	53.14	50.48	51.27	52.71	53.77	53.18	53.32	52.16
Cool at	g	9.51	12.24	11.08	10.61	10.35	11.44	8.31	10.26
–5°C	%	11.12	14.32	12.96	12.41	12.11	13.38	9.71	12.00
Total	g	54.94	55.40	54.91	55.67	56.32	56.91	53.90	54.85
	%	64.25	64.79	64.23	65.12	65.88	66.56	63.03	64.16
PE/Beta 2%		**Time (hours)**							
T = 400°C		**1**	**2**	**3**	**4**	**5**	**6**	**7**	**8**
Cool at	g	32.53	38.11	38.31	37.97	35.56	36.11	36.22	37.11
20°C	%	36.88	43.20	43.44	43.04	40.32	40.93	41.06	42.07
Cool at	g	5.33	5.86	6.28	7.25	8.16	7.80	7.54	9.23
–5°C	%	6.04	6.64	7.12	8.22	9.25	8.84	8.55	10.46
Total	g	37.86	43.97	44.59	45.22	43.72	43.91	43.76	46.34
	%	42.92	49.84	50.55	51.26	49.57	49.77	49.61	52.53

Table H.5 Distribution of gaseous products from thermal and catalytic cracking of polyethylene at temperatures range between 375°C and 430°C

Sample	Temp (°C)	Product Distribution (%)			
		C_3	C_4	C_5	C_6
Pure PE	350	49.49	22.50	14.36	13.65
Pure PE	350	50.21	20.21	14.15	15.43
Pure PE	350	47.82	20.57	15.88	15.73
Pure PE	350	49.44	22.36	13.17	15.03
Pure PE	350	48.1	23.55	15.88	12.47
Pure PE	350	47.58	20.64	13.55	18.23
Pure PE	350	47.77	20.42	14.68	17.12
% Total Average		**48.63**	**21.46**	**14.52**	**15.38**
Pure PE	375	49.55	24.80	23.29	2.35
Pure PE	375	32.42	49.75	15.81	2.02
Pure PE	375	42.46	30.01	24.54	2.99
Pure PE	375	47.17	25.49	24.73	2.61
Pure PE	375	43.92	24.98	26.55	4.55
Pure PE	375	44.87	24.65	27.29	3.20
Pure PE	375	44.55	24.11	27.46	3.88
% Total Average		**43.56**	**29.11**	**24.24**	**3.09**
Pure PE	400	24.64	49.02	22.35	4.00
Pure PE	400	31.02	39.19	25.73	4.07
Pure PE	400	26.85	34.61	27.75	10.79
Pure PE	400	20.19	44.39	22.39	13.02
Pure PE	400	36.05	19.3	26.75	17.9
Pure PE	400	33.49	26.27	23.18	17.06
Pure PE	400	29.87	34.88	23.53	11.72
% Total Average		**28.87**	**35.38**	**24.53**	**11.22**

Table H.5 (continued)

Sample	Temp (°C)	Product Distribution (%)			
		C_3	C_4	C_5	C_6
Pure PE	430	52.83	29.25	17.04	0.88
Pure PE	430	50.77	30.79	17.91	0.53
Pure PE	430	48.50	30.69	18.79	2.02
Pure PE	430	47.63	30.68	19.34	2.35
Pure PE	430	51.48	27.92	17.87	2.73
Pure PE	430	46.94	28.47	19.05	5.54
Pure PE	430	47.15	28.37	19.58	4.90
% Total Average		**49.33**	**29.45**	**18.51**	**2.71**
PE/Beta5%	350	38.59	20.44	17.48	23.49
PE/Beta5%	350	34.26	29.45	20.94	15.35
PE/Beta5%	350	33.78	28.74	19.54	17.94
PE/Beta5%	350	41.42	24.03	17.2	17.35
PE/Beta5%	350	37.46	24.98	22.67	14.90
PE/Beta5%	350	37.66	20.28	17.45	24.61
PE/Beta5%	350	32.26	43.92	19.30	4.52
% Total Average		**36.49**	**27.41**	**19.23**	**16.88**
PE/Beta5%	375	46.10	39.00	13.56	1.34
PE/Beta5%	375	51.37	35.73	12.91	-
PE/Beta5%	375	64.25	24.82	10.94	-
PE/Beta5%	375	50.93	37.42	11.46	0.19
PE/Beta5%	375	51.76	37.44	10.80	-
PE/Beta5%	375	53.42	33.52	12.84	0.21
PE/Beta5%	375	52.33	36.24	11.03	0.4
% Total Average		**52.88**	**34.88**	**11.93**	**0.31**

Table H.5 (continued)

Sample	Temp (°C)	Product Distribution (%)			
		C_3	C_4	C_5	C_6
PE/Beta5%	400	51.69	34.11	14.20	-
PE/Beta5%	400	46.38	38.38	14.58	0.66
PE/Beta5%	400	54.71	26.47	18.05	0.77
PE/Beta5%	400	51.52	31.77	15.97	0.75
PE/Beta5%	400	49.82	32.17	16.76	1.25
PE/Beta5%	400	56.20	22.79	20.45	0.56
PE/Beta5%	400	43.49	41.32	14.19	1.00
% Total Average		**50.54**	**32.43**	**16.31**	**0.71**
PE/Beta5%	430	42.79	41.09	14.95	1.18
PE/Beta5%	430	45.24	30.36	22.00	2.41
PE/Beta5%	430	43.50	32.58	21.94	1.98
PE/Beta5%	430	44.88	26.83	25.04	3.25
PE/Beta5%	430	42.87	32.68	22.07	2.38
PE/Beta5%	430	42.87	32.68	22.07	2.38
PE/Beta5%	430	42.43	28.55	25.91	3.12
PE/Beta5%	430	41.95	28.71	26.18	3.16
% Total Average		**43.32**	**31.69**	**22.52**	**2.48**
PE/Beta2%	400	42.36	29.83	23.10	4.72
PE/Beta2%	400	39.86	39.62	18.81	1.72
PE/Beta2%	400	39.90	39.18	19.20	1.73
PE/Beta2%	400	40.16	38.80	18.59	2.45
PE/Beta2%	400	39.20	37.84	19.95	3.01
PE/Beta2%	400	39.74	37.93	19.94	2.39
PE/Beta2%	400	39.88	37.00	20.56	2.56
PE/Beta2%	400	39.72	37.75	20.21	2.32
% Total Average		**40.10**	**37.24**	**20.05**	**2.61**

Table H.6 Distribution of light cracked liquid products from thermal and catalytic cracking of polyethylene at temperatures range between 375°C and 430°C

Sample	Temp (°C)	Hour	Product Distribution (%)					
			C_4	C_5	C_6	C_7	C_8	C_9^+
Pure PE	375	1	10.27	47.88	30.26	7.55	4.00	0.04
Pure PE	375	2	12.58	54.70	24.41	4.91	3.07	0.33
Pure PE	375	3	8.48	46.40	34.84	6.58	3.62	0.08
Pure PE	375	4	8.67	42.59	40.73	4.70	2.81	0.51
Pure PE	375	5	7.30	32.20	34.18	8.69	13.08	4.55
Pure PE	375	6	8.03	38.18	43.78	6.30	3.66	0.05
Pure PE	375	7	9.48	36.41	42.15	8.12	3.84	-
Pure PE	375	8	2.80	28.98	41.72	15.56	9.85	1.09
% Total Average			**8.45**	**40.92**	**36.51**	**7.80**	**5.49**	**0.83**
Pure PE	400	1	9.53	45.12	35.99	6.08	3.21	0.07
Pure PE	400	2	6.89	41.98	38.32	9.12	3.61	0.08
Pure PE	400	3	3.81	27.69	43.62	16.01	8.68	0.20
Pure PE	400	4	3.14	27.75	44.82	16.33	7.59	0.36
Pure PE	400	5	3.78	24.88	43.92	18.85	7.97	0.60
Pure PE	400	6	1.35	13.79	39.86	27.52	15.97	1.52
Pure PE	400	7	1.57	16.74	44.85	22.93	12.61	1.31
Pure PE	400	8	1.45	13.07	41.05	25.03	17.89	1.51
% Total Average			**3.94**	**26.38**	**41.55**	**17.73**	**9.69**	**0.71**

Table H.6 (continued)

Sample	Temp (°C)	Hour	Product Distribution (%)					
			C_4	C_5	C_6	C_7	C_8	C_9^+
Pure PE	430	1	8.59	47.58	31.29	7.24	4.68	0.62
Pure PE	430	2	14.44	50.98	27.46	4.79	2.10	0.22
Pure PE	430	3	12.99	48.54	31.40	5.36	1.55	0.15
Pure PE	430	4	10.11	45.82	36.48	5.16	2.30	0.13
Pure PE	430	5	7.20	36.96	42.62	8.70	4.14	0.37
Pure PE	430	6	3.42	27.04	45.35	15.40	7.94	0.84
Pure PE	430	7	4.53	29.49	44.88	13.63	6.66	0.81
Pure PE	430	8	4.79	45.47	38.52	8.27	2.87	0.09
% Total Average			**8.26**	**41.49**	**37.25**	**8.57**	**4.03**	**0.40**
PE/Beta 5%	375	1	11.89	55.03	22.92	5.89	3.56	0.71
PE/Beta 5%	375	2	17.54	53.51	24.89	2.88	1.12	0.07
PE/Beta 5%	375	3	15.96	52.39	26.66	3.58	1.34	0.06
PE/Beta 5%	375	4	17.13	52.37	25.44	3.92	1.12	0.02
PE/Beta 5%	375	5	15.94	51.79	27.13	3.89	1.22	0.02
PE/Beta 5%	375	6	16.42	52.15	26.32	3.91	1.17	0.02
PE/Beta 5%	375	7	15.22	55.35	25.63	2.65	1.09	0.05
PE/Beta 5%	375	8	17.70	59.43	18.94	2.90	1.00	0.04
% Total Average			**15.98**	**54.00**	**24.74**	**3.70**	**1.45**	**0.12**

Table H.6 (continued)

Sample	Temp (°C)	Hour	Product Distribution (%)					
			C_4	C_5	C_6	C_7	C_8	C_9^+
PE/Beta 5%	400	1	13.27	60.24	22.24	3.01	1.24	-
PE/Beta 5%	400	2	12.59	61.98	21.65	2.73	1.05	0.01
PE/Beta 5%	400	3	11.23	61.93	22.53	3.17	1.13	0.01
PE/Beta 5%	400	4	10.65	56.32	29.11	2.74	1.19	-
PE/Beta 5%	400	5	10.65	54.19	29.58	3.87	1.71	-
PE/Beta 5%	400	6	10.58	56.29	29.12	2.72	1.28	0.01
PE/Beta 5%	400	7	8.01	56.04	24.83	5.13	4.64	1.36
PE/Beta 5%	400	8	8.64	52.06	34.00	3.24	2.06	-
% Total Average			**10.70**	**57.38**	**26.63**	**3.33**	**1.79**	**0.17**
PE/Beta 5%	430	1	15.55	59.78	21.09	2.58	0.97	0.03
PE/Beta 5%	430	2	13.60	59.02	23.58	2.63	1.16	-
PE/Beta 5%	430	3	16.56	59.43	20.55	2.37	1.09	-
PE/Beta 5%	430	4	16.27	58.94	21.15	2.41	1.24	-
PE/Beta 5%	430	5	16.74	58.98	20.84	2.34	1.10	-
PE/Beta 5%	430	6	18.49	61.92	17.54	1.37	0.69	-
PE/Beta 5%	430	7	15.72	60.61	20.19	2.64	0.84	0.01
PE/Beta 5%	430	8	15.73	60.16	20.21	2.98	0.92	0.01
% Total Average			**16.08**	**59.86**	**20.64**	**2.42**	**1.00**	**0.01**

Table H.6 (continued)

Sample	Temp (°C)	Hour	Product Distribution (%)					
			C_4	C_5	C_6	C_7	C_8	C_9^-
PE/Beta 2%	400	1	15.53	58.28	21.91	3.39	0.88	0.01
PE/Beta 2%	400	2	15.61	58.90	21.85	2.75	0.88	0.01
PE/Beta 2%	400	3	14.64	60.28	21.89	2.43	0.77	-
PE/Beta 2%	400	4	17.12	57.75	22.22	2.21	0.70	-
PE/Beta 2%	400	5	15.77	57.48	23.65	2.32	0.78	-
PE/Beta 2%	400	6	16.68	56.70	23.18	2.68	0.76	-
PE/Beta 2%	400	7	17.38	55.59	23.27	2.95	0.79	0.01
PE/Beta 2%	400	8	13.79	52.30	27.99	4.44	1.44	0.04
% Total Average			**15.82**	**57.16**	**23.25**	**2.90**	**0.88**	**0.01**

Table H.7 Distribution of heavy cracked liquid products from thermal and catalytic cracking of polyethylene at temperatures range between 375°C and 430°C

Sample	Temp (°C)	Hour	Product Distribution (%)				
			C_5	C_6	C_7	C_8	C_9^+
Pure PE	375	1	21.66	20.02	17.38	13.78	27.16
Pure PE	375	2	21.35	19.97	17.33	13.82	27.53
Pure PE	375	3	24.53	22.72	17.77	12.25	22.73
Pure PE	375	4	23.75	23.03	18.73	13.11	21.38
Pure PE	375	5	21.63	21.21	17.90	13.14	26.11
Pure PE	375	6	21.14	21.62	18.78	13.78	24.67
Pure PE	375	7	18.60	19.83	18.03	13.95	29.58
Pure PE	375	8	19.98	21.98	20.24	15.65	22.14
% Total Average			**21.58**	**21.30**	**18.27**	**13.69**	**25.16**
Pure PE	400	1	22.25	22.66	18.72	12.25	24.12
Pure PE	400	2	24.21	24.99	20.19	12.66	17.95
Pure PE	400	3	18.70	21.35	19.14	13.00	27.82
Pure PE	400	4	16.43	20.34	19.45	13.68	30.10
Pure PE	400	5	14.37	19.11	19.52	14.36	32.64
Pure PE	400	6	11.56	17.05	19.47	15.14	36.77
Pure PE	400	7	12.98	18.68	20.16	14.93	33.25
Pure PE	400	8	12.64	18.88	21.02	15.97	31.49
% Total Average			**16.64**	**20.38**	**19.71**	**14.00**	**29.27**

Table H.7 (continued)

Sample	Temp (°C)	Hour	Product Distribution (%)				
			C_5	C_6	C_7	C_8	C_9^+
Pure PE	430	1	48.91	15.63	10.09	7.08	18.30
Pure PE	430	2	31.97	22.73	15.57	9.99	19.74
Pure PE	430	3	24.89	19.88	15.12	10.78	29.34
Pure PE	430	4	24.72	20.10	15.60	10.85	28.75
Pure PE	430	5	19.84	17.52	15.27	11.29	36.08
Pure PE	430	6	19.84	17.78	15.72	11.52	35.14
Pure PE	430	7	17.72	16.71	15.98	11.93	37.66
Pure PE	430	8	16.54	15.97	15.91	11.79	39.78
% Total Average			**25.55**	**18.29**	**14.91**	**10.65**	**30.60**
PE/Beta 5%	350	1	-	4.45	4.90	8.71	81.94
PE/Beta 5%	350	2	-	4.46	5.55	9.69	80.29
PE/Beta 5%	350	3	1.36	8.48	8.70	13.70	67.75
PE/Beta 5%	350	4	3.61	9.12	10.20	11.38	65.69
PE/Beta 5%	350	5	4.24	10.16	11.36	11.76	62.49
PE/Beta 5%	350	6	2.90	6.75	7.78	8.36	74.21
PE/Beta 5%	350	7	4.68	10.99	12.42	12.63	59.28
PE/Beta 5%	350	8	3.96	9.99	11.40	11.88	62.78
% Total Average			**2.59**	**8.05**	**9.04**	**11.01**	**69.30**

Table H.7 (continued)

Sample	Temp (°C)	Hour	Product Distribution (%)				
			C_5	C_6	C_7	C_8	C_9^+
PE/Beta 5%	375	1	29.40	23.16	17.37	10.97	19.10
PE/Beta 5%	375	2	33.51	23.98	17.43	10.27	14.82
PE/Beta 5%	375	3	26.92	19.70	13.78	8.72	30.87
PE/Beta 5%	375	4	33.62	24.86	17.08	10.16	14.27
PE/Beta 5%	375	5	32.38	25.04	17.48	10.45	14.64
PE/Beta 5%	375	6	34.66	25.53	17.60	10.99	11.21
PE/Beta 5%	375	7	35.29	24.35	16.48	10.55	13.33
PE/Beta 5%	375	8	36.42	25.89	17.01	9.88	10.80
% Total Average			**32.78**	**24.06**	**16.78**	**10.25**	**16.13**
PE/Beta 5%	400	1	28.67	23.03	16.72	11.45	20.13
PE/Beta 5%	400	2	30.56	24.98	16.97	10.83	16.66
PE/Beta 5%	400	3	30.30	22.98	15.64	10.28	20.80
PE/Beta 5%	400	4	32.46	24.85	16.54	10.34	15.82
PE/Beta 5%	400	5	32.34	23.89	15.95	10.51	17.31
PE/Beta 5%	400	6	30.47	24.12	16.31	10.38	18.72
PE/Beta 5%	400	7	31.36	24.72	16.77	10.78	16.35
PE/Beta 5%	400	8	31.99	24.96	16.37	10.36	16.32
% Total Average			**31.02**	**24.19**	**16.41**	**10.62**	**17.76**

Table H.7 (continued)

Sample	Temp (°C)	Hour	Product Distribution (%)				
			C_5	C_6	C_7	C_8	C_9^+
PE/Beta 5%	430	1	31.43	29.92	14.73	9.39	14.52
PE/Beta 5%	430	2	38.30	22.41	13.90	10.14	15.25
PE/Beta 5%	430	3	39.37	25.51	14.45	8.52	12.16
PE/Beta 5%	430	4	37.35	24.64	13.40	9.55	15.06
PE/Beta 5%	430	5	39.28	26.07	13.79	9.01	11.84
PE/Beta 5%	430	6	40.34	26.45	13.66	8.71	10.84
PE/Beta 5%	430	7	39.23	25.63	13.67	9.05	12.42
PE/Beta 5%	430	8	36.80	25.90	14.81	9.80	12.68
% Total Average			**37.76**	**25.82**	**14.05**	**9.27**	**13.10**
PE/Beta 2%	400	1	31.00	24.53	17.48	10.56	16.43
PE/Beta 2%	400	2	35.52	29.64	18.06	8.49	8.29
PE/Beta 2%	400	3	32.90	26.89	17.77	10.04	12.40
PE/Beta 2%	400	4	34.07	26.43	17.18	9.74	12.58
PE/Beta 2%	400	5	33.56	26.07	17.43	10.09	12.84
PE/Beta 2%	400	6	33.59	26.19	17.37	9.97	12.88
PE/Beta 2%	400	7	34.19	26.35	17.20	9.79	12.48
PE/Beta 2%	400	8	36.34	28.41	16.54	7.35	11.36
% Total Average			**33.90**	**26.81**	**17.38**	**9.50**	**12.41**

Table H.8 Distribution of all cracked liquid products from thermal and catalytic cracking of polyethylene at temperatures range between 375°C and 430°C

Sample	Temp (°C)	Hour	Product Distribution (%)					
			C_4	C_5	C_6	C_7	C_8	C_9^+
Pure PE	375	1	3.06	29.47	23.07	14.45	10.87	19.08
Pure PE	375	2	2.74	28.62	20.94	14.62	11.48	21.60
Pure PE	375	3	1.50	28.40	24.86	15.79	10.72	18.72
Pure PE	375	4	1.51	27.02	26.10	16.29	11.32	17.76
Pure PE	375	5	1.26	23.45	23.44	16.31	13.13	22.40
Pure PE	375	6	1.75	24.84	26.44	16.07	11.58	19.32
Pure PE	375	7	1.95	22.27	24.42	15.99	11.87	21.51
Pure PE	375	8	0.57	21.82	26.01	19.28	14.47	17.84
% Total Average			**1.76**	**25.60**	**24.46**	**16.10**	**11.98**	**20.11**
Pure PE	400	1	1.62	26.14	24.93	16.57	10.71	20.03
Pure PE	400	2	0.98	26.72	26.88	18.62	11.38	15.42
Pure PE	400	3	0.59	20.10	24.81	18.65	12.33	23.53
Pure PE	400	4	0.35	17.68	23.05	19.10	13.01	26.81
Pure PE	400	5	0.44	15.60	22.02	19.44	13.61	28.88
Pure PE	400	6	0.17	11.83	19.86	20.46	15.24	32.42
Pure PE	400	7	0.17	13.40	21.59	20.47	14.67	29.70
Pure PE	400	8	0.18	12.69	21.66	21.52	16.21	27.73
% Total Average			**0.51**	**17.91**	**23.14**	**19.45**	**13.44**	**25.55**

Table H.8 (continued)

Sample	Temp (°C)	Hour	Product Distribution (%)					
			C_4	C_5	C_6	C_7	C_8	C_9^+
Pure PE	430	1	0.51	48.83	16.56	9.92	6.94	17.25
Pure PE	430	2	0.91	33.17	23.03	14.89	9.49	18.51
Pure PE	430	3	1.02	26.74	20.78	14.36	10.06	27.06
Pure PE	430	4	0.66	26.10	21.17	14.92	10.29	26.88
Pure PE	430	5	0.27	20.48	18.46	15.02	11.02	34.74
Pure PE	430	6	0.22	20.30	19.56	15.70	11.29	32.93
Pure PE	430	7	0.20	18.24	17.97	15.88	11.70	36.02
Pure PE	430	8	0.22	17.90	17.03	15.55	11.37	37.92
% Total Average			**0.47**	**26.46**	**19.37**	**14.55**	**10.27**	**28.87**
PE/Beta 5%	350	1	-	-	4.45	4.9	8.71	81.94
PE/Beta 5%	350	2	-	-	4.46	5.55	9.69	80.29
PE/Beta 5%	350	3	-	1.36	8.48	8.7	13.7	67.75
PE/Beta 5%	350	4	-	3.61	9.12	10.2	11.38	65.69
PE/Beta 5%	350	5	-	4.24	10.16	11.36	11.76	62.49
PE/Beta 5%	350	6	-	2.9	6.75	7.78	8.36	74.21
PE/Beta 5%	350	7	-	4.68	10.99	12.42	12.63	59.28
PE/Beta 5%	350	8	-	3.96	9.99	11.4	11.88	62.78
% Total Average			**-**	**2.59**	**8.05**	**9.04**	**11.01**	**69.30**

Table H.8 (continued)

Sample	Temp (°C)	Hour	Product Distribution (%)					
			C_4	C_5	C_6	C_7	C_8	C_9^+
PE/Beta 5%	375	1	0.89	31.32	23.14	16.51	10.41	17.72
PE/Beta 5%	375	2	1.63	35.37	24.06	16.08	9.42	13.45
PE/Beta 5%	375	3	1.38	29.13	20.30	12.90	8.08	28.20
PE/Beta 5%	375	4	1.87	35.67	24.92	15.64	9.17	12.71
PE/Beta 5%	375	5	2.25	35.11	25.33	15.57	9.15	12.58
PE/Beta 5%	375	6	2.44	37.26	25.65	15.57	9.53	9.55
PE/Beta 5%	375	7	2.62	38.74	24.57	14.10	8.92	11.04
PE/Beta 5%	375	8	2.72	39.96	24.82	14.84	8.51	9.14
% Total Average			**2.01**	**35.44**	**24.15**	**15.13**	**9.14**	**14.12**
PE/Beta 5%	400	1	1.95	33.30	22.91	14.71	9.95	17.18
PE/Beta 5%	400	2	2.79	37.52	24.24	13.82	8.66	12.97
PE/Beta 5%	400	3	2.32	36.84	22.89	13.06	8.39	16.50
PE/Beta 5%	400	4	2.14	37.26	25.71	13.77	8.50	12.64
PE/Beta 5%	400	5	2.26	36.98	25.10	13.38	8.64	13.63
PE/Beta 5%	400	6	2.12	35.64	25.12	13.59	8.56	14.97
PE/Beta 5%	400	7	1.75	36.75	24.74	14.23	9.44	13.08
PE/Beta 5%	400	8	2.11	36.90	27.17	13.16	8.33	12.33
% Total Average			**2.22**	**36.48**	**24.70**	**13.70**	**8.79**	**14.12**

Table H.8 (continued)

Sample	Temp (°C)	Hour	Product Distribution (%)					
			C_4	C_5	C_6	C_7	C_8	C_9^+
PE/Beta 5%	430	1	2.69	36.34	28.39	12.63	7.93	12.01
PE/Beta 5%	430	2	3.01	42.88	22.67	11.41	8.16	11.88
PE/Beta 5%	430	3	3.34	43.42	24.51	12.01	7.02	9.71
PE/Beta 5%	430	4	3.10	41.46	23.97	11.31	7.97	12.19
PE/Beta 5%	430	5	3.08	42.90	25.11	11.69	7.56	9.66
PE/Beta 5%	430	6	3.72	44.68	24.66	11.19	7.10	8.66
PE/Beta 5%	430	7	2.42	42.52	24.79	11.97	7.78	10.51
PE/Beta 5%	430	8	2.94	41.17	24.84	12.60	8.14	10.31
% Total Average			**3.04**	**41.94**	**24.84**	**11.85**	**7.71**	**10.62**
PE/Beta 2%	400	1	2.19	34.84	24.16	15.50	9.20	14.12
PE/Beta 2%	400	2	2.08	38.63	28.60	16.02	7.48	7.19
PE/Beta 2%	400	3	2.06	36.75	26.19	15.61	8.74	10.65
PE/Beta 2%	400	4	2.74	37.87	25.76	14.78	8.29	10.56
PE/Beta 2%	400	5	2.94	38.02	25.62	14.61	8.35	10.44
PE/Beta 2%	400	6	2.96	37.69	25.66	14.76	8.33	10.59
PE/Beta 2%	400	7	3.00	37.88	25.82	14.74	8.24	10.33
PE/Beta 2%	400	8	2.75	39.52	28.33	14.13	6.17	9.11
% Total Average			**2.60**	**37.72**	**26.23**	**15.00**	**8.09**	**10.37**

APPENDIX J

NMR DATA

Table J.1 Intergrated area of the spectral regions

Sample	Hour	T (^{o}C)	A	B	C	D	E	F
LCL (Cool at -5^{o}C)								
PE/Beta5%	2	375	0.999	18.488	19.030	71.234	13.662	85.475
PE/Beta5%	3	375	1.002	77.949	73.425	317.493	31.068	263.500
PE/Beta5%	4	375	1.001	40.540	37.106	144.846	21.465	151.581
PE/Beta5%	5	375	0.999	130.546	118.184	493.223	167.996	541.799
PE/Beta5%	6	375	1.003	37.549	35.249	153.668	18.943	143.103
PE/Beta5%	7	375	1.003	65.742	57.408	250.864	19.545	218.619
PE/Beta5%	8	375	1.004	81.880	67.950	290.476	27.668	261.398
PE/Beta5%	2	430	1.002	22.374	26.692	73.513	16.690	94.342
PE/Beta5%	3	430	1.007	72.168	58.393	234.455	20.334	169.266
PE/Beta5%	4	430	1.002	33.293	27.144	109.749	14.807	98.905
PE/Beta5%	5	430	1.001	33.833	23.664	117.008	11.460	105.717
PE/Beta5%	6	430	1.001	26.609	22.670	90.991	11.573	83.537
PE/Beta5%	7	430	1.002	33.241	28.935	124.772	13.164	107.042
PE/Beta5%	8	430	1.000	53.875	42.048	180.642	19.518	164.017
PE/Beta2%	4	400	0.995	36.386	27.241	110.538	14.764	107.431
PE/Beta5%	4	400	0.998	53.863	44.222	178.105	14.957	138.742
HCL (Cool at 20^{o}C) and Commercial gasoline								
PE/Beta5%	4	375	0.999	2.449	4.532	8.835	8.516	20.746
PE/Beta5%	4	430	1.000	2.409	5.430	7.450	7.003	16.978
PE/Beta5%	4	400	1.000	2.338	4.528	7.857	5.194	13.818
PE/Beta2%	4	400	1.000	9.281	15.924	28.235	19.758	50.592
Octane91	-	-	1.000	0.179	1.548	0.639	1.835	3.274
Octane95	-	-	1.000	0.195	1.593	0.663	1.720	3.737

Table J.2 Hydrocarbon types and octane number of cracked liquid products with commercial products

Sample	Hour	T (°C)	Aromatic %	Paraffin %	Olefin %	Isoparaffin index	RON	MON
LCL (Cool at -5°C)								
PE/Beta5%	2	375	5.10	50.82	44.08	4.171	117.9	113.0
PE/Beta5%	3	375	4.46	48.74	46.81	5.654	131.0	127.8
PE/Beta5%	4	375	4.71	46.29	49.00	4.708	122.6	118.4
PE/Beta5%	5	375	4.00	51.67	44.33	2.150	99.8	92.7
PE/Beta5%	6	375	4.48	50.19	45.33	5.036	125.5	121.6
PE/Beta5%	7	375	4.39	46.36	49.25	7.457	147.0	145.8
PE/Beta5%	8	375	4.35	44.00	51.66	6.298	136.7	134.2
PE/Beta5%	2	430	6.23	45.40	48.37	3.768	114.4	109.1
PE/Beta5%	3	430	4.73	38.06	57.22	5.550	130.1	126.8
PE/Beta5%	4	430	4.74	41.40	53.87	4.453	120.3	115.8
PE/Beta5%	5	430	4.04	43.17	52.79	6.150	135.4	132.7
PE/Beta5%	6	430	4.89	42.91	52.20	4.812	123.6	119.4
PE/Beta5%	7	430	4.62	45.87	49.51	5.421	128.9	125.5
PE/Beta5%	8	430	4.36	41.93	53.71	5.602	130.5	127.3
PE/Beta2%	4	400	4.58	38.68	56.75	4.851	123.9	119.8
PE/Beta5%	4	400	4.75	39.41	55.84	6.184	135.7	133.1
HCL (Cool at 20°C) and Commercial gasoline								
PE/Beta5%	4	375	9.36	59.27	31.36	1.624	95.7	88.0
PE/Beta5%	4	430	11.97	52.81	35.22	1.616	95.9	88.2
PE/Beta5%	4	400	11.70	50.89	37.41	1.774	97.2	89.7
PE/Beta2%	4	400	8.25	50.08	41.67	1.707	96.3	88.7
Octane91	-	-	33.40	53.06	13.54	1.189	94.4	86.1
Octane95	-	-	32.56	53.20	14.24	1.448	96.6	88.6

AUTHOR BIOGRAPHY

Mr. Chaiwat Tachakritikul was born on May 11, 1976 in Bangkok. He received a Bachelor Degree in Industrial Chemistry from the Department of Chemistry, Faculty of Science, King Mongkut's Institute of Technology Ladkrabang in 1998. He has been a graduate student of the Program of Petrochemicals and Hydrocarbon Chemistry, Graduate School, King Mongkut's Institute of Technology Ladkrabang since 1998.